THE APPLICABILITY OF ELECTRODES MODIFIED WITH NANOMATERIALS IN POTENTIOMETRIC TITRATIONS AND IN CYCLIC VOLTAMMETRIC DETERMINATIONS OF SOME DRUGS

BY

Khaled M. AlAqad

A Thesis Presented to the

DEANSHIP OF GRADUATE STUDIES

KING FAHD UNIVERSITY OF PETROLEUM & MINERALS

DHAHRAN, SAUDI ARABIA

In Partial Fulfillment of the
Requirements for the Degree of

MASTER OF SCIENCE

In

CHEMISTRY

MAY 2016

KING FAHD UNIVERSITY OF PETROLEUM & MINERALS

DHAHRAN- 31261, SAUDI ARABIA

DEANSHIP OF GRADUATE STUDIES

This thesis, written by **Khaled M. ALaqad** under the direction his thesis advisor and approved by his thesis committee, has been presented and accepted by the Dean of Graduate Studies, in partial fulfillment of the requirements for the degree of **MASTER OF SCIENCE IN CHEMISTRY.**

Dr. Abdallah Abulkibash 4-5-16
(Advisor)

8/5/2016
Dr. Abdulaziz AL-Saadi
Department Chairman

Dr. Tawfik Saleh
(Member)

Dr. Salam A. Zummo
Dean of Graduate Studies

Dr. Othman AL-Hamouz
(Member)

15/5/16
Date

DEDICATION

My parents, wife, son Mohammed, brothers & sister

ACKNOWLEDGMENTS

All praise and thanks are due to Almighty Allah. He bestowed upon me health, knowledge and patience to complete this work.

I will take this opportunity to acknowledge, with deep gratitude and appreciation, the encouragement, valuable time and guidance given to me by my thesis advisor, Dr. Abdallah Abulkibash. I am also highly grateful to my thesis committee members: Dr. Tawfik Saleh and Dr. Othman AL-Hamouz for their valuable guidance, comments, suggestions and motivation throughout the research period. Thanks to all faculty members, staffs and students of the chemistry department. Sincere thanks to KFUPM for the support extended towards my research and for granting me the opportunity to pursue graduate studies. My heartfelt thanks are due to my parents, small beloved family my wife and son Mohamed for their prayers, guidance, love, care and moral support throughout my academic life. My heartfelt thanks to my brothers and sister for their prayers and guidance. Finally, many thanks are due to my senior colleagues at KFUPM for their help and prayers.

TABLE OF CONTENTS

LIST OF FIGURES

LIST OF SCHEME

LIST OF ABBREVIATIONS

Ag/CNTs : Silver Metal coated with Carbon NanoTubes

AuNPs : Gold NanoParticles

AuNPs/CPE : Gold NanoParticles Carbon Paste Electrode

AgNPs : Silver NanoParticles

AgNPs/CPE : Silver NanoParticles Carbon Paste Electrode

AgNPs/GO : Silver NanoParticles Decorated with Graphene Oxide

AgNPs/GO/CPE : Silver NanoParticles and Graphene Oxide Carbon Paste Electrode

AgNPs/CNT : Silver NanoParticles Decorated with Carbon Nanotube

AgNPs/CNT/CPE : Silver NanoParticles Carbon Nanotube Carbon Paste Electrode

CNTs : Carbon NanoTubes

CPE : Carbon Paste Electrode

GO : Graphene Oxide

GCPE : Graphene Carbon Paste Electrode

KCZ : Ketoconazole

MMZ : Methimazole

PZ : Promazine

ABSTRACT

Full Name : Khaled M. ALAqad

Thesis Title : The Applicability of Electrode Modified with Nanomaterials in Potentiometric Titration and in Cyclic Voltammetric Determination of some Drugs.

Major Field : Chemistry

Date of Degree : May, 2016

The chemical vaporization method (CVD) was applied for the preparation of silver electrodes coated with carbon nanotubes. These electrodes were characterized by different techniques, including (TEM) and (SEM) to study the size, morphology and the chemical composition of the nanostructure of the carbon nanotubes. During the application of potentiometry in titration reactions, the silver electrodes coated with carbon nanotubes were found to show a response to all types of titration reactions, such as acid-base, precipitation; complexation and electron transfer reactions. In addition, modified Hummer method was applied for the synthesis of nanomaterials such as graphene nanosheet. Nobel metal nanoparticles like gold and silver nanoparticles were prepared by chemical reduction method. Furthermore, Raman spectroscopy and FT-IR were used to characterize functional groups of graphene oxide and carbon nanotubes. The silver nanoparticles with graphene oxide or multi- walled carbon nanotubes were used to investigate some of the pharmaceutical compounds using electrochemical techniques. The applicability of carbon paste electrode which was modified by nanomaterials such as graphene oxide, gold nanoparticles, silver nanoparticles, and multi- walled carbon nanotubes was investigated in the determination of pharmaceutical drugs like Promazine, Ketoconazole, and Methimazole.

ملخص الرسالة

الاسم الكامل: خالد محمد منصور العقاد

عنوان الرسالة: تطبيقات الاقطاب المعدلة بالمواد النانونية في المعايرات الجهدية والقياس الفولطي الحلقي لبعض الادوية.

التخصص: الكيمياء

تاريخ الدرجة العلمية: مايو 2016.

تم استخدام طريقة التبخير الكيميائية لتحضير أقطاب الفضة المغطاة بأنابيب الكربون النانونية، وتم توصيف هذه الأقطاب بواسطة تقنيات مختلفة تشمل الميكروسكوب الإلكتروني المنفذ والميكروسكوب الإلكتروني الماسح لدراسة الحجم، والتشكل والتركيب الكيميائي للأبنية النانونية لأنابيب الكربون النانونية. أثناء اجراء المعايرة الجهدية في تفاعلات المختلفة وجد بأن أقطاب الفضة المغطاة بأنابيب الكربون النانونية تعمل بكفاءة في معايرة كل من الحمض والقاعدة، والترسيب، والمعقدات، وفي تفاعلات الأكسدة والاختزال. هذا ولقد تم استخدام طريقة هامر المعدلة لتخليق المواد النانونية مثل الجرافين الورقي النانوني، وكذلك تم استخدام طريقة الاختزال الكيميائية لتحضير الجسيمات النانونية المعدنية النبيلة مثل جسيمات الفضة النانونية وجسيمات الذهب النانونية. علاوة على ذلك تم استخدام مطياف رامان لتمييز المواد النانونية وناقل فوريد للأشعة التحت الحمراء لإظهار وجود المجموعات الوظيفية لأكسيد الجرافين والأنابيب الكربونية النانونية. تم تخليق جسيمات الفضة النانونية المزخرفة مع أكسيد الجرافين أو أنابيب الكربون النانونية لتعيين بعض المركبات الصيدلانية باستخدام التقنيات الكهروكيميائية. ولقد تم استخدام قطب عجينة الكربون المعدل بواسطة المواد النانونية مثل أكسيد الجرافين، وجسيمات الذهب النانونية، وجسيمات الفضة النانونية، وأنابيب الكربون النانونية في تعيين الأدوية الصيدلانية مثل البرومازين والكيتونازول والميثامزول.

CHAPTER 1

INTRODUCTION

The term nano is a word of Greek origin, which means small in amount and size and it is used as the prefix for billionth from range 9 to 10 [1]. Nanomaterials such as carbon nanotubes, graphene, silver nanoparticles and gold nanoparticles, each has the size between 1nm to 100nm. Nanoparticles have unique chemical and physical properties as compared to their solid bulk materials because of high surface area and electronic properties [2]. The novel properties of nanomaterials and nanoparticles have been used in different applications such as medicine, cosmetics [3], photography, catalysis, and sensors [4]. There are different methods and techniques that can be applied in the syntheses of the nanomaterials in the form of particles or colloids. The chemical method involves a solid-state reaction and a sol-gel. The physical methods include vapor phase transport. The other method is a physical-chemical method like sono-chemical synthesis and Mechano-chemical synthesis. The biological methods such as Lactobacillus - assisted biosynthesis and Fusarium – oxysporum, were reported [5]. These methods are very useful to control the size, the morphology, the colors and the structure of the nanoparticles [6]. Carbon nanotubes (CNTs) have different structures, like single-walled carbon nanotubes, and multi-walled carbon nanotubes. CNTs are linked with each other's CNTs by Van Der Waals forces. The orbital hybridization theory is the best to show the chemical bond in

nanomaterial. The CNTs bonding is strong due to the sp^2 hybridization, like hybridization of graphite [7].

1.1. Literature Review

There are different methods that have been applied to prepare the nanomaterial such as carbon nanotubes, graphene nanosheet, and nanoparticles. Each method has its advantages and disadvantages regarding the cost, the particles size and the stability of the particles. The chemical vapor deposition method (CVD) has been commonly used in synthesizing carbon nanotubes and graphene and graphene [8]. Graphene is a suitable material and wildly used in electrochemistry applications because it has a high signal electrical of conductivity, high surface area, low costs of production and a special heterogeneous electron transfer rate [9]. Hummer method is generally used widely in the synthesis of graphene nanosheet [10]. Gold nanoparticles are widely used in the biotechnology field and biomedicine field because of their large surface area, and high electron conductivity which enhances the bioconjugation with molecule plumb-line and they also have unique optical properties [11]. The gold nanoparticles have good physical, chemical and optical properties [12]. On the other hand, the physical, chemical, and photo properties of gold nanoparticles are innovative ways to control the transport of the pharmaceutical compounds [13]. The gold nanoparticles were carried on huge number of drug molecules due to the high surface area to volume ratio [14]. The synthesis of Au/NPs has been made by different precursor metals, stabilizing, and reducing agents. The method used for syntheses of Au/NPs include tetrachloroauric acid ($HAuCl_4$) as a metal precursor and a citric acid ($C_6H_8O_7$) as stabilizing and reducing agents. The mechanism of the reaction of this method has been reported [15]. However, the researcher has used various precursors

like trisodium citrate and sulfur dioxide respectively [16-17]. Silver (Ag) metal that has distinctive properties such as, high conductivity, good stability, catalytic activity and antimicrobial. So silver nanoparticles were considered as an attractive material and used in antimicrobial applications [18-19]. The common method that has been utilizing to prepare colloidal AgNPs is the chemical reduction method, this method includes three main components the precursor, the stabilizing agents, and the reducing agents. Silver nitrate ($AgNO_3$) has been used as the metal precursor, and trisodium citrate ($C_6H_5O_7Na_3$) as a stabilizing and reducing agent. The mechanism of this reaction has been discussed [20]. In addition, other researchers have used silver nitrate as a precursor and ethylene glycol as reducing agent [21].

Titration is a widespread method, which is usually used in chemical laboratories. Normal potentiometry is based on the initial work of Nernst [22]. Normal potentiometry depends on measuring the difference in potential (ΔE) between the indicator electrode and Ag/AgCl as a reference electrode and immersed in the titration solution. The difference in potential is plotted against the volume of titrant added. An S-shaped curve is obtained with the end point occurring at the point of inflection. This technique has been applied for different types of titration processes. Potentiometric sensors play an important role in electrochemistry, which detected the activity of the analyte and the potential response are consider [23]. In addition, Classical potentiometry has been applied to all types of chemical reactions of ion combination in aqueous solutions by using different types of electrodes. For instance, acid-base reactions using antimony electrodes [24] while in precipitation reactions, silver-silver halide electrodes have been used [25]. In redox reactions, the platinum electrodes have been used [26] while in the case of complexation reactions, Pt/Hg

can be used [27]. The main objective of applying solid electrodes coated with nanomaterial find a universal electrode that can be applied in all types of titrimetric reactions.

1.2. Methodology

1.2.1. Synthesis of Nanomaterials

The noble metals nanomaterials such as gold nanoparticles and silver nanoparticles can be prepared by chemical reduction method. Silver nitrate used as a precursor in the synthesis of silver nanoparticles. Sodium boron tetra hydrate can be used as reducing agent in the synthesis of silver nanoparticles. Hummer method was used to prepared graphene oxide by reacting sodium nitrate with sulfuric acid and using potassium permanganate and hydrogen peroxide as a precursor and as a stabilizer respectively. The silver nano particles were used to decorate graphene oxide, and silver ions could be attached to COOH functional group of graphene oxide. Modified electrodes with carbon paste were prepared to make a working electrode by different metal nanoparticles and nanosheet. Carbon nanotubes have been used to coat a silver wire by the chemical vapor deposition method. In this method ferrocene was used as a catalyst and argon gas as a carrier. Working electrodes prepared by physical attachment of nanomaterials with silver metals have been investigated.

1.2.2. Instrumentals and Techniques

Electrochemical techniques like cyclic voltammetry and square wave voltammetry are widely used to determine the pharmaceutical compounds. In this work, some of the parameters were considered. For example, the window potential range for CV and SWV techniques were from (-1.2 – 1.4) V and scan rate range from (0 – 260) mV/s. Furthermore,

optimum parameters such as the frequency, the amplitude, and the increment potential with values from range (5 – 25) Hz, (1 – 20) mV, and (0.025 – 0.04) V were found to affect the signals by utilizing SWV. In this work, the pretreatment potential, the pretreatment time, and pH were found to affect the signals. Raman spectroscopy was used as a technique for nanomaterials to illustrate the element composition and the structure. The CCD detector with 400 mm monochromator was used in Raman spectroscopy. The wavenumber range was used from (50 – 4000) cm^{-1}. The laser source is consisted from two UV- Vis wavelength from (532 – 633) nm while the 633 nm wavelength was used because the higher energy causes high fragments in solution and the ND filter. Laser light of 50% magnification was used due to its high energy to fragments the sample. Depending on the concentration of the sample objective lenses of (10x, 50x, and 100x) were used. The optimum parameters of Raman spectroscopy such as 532 nm of laser, 2 V of accumulation time, and 2 s of acquisition Time. FT-IR technique was used to identify the functional groups of the nanomaterials and the sample prepared in a ratio of 1 sample: 99 potassium bromide (KBr) to construct the pellet. The wavenumber of IR was recorded from 400 – 4000 cm^{-1}.

1.3. REFERENCES

[1] F.K. Alanazi, A.A. Radwan, I.A. Alsarra, Saudi Pharm J., 18, 2010, 179-193.

[2] D. Guglielmo C, Lopez DR, Suarez MB., Reproduct Toxicol, 30,2010, 271-276.

[3] Q. H. Tran, V. Q. Nguyen, Anh-Tuan Le, Adv. Nat. Sci., 4, 2013, 033001.

[4] Z. Khan, Sh. A. Al-Thabaiti, A.O. Al-Youbi, Colloids and Surfaces, 82, 2011.

[5] Yuriy G., Advances in Ferroelectrics - Materials Science, 2012, 10-5772.

[6] Umme T K, K. V. Rao, Y. Aparna, IEEE. 2011, 978-1-4673-0074-2.

[7] Harry M., Francisco R. R., Elsevier, Activated Carbon, 2006, 13-86.

[8] C.E.Baddour, D.Nasuhoglu, Elsevier, Carbon, 47, 2008, 313-347.

[9] M. Liang, L. Zhi, J. Mater. Chem., 19, 2009, 5871.

[10] Priti Xavier,keshav sharma, Royal socity of chemistry,RSC Adv., 4, 2014, 12376.

[11] Tedesco S, Doyle H, Blasco J, Redmond G, Aquatic Toxicol, 100 2010, 178-186.

[12] Valenzuela SM, Trends Biotechnol., 2006, 7-62.

[13] Po C Chen, Sandra C Mwakwari, Nanotech, Science and application, 1, 2008.

[14] Grace, N.A.; Pandian, K., Colloids Surf, 297, 2007, 63–70.

[15] Verma HN, Singh P and Chavan RM, Veterinary World, EISSN, 7, 2014.

[16] T. Ahner, F. Delissen, S. Sokolov, J. Am. Chem. Soc., 132, 2010.

[17] N. Prior, EMC Conference, Precious metals, 2011, 1087–1102.

[18] Frattini, N. Pellegri, D. Nicastro, Chem. Phys. 94, 2005, 148-152.

[19] P. Li, J. Li, C. Wu, Q.Wu, J. Li, , J. Nanotechnol., 16 , 2005, 1912.

[20] Ratyakshi and R.P. Chauhan, Asian J. Chem, 21, No. 10, 2009.

[21] Yugang Sun, Younan Xia, MATERIALS SCIENCE, 298, 2002.

[22] Nernst, W., Z.phys.chem.,4,1889,129.

[23] Abdennabi A. differential electrolytic potentiometric titrimetry in non-aqueous media, PhD thesis, 1979.

[24] E. Bishop, G.D. Short, Analyst, 87, 1962, 467.

[25] E. Bishop, R.B. Dhaneshwer, Analyst, 87, 1962, 207.

[26] E. Bishop, Mikrochim. Acta, 40, 1956,619.

[27] H.V. Malmstadt, E.R. Fett, Anal. Chem., 27.

CHAPTER 2

Silver Coated with Carbon NanoTubes as an Indicator Electrode in Potentiometry

2.1. Introduction

Carbon nanotubes (CNTs) have different applications in chemistry, and material science because of their unique properties attributed to the atomic structure [1] [2]. CNTs behave as semiconductor [3]. The CNTs have electronic properties, which enable electron transfer [4]. Different techniques are used to prepare the CNTs. The common techniques employed include arc discharge [5], laser ablation [6] and chemical vapor deposition (CVD) [7]. Classical potentiometry has been applied in all types of a chemical reaction like ion combination in aqueous solution and electron transfer reaction using different types of indicator electrodes. Acid-base reactions using antimony electrodes [8-10] while in precipitation reactions, silver-silver halide electrodes have been used [11-12]. In redox reactions, the platinum or gold electrodes have been used [13-14] while in the case of complexation reactions, Pt/Hg was used [15].

2.2. Experimental

2.2.1. Apparatus

The potentiometry setup included a cell, a potentiometer, an indicator electrode and a reference electrode. In this work, Ag/AgCl electrode was used as a reference electrode. For the first time, the Ag/CNTs electrode was used as an indicator electrode in all of the titrimetric reactions. All of these electrodes inserted in a cell glass by using a stand of Teflon cover.

2.2.2. Reagents and Solutions

Precipitation: A standard solution of 0.05 M sodium chloride was prepared. A solution of 0.05 M NaCl was prepared in 0.1 M KNO_3. Solutions of 0.05 M of bromide and 0.05 M iodide were also prepared. A standard solution of 0.05 M silver nitrate was prepared in distilled water. A volume of 2 ml of each solution was transferred to a titration cell, then 18 ml of 0.1 M KNO_3 was added and the titration was started by adding the titrant from the burette. Complexometric titration; A standard solution of 0.05 M EDTA was prepared and a solution of 0.05 M magnesium chloride was also prepared and diluted in a buffer of pH 9. A solution of 0.05M calcium chloride was prepared in a buffer of pH 10. Similarly, a volume of 2 ml of Ca^{+2} or Mg^{+2} solution was transferred to the titrant cell, then 18 ml of the buffer solution was added. Acid-base reactions: A solution of 0.05M of NaOH was prepared and used as a titrant. Similarly, a volume of 2 ml of HCl solution was transferred to the titrant cell, then 18 ml of distilled water was added. Oxidation- reduction reactions: A solution of 0.05 M cerium sulfate was prepared and used as a titrant. A solution of 0.05

M Ferrous sulfate was prepared. Similarly, a volume of 2 ml of Fe^{+2} solution was transferred to the titrant cell, then 18 ml of 0.1 M H_2SO_4 was added.

2.2.3. Synthesis of Carbon Nanotubes on Silver Metal Electrode

A silver wire of length of 2 cm and 1 mm diameter was placed in the reactor. The reactor of floating catalyst (FL-CVD) was used to produce solid Ag/CNTs electrodes. A tube of quartz with a diameter 2.5 cm and a length of 100 cm placed in each reactor. The reactors were heated by silicon carbide, which is illustrated in Scheme 2.1. Ferrocene (Fe $C_{10}H_{10}$) was placed in the first reactor as a catalyst while the silver wire electrode was placed in the second reactor. Acetylene gas with a percentage purity of 99.5% was used as a hydrocarbon source and H_2 was used as a carrier gas. The reactor was flushed with argon gas to expel air from the reactor. The temperature of the system was adjusted from (600 – 900) C˚. The flow rate of H_2 was varied from (10 – 150) ml /minutes while the flow rate of the source of hydrocarbon was varied from (75– 300) ml/minutes. The reaction time was 30 min. The resulting modified electrode Ag/CNTs was used as an indicator electrode in classical potentiometry. A titration cell that accommodates the indicator electrode Ag/CNTs and the Ag/AgCl reference electrode. The solid Ag/CNTs modified electrodes was washed with a solution of 1 M of HNO3 then rinsed with distilled water [43]. Another the modified electrode was prepared by physical attachment using silver glue as a conducting material.

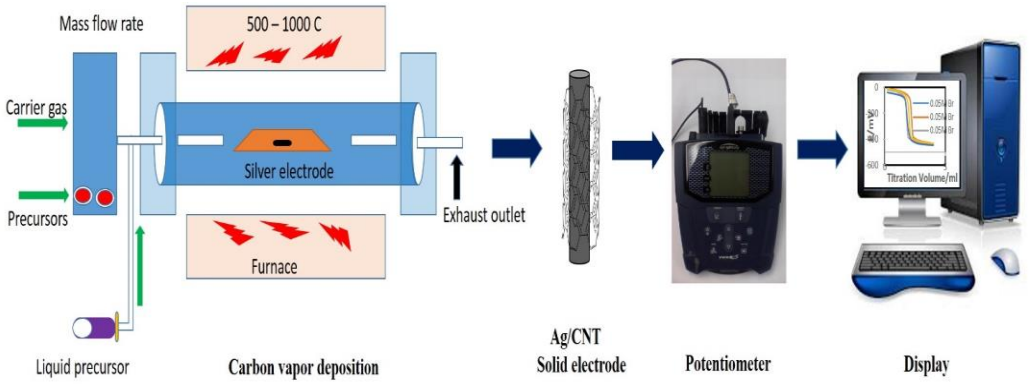

Scheme 2.1: Synthesis of CNTs by Chemical vapor deposition.

2.2.4. Procedure

Potentiometric titrations were performed by using of Ag/CNTs electrode as an indicator electrode in the precipitation, complexation, acid-base and redox reaction. A reagent such as KNO_3 and H_2SO_4 were used in precipitation and redox reactions respectively. In addition, buffer solutions of different pH values were used in complexation reactions. The Ag/CNTs electrode was immersed in the titration cell containing a volume of 20 ml of the reagent and the analyte. The electrodes were connected to the potentiometric device. The following titrant solutions EDTA, $AgNO_3$, NaOH, and cerium sulfate were used. During the titration process, small drops were added and the results were recorded.

2.3. Results and Discussions

2.3.1. Characterization of Solid Ag/CNTs Sensor Electrode

The scanning electron microscope (SEM) Fig. 2.1a, was used to characterize the morphology of the solid silver coated with CNTs while the structure of the carbon nanotubes coated with silver metal were characterized using the transmission electron microscope (TEM) in Fig. 2.1b. Furthermore, the Ag/CNTs electrode coated with CNTs using physical attachment method. The silver glue was used as a conducting material and characteristics of Ag/CNTs electrode was shown in Fig 2.1c, d.

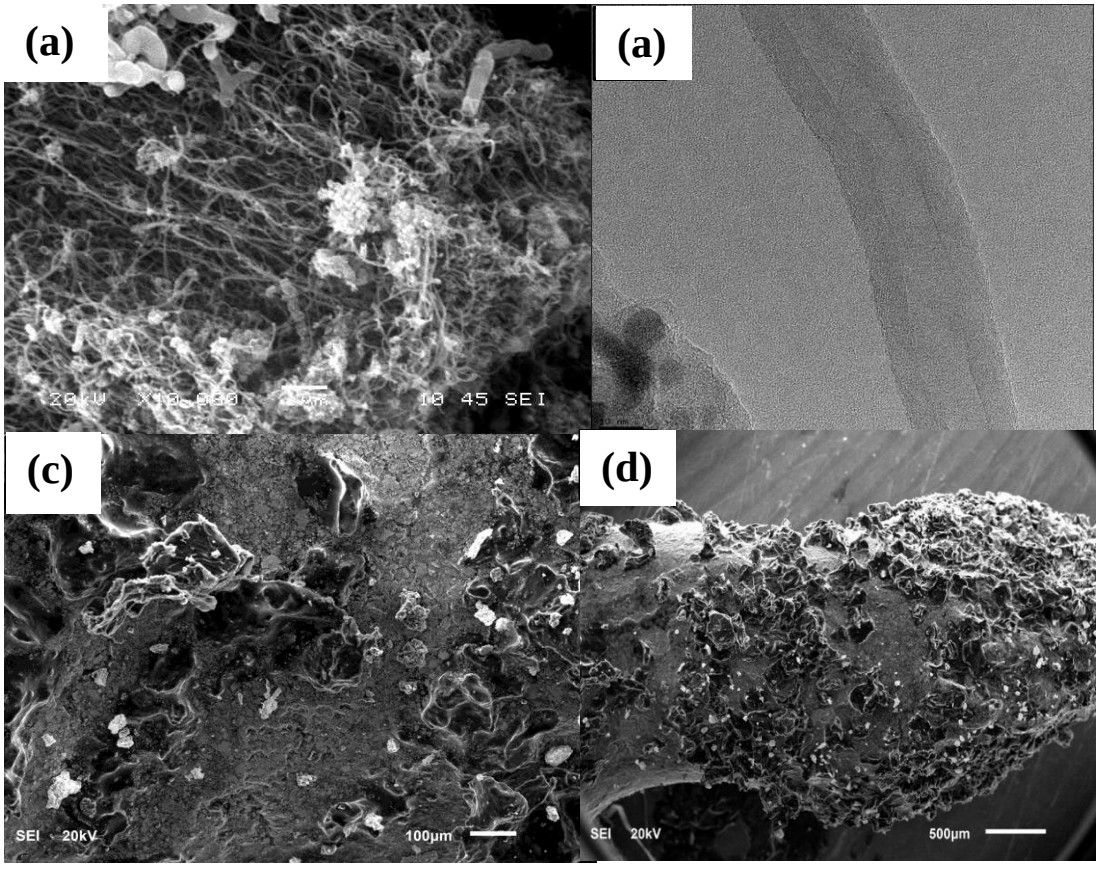

Figure 2.1: (a) SEM of Ag/CNTs at 10 µm, (b) TEM of Ag/CNTs at 10 µm, (c) SEM of Ag/CNTs physical attachment at 100 µM, and (d) SEM of Ag/CNTs phys.attach. at 500µM.

2.3.2. Precipitation Titrations

The titration curve using Ag/CNTs indicator electrode in the titration of 0.05 M bromide and 0.05 M iodide with 0.05 M $AgNO_3$ are depicted in Fig 2.2. The ionic strength was maintained by using a solution of 0.1M KNO_3. The plot showed S-shaped and the first differential curves are also shown end points of all ions. In addition, the titration mixture of 0.05 M Br^- with 0.05 M I^- and the mixture of 0.05 M Cl^- with 0.05 M I^- were illustrated in Fig. 2.3. Furthermore, the potentiometric response behavior of the Ag/CNTs physically attached electrode in potentiometric titration of 0.05 M chloride ion with 0.05 M $AgNO_3$ were obtained by measuring the cell potential (EMF) at 25 C °. The response enhanced was investigated as the potential increased with jump response. The ionic strength was maintained by using a solution of 0.1M KNO_3 solution. The titration curve is shown in Fig. 2.4a. The plot mixture curve between iodide and chloride is shown in Fig. 2.4b.

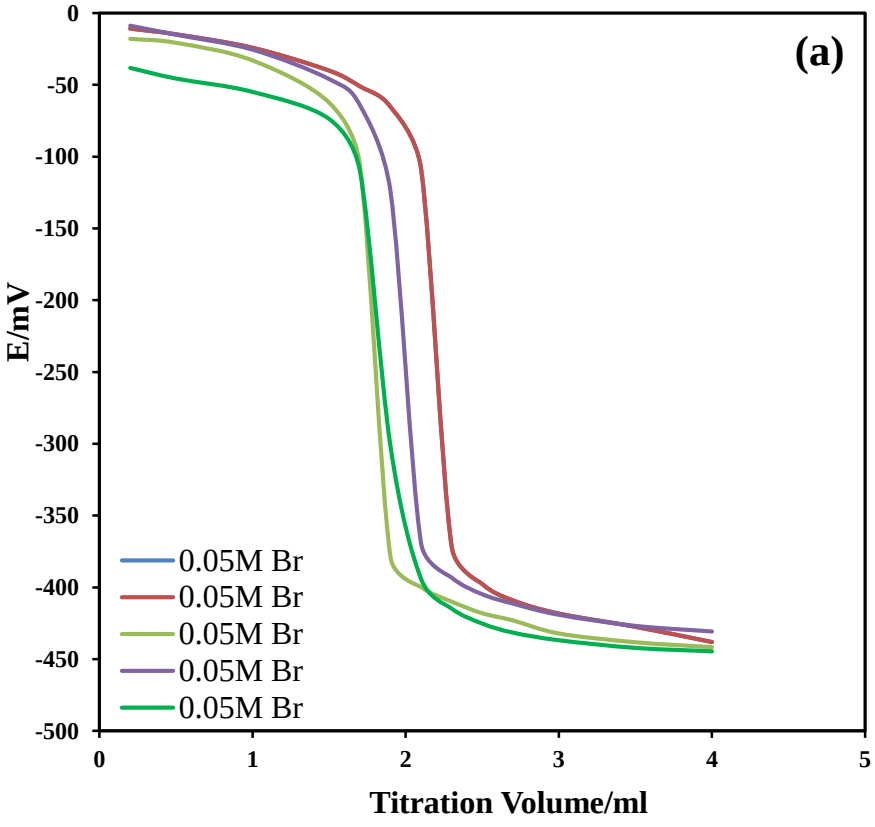

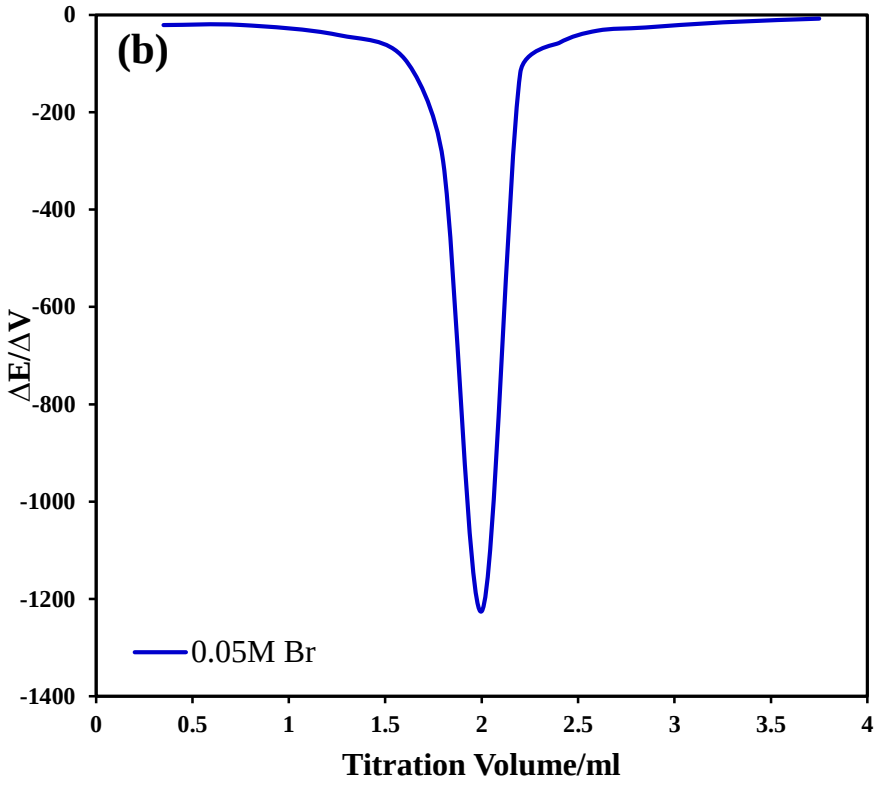
(b)
0
-200
-400
-600
-800
-1000
-1200
-1400
ΔE/ΔV
0.05M Br
0
0.5
1
1.5
2
2.5
3
3.5
4
Titration Volume/ml

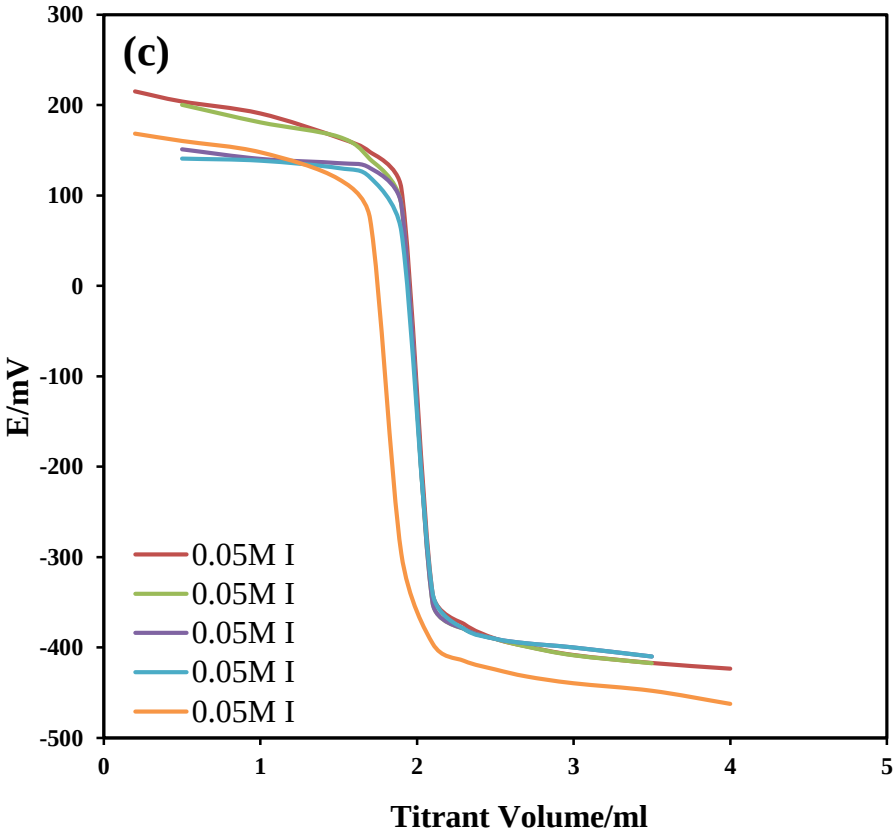
(c)
300
200
100
0
-100
-200
-300
-400
-500
E/mV
0.05M I
0.05M I
0.05M I
0.05M I
0.05M I
0
1
2
3
4
5
Titrant Volume/ml

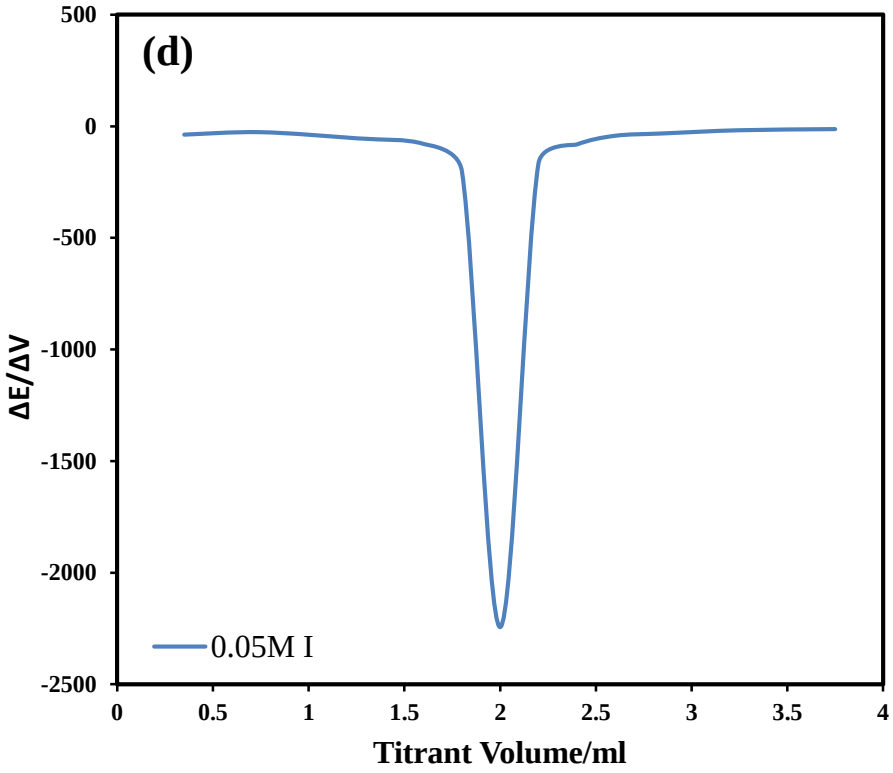

Figure 2.2: (a) Titration of 20 ml of 0.05 M bromide with 0.05 M $AgNO_3$, (b) first differential curve of 0.05 M Br^-, (c) titrate of 20 ml of 0.05 M iodide with 0.05 M $AgNO_3$, and (d) The first differential curve of 0.05 M I^-.

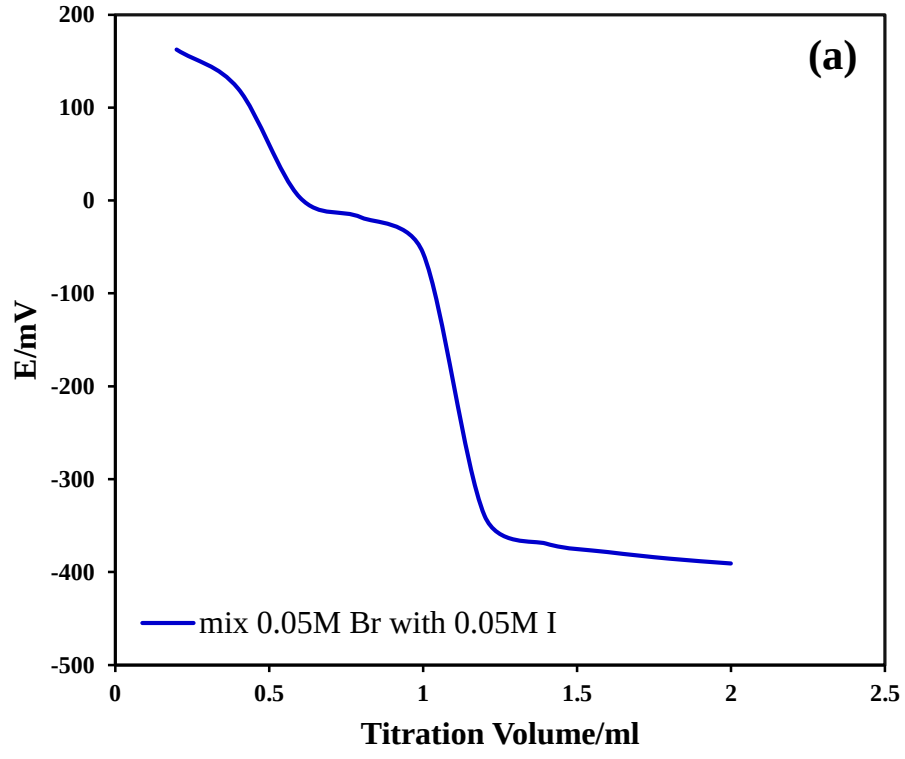

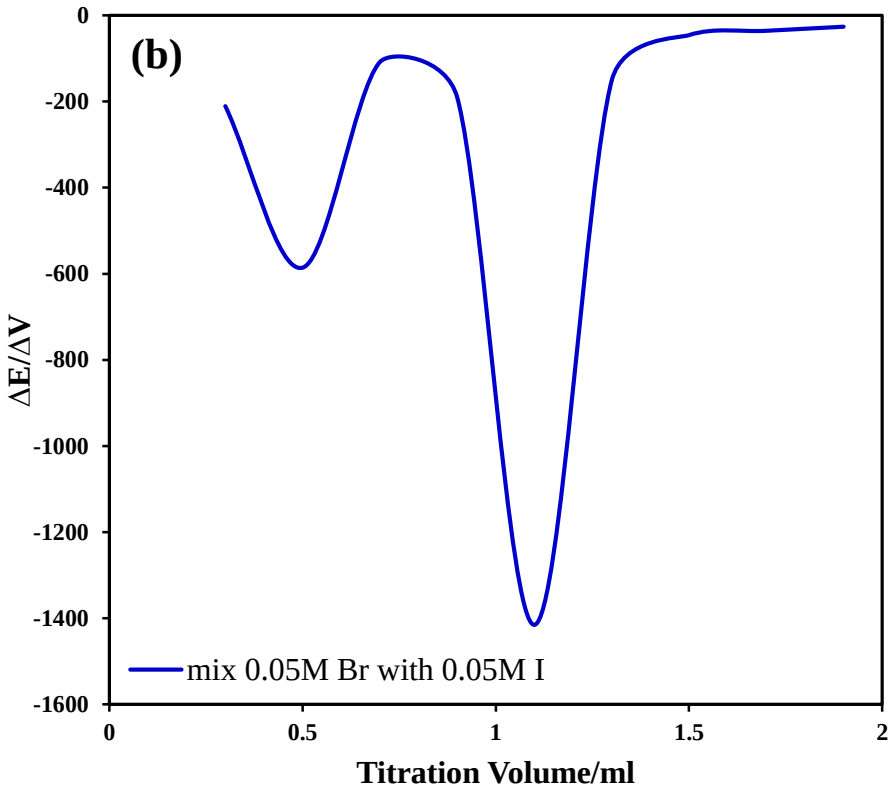
(b)
0
-200
-400
-600
-800
-1000
-1200
-1400
-1600
ΔE/ΔV
0
0.5
1
1.5
2
Titration Volume/ml
mix 0.05M Br with 0.05M I

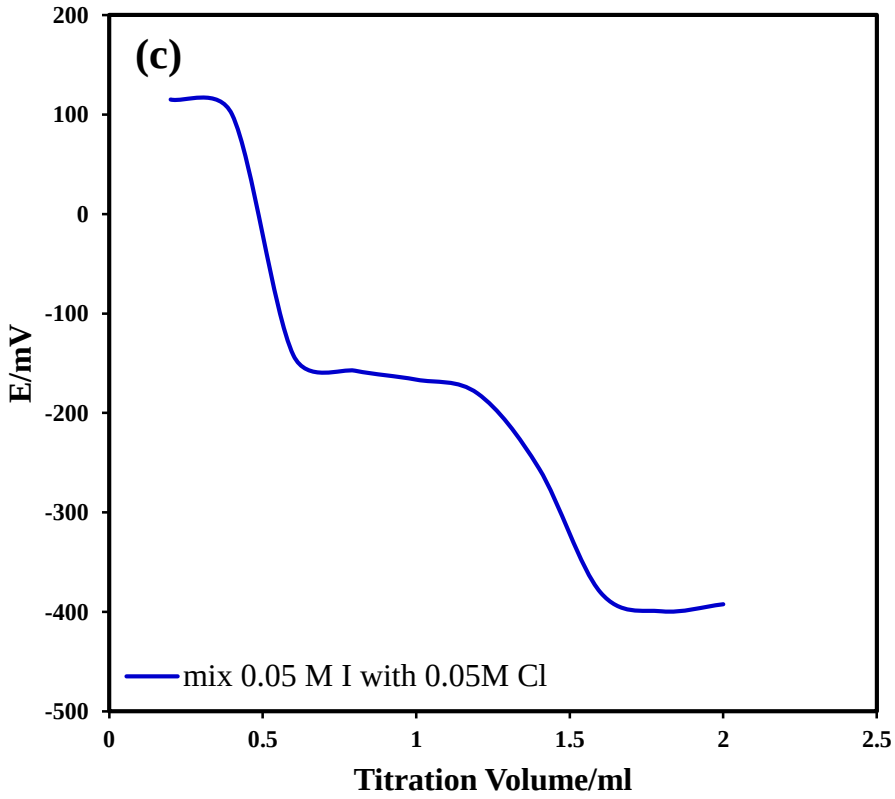
(c)
200
100
0
-100
-200
-300
-400
-500
E/mV
0
0.5
1
1.5
2
2.5
Titration Volume/ml
mix 0.05 M I with 0.05M Cl

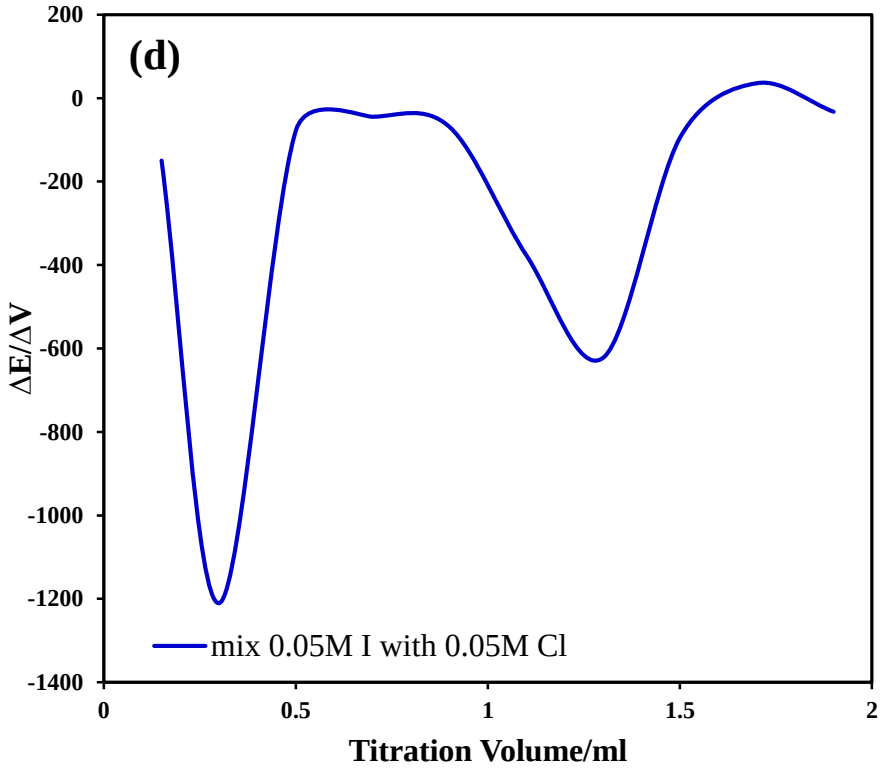

Figure 2.3: (a) Titration of 20 ml of a mixture 0.05 M bromide and 0.05 M iodide with 0.05 M $AgNO_3$, (b) The first differential curve of the mixture of 0.05 M bromide and 0.05 M iodide, (c) titration of 20 ml of mixture of 0.05 M iodide and 0.05 M chloride with 0.05 M $AgNO_3$, and (d) the first derivative curve of the mixture 0.05 M I^- and 0.05 M Cl^-.

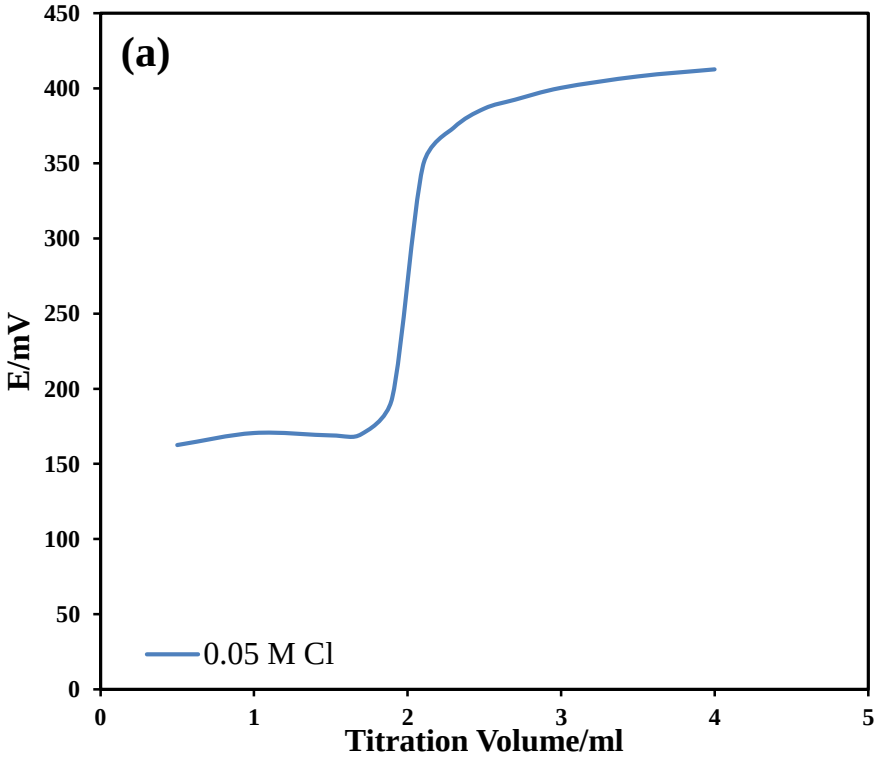

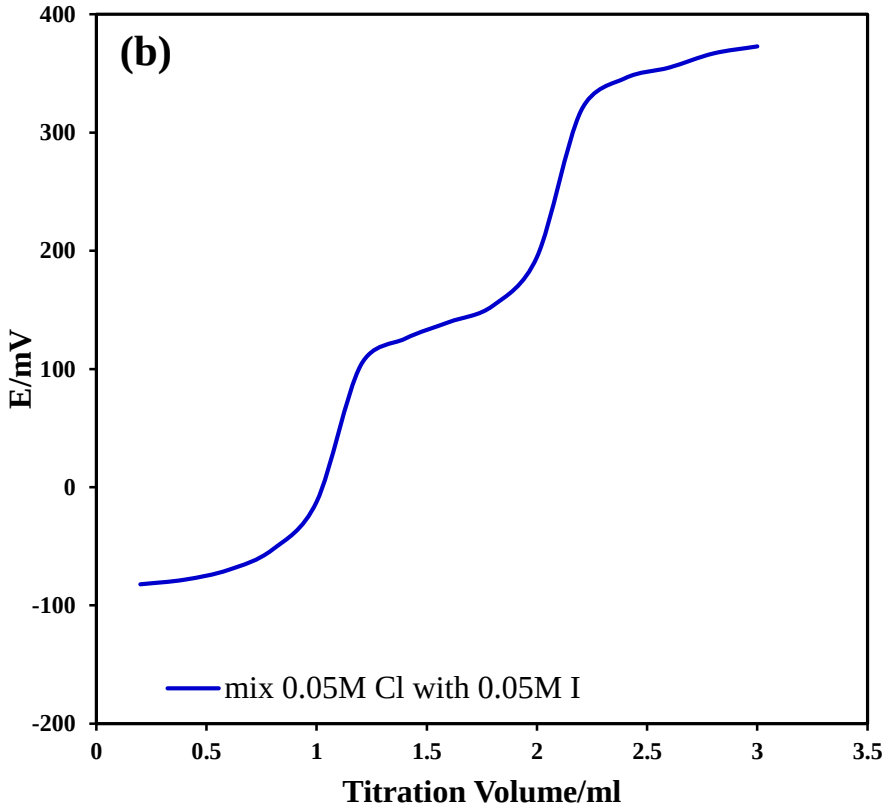

Figure 2.4: (a) Titration of 20 ml of 0.05 M chloride and 0.05 M I^- with 0.05 M $AgNO_3$, and (b) Titration of 20 ml of a mixture of 0.05M I^- and 0.05 M Cl^- with 0.05 M $AgNO_3$.

2.3.3. Complexometric Titrations

The response of the Ag/CNTs sensor electrode in the titration of 0.05 M calcium ion and 0.05M Magnesium ion with 0.05 M EDTA were conducting by measuring the cell potential (EMF) at 25°C under steering. The ionic strength was maintained by using a buffer solution of pH 10 and pH 9 for Ca^{+2} and Mg^{+2} respectively. The potentiometric curve of magnesium and calcium ions are shown in Fig. 2.4 and Fig. 2.5 respectively. Each plot shows an S-shaped curve and the first differential curves. In addition, the titration curve of a mixture of Mg^{+2} and Ca^{+2} ions at pH 10 is shown in Fig. 2.6.

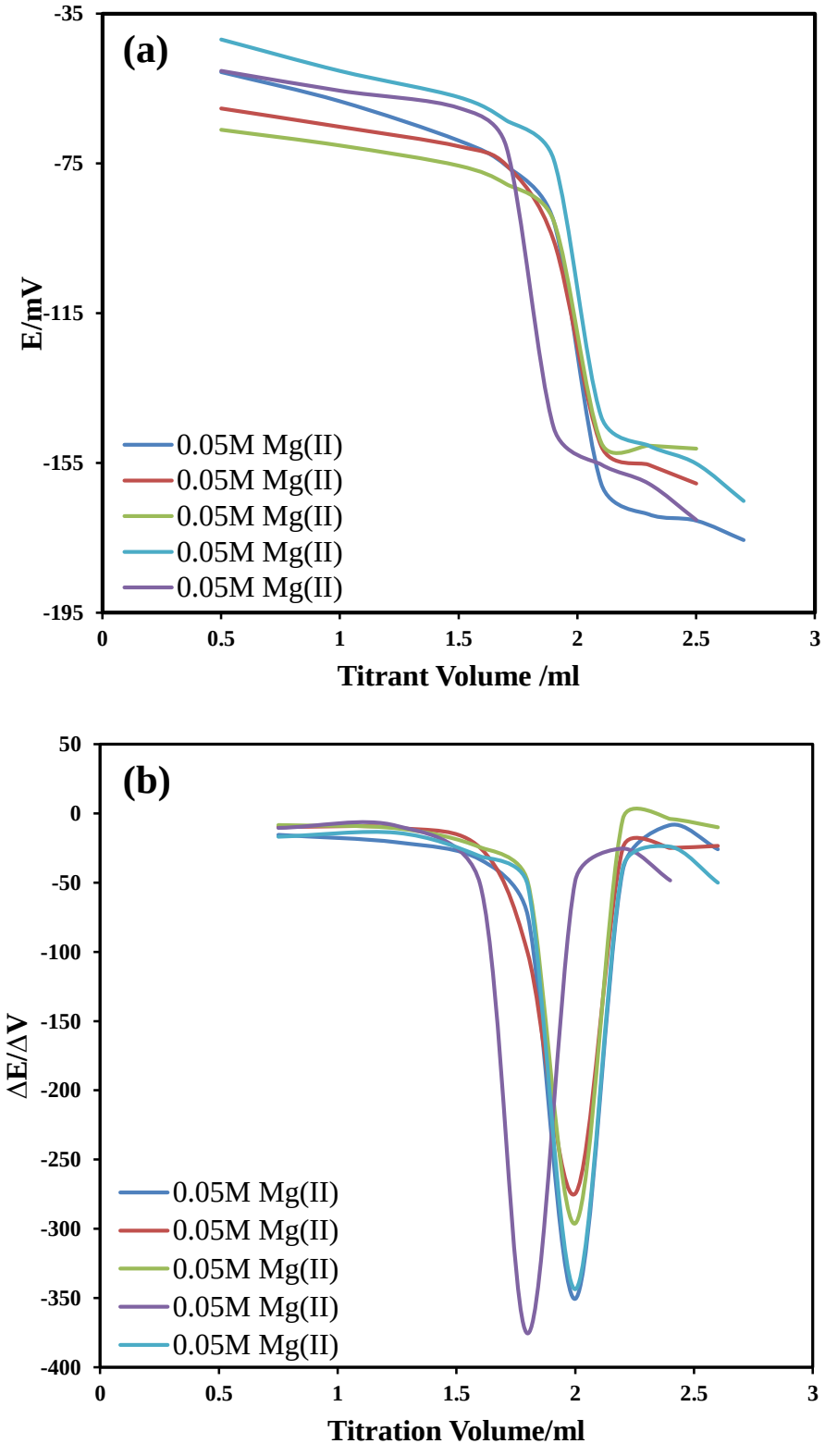

Figure 2.5: (a) Titration of 20 ml of 0.05 M Mg^{+2} with 0.05 M EDTA and (b) the first differential curve of 0.05 M Mg^{+2}.

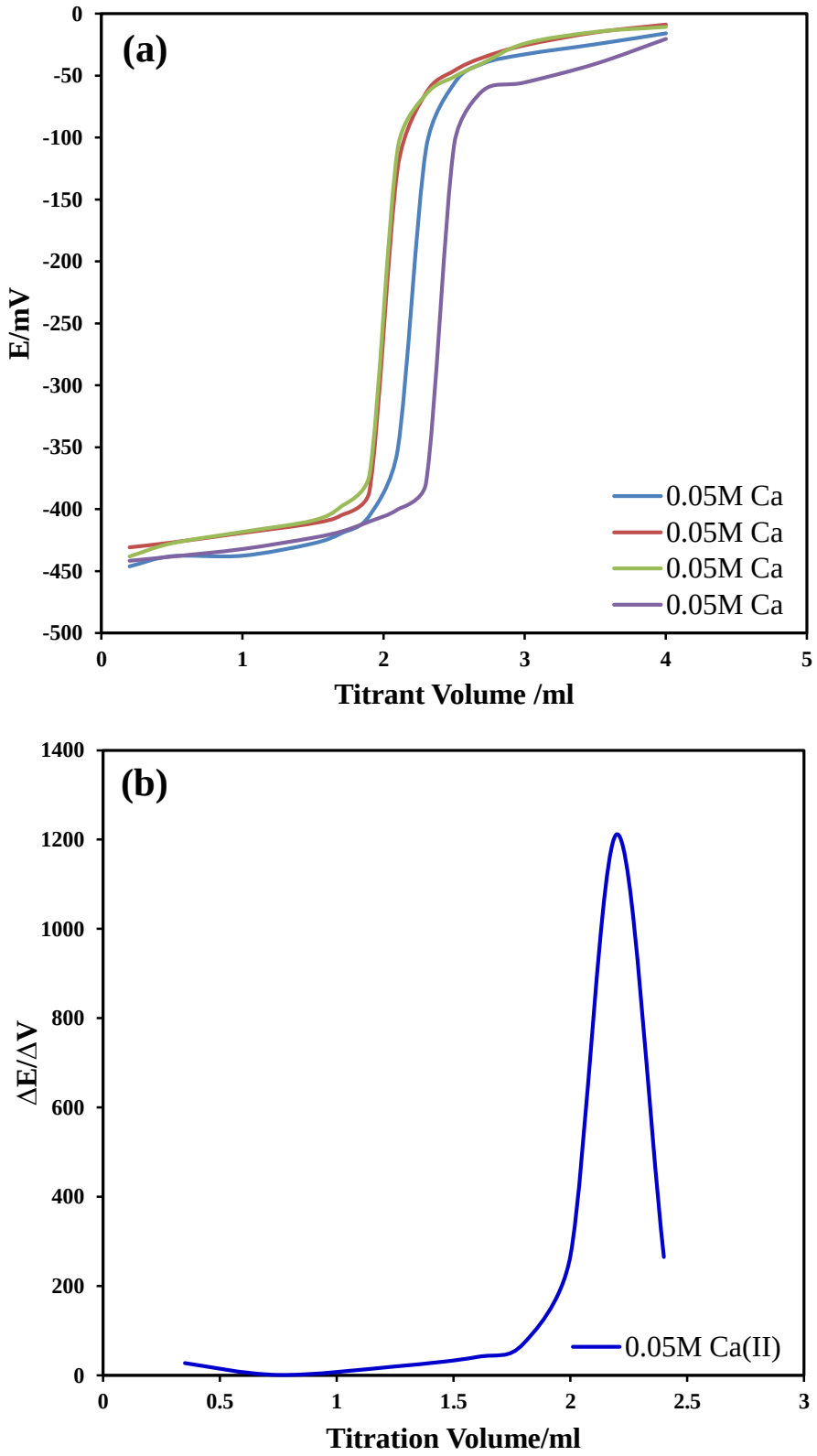

Figure 2.6: (a) Titration of 20 ml of 0.05 M Ca^{+2} with 0.05 M EDTA and (b) the first differential curve of 0.05 M Ca^{+2}.

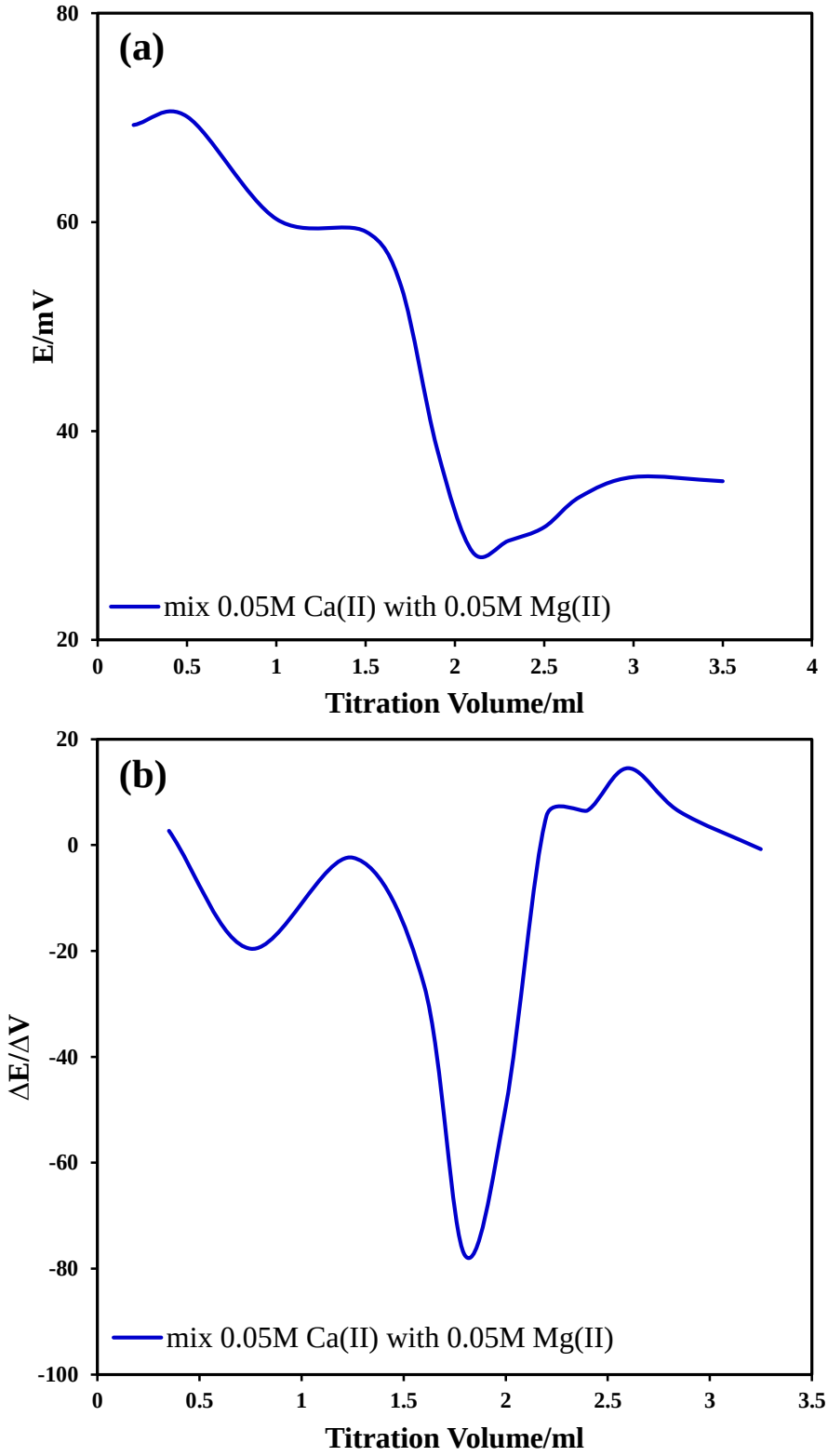

Figure 2.7: (a) Titration of 20 ml of mixture of 0.05 M Ca^{+2} and 0.05 M Mg^{+2} with 0.05 M EDTA and (b) the first differential curve of mixture.

2.3.4. Acid - Base Titrations

The potentiometric response of Ag/CNTs indicator electrode during the titration of 0.05M HCl with 0.05 M NaOH. The plot shows an S-shaped curve and the first differential curve is shown in Fig. 2.9. The end point can be easily located from these two curves.

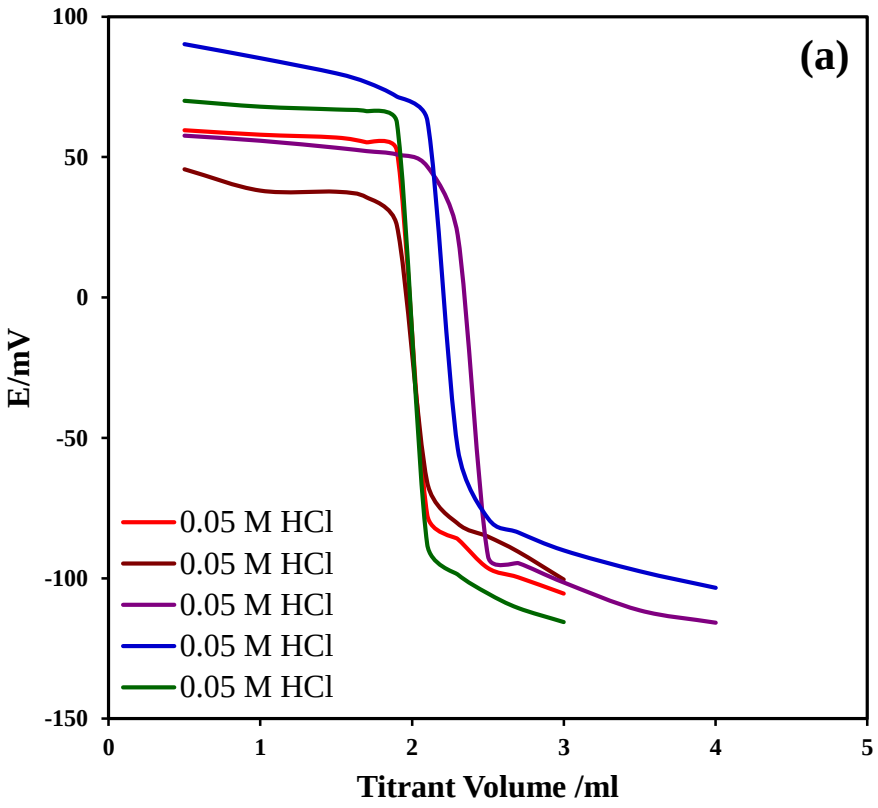

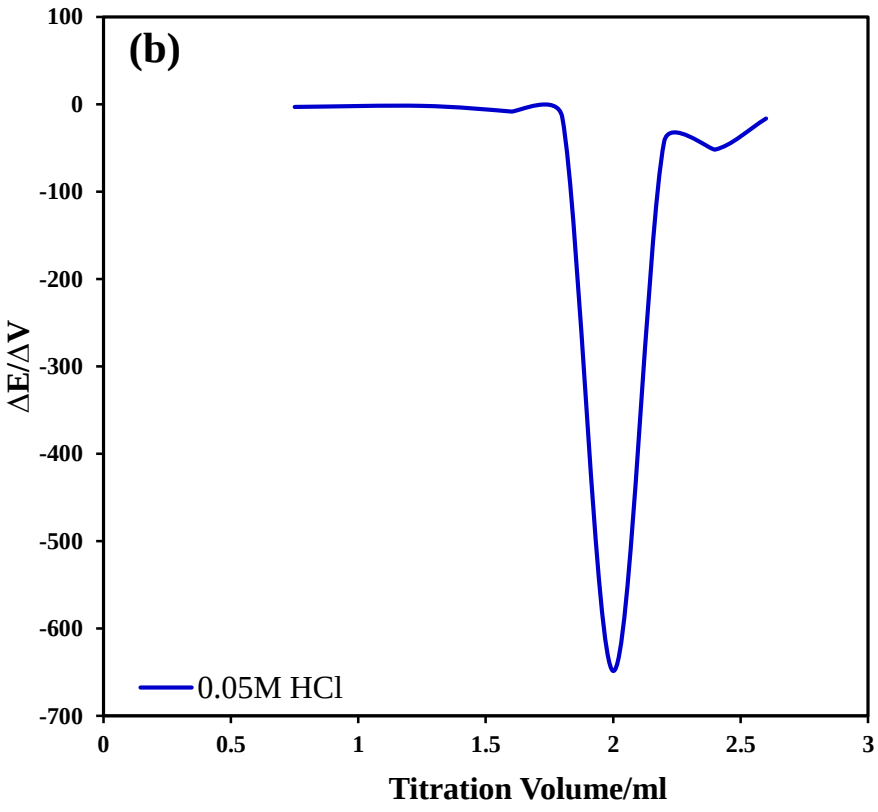

Figure 2.8: (a)Titration of 20 ml of 0.05 M HCl with 0.05 M NaOH and (b) the first differential curve of reaction.

2.3.5. Oxidation - Reduction Titrations

The response of Ag/CNTs indicator electrode in the titration of 0.05 M ferrous ion with 0.05 M cerium ion. The ionic strength was maintained by using 0.1 M H_2SO_4 as a strong acid. The record result was shown in Fig. 2.10. The plot showed S-shaped and differential curves were observed sharp end points of ferrous ions.

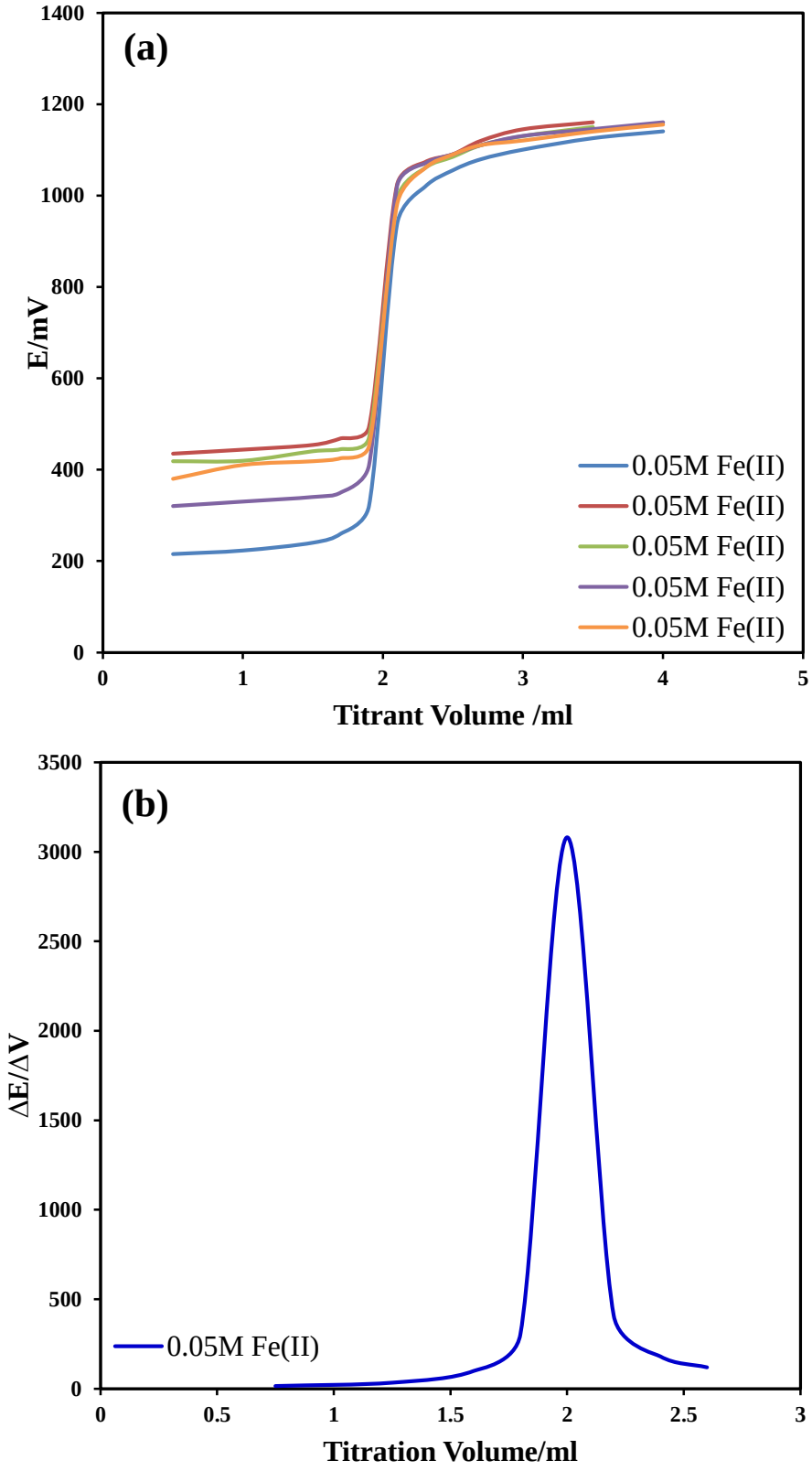

Figure 2.9: (a) Titrate of 20 ml of 0.05 M Ce^{+4} with 0.05 M Fe^{+2} and (b) first derivative curves of 0.05 M Fe^{+2}.

2.4. REFERENCES

[1] Ajayan, P.M., Chemical Reviews, 99, 1999, 1787-1800.

[2] Odom, T.W., Huang, J.L., Kim, P., Lieber, C.M. Nature, 391, 1998, 62-64.

[3] Jang, J.W., Lee, D.K., Lee, C.E., Lee, T.J., Lee, C.J. and Noh, S.J., Elsevier, Solid State Communications, 122, 2002, 619-622.

[4] Nugent, J.M., Santhanam, K.S.V., Rubio, A., Nano Letters, 1, 2009, 87-91.

[5] Merkoçi, A., Pumera, M., Llopis, X., Pérez, B., Del Valle, M., Carbon Nanotubes. TrAC Trends in Analytical Chemistry, 24, 2005, 826-838.

[6] Ebbesen, T.W. and Ajayan, P.M. Nature, 358, 6383, 1992, 220-222.

[7] Guo, T., Nikolaev, P., Thess, A., Chemical Physics Letters, 243, 1995, 49-54.

[8] G.D. Short, E. Bishop, Analyst, 87, 1962, 724.

[9] G.D. Short, E. Bishop, Analyst, 87, 1962, 415.

[10] E. Bishop, G.D. Short, Analyst, 89, 1964, 587

[11] E. Bishop, R.B. Dhaneshwer, Analyst, 87, 1962, 845.

[12] E. Bishop, R.B. Dhaneshwer, Anal. Chem., 36, 1964, 726.

[13] E. Bishop, Analyst, 83, 1958, 212.

[14] E. Bishop, Analyst, 85, 1960, 422.

[15] R.G. Monk, K.C. Steed, Anal. Chim. Acta, 26, 1962, 305.

CHAPTER 3

Electrochemical Behaviour of Graphene Modified Carbon Paste Electrode and Promazine Detection by Square Wave Voltammetry

3.1. Introduction

Graphene is an intrinsic two-dimensional sheet in a hexagonal configuration with carbon atoms bonded by sp^2 carbon hybridization. Graphene has attracted extensive attention due to its unique electronic structure, two-dimensional nature, flexibility, and chemical stability. It is considered to be of good electronic conductivity and high surface area [1-3]. Graphene was used in some areas, such as fuel cells [4-5] and modification with electro–catalytic nanoparticles [6], electrochemical sensor of nanotechnology [7] and used as the anode in batteries of lithium [8]. Graphene is used in electrochemistry-related applications because of its high signal electrical of conductivity, high surface area, low cost of production and heterogeneous electron transfer rate [9-13]. The graphene can be used in sensing of various targets, such as biosensing of glucose [14], assaying of hydrogen peroxide [15], and determination of bimolecular, organic molecules and pharmaceutical compounds. This is because of its individual properties, such as good conductivity and good carrier charge mobility [18]. Graphene is a common material used in electrochemistry-based applications due also to having properties of the individual planar structure [16-17]. There are various classes of the carbon substrates such as graphite,

carbon nanotube, and glassy carbon has been used to make modified carbon paste electrode via different methods [18-22]. Graphite is commonly used in electrochemistry because of its less background current and wide potential [23]. Graphite paste electrode used for determination of redox reaction by utilizing the electrochemical technique which has high sensitivity with low cost [24]. Graphite is used as a paste electrode in because of its low current compared to solid graphite electrodes. Graphite paste electrode is used as a working electrode in electrochemical techniques, such as cyclic voltammetry measurements, characterization, and identification of a pharmaceutical compound. Examples are its use in the determination of phenolic compounds [25] and glutathione [26]. Graphite paste has been popular due to the low background and easy to modify and miniaturization. [27]. The monitoring of promazine is significant for quality assurance in the pharmaceutical industry. Therefore, the detection of this drug is important in biological samples such as urine and drug tablets. In addition, there are more analytical procedures have been reported for the promazine analysis involving electrophoresis [28], spectrophotometry [29], and electrochemistry [30]. The CVs shows the two oxidation peaks of promazine first one is reversible and the second one is irreversible [31]. In the present work, the graphene prepared from graphite was used to fabricate carbon paste modified with graphene (GCPE). The electrochemical behavior of the fabricated electrode was evaluated using CV and SWV. The electrode was investigated for the determination of promazine. The structure of promazine was shown in scheme 3.1.

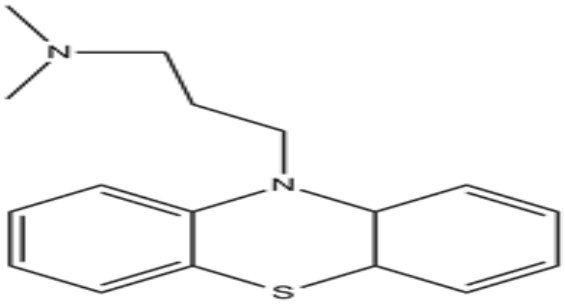

Scheme 3.1: Show the structure of promazine drug.

3.2. Experimental

3.2.1. Chemical and Material

Promazine (PZ) drug powder and graphite powder were been taken from Aldrich-Sigma Company. In addition, 30% H_2O_2 was used and production from sigma company. Sodium nitrate and potassium permanganate were used and produced by Sigma Company. Paraffin oil with low density and sulfuric acid were used.

3.2.2. Apparatus

Square wave voltammetry (SWV) technique and Cyclic voltammetry (CV) technique were utilized in electrochemical measuring station (CHI1140A, CH instrument Inc, Austin, TX, US). Electrochemical apparatus included electrochemical analyzer device, Ag/AgCl as a reference electrode (in 1 M KCl CHI11, CH Instruments INC), platinum wire as an auxiliary electrode (CHI115, CH Instilments Inc.) and a paste composite electrode as a working electrode. The electrodes immersed in a cell glass by using a stand of Teflon cover. The electrochemical cell contains three electrodes; a working electrode, a reference electrode, and an auxiliary electrode in order to measure the current and potential. Raman

spectroscopy (Lab Ram HP Evolution), and equipped with He-Ne have 17 mV with laser 633 nm of wavelength. FT-IR spectrophotometer was used.

3.2.3. Reagents and Solutions

A solution of $1*10^{-4}$ M promazine (PZ) was prepared by dissolving a certain weight of PZ in a pH 4.0 of phosphate buffer to make an analyte; the solution under sonication for 10 min. to complete the desolvation. The buffer solution was prepared of 100 g of pH 4 phosphate powder by dissolved into 100 ml of distilled water in 100 ml volumetric flask. The standard solution was prepared and used to diluting solutions from its. Buffer phosphate of pH 4 was utilized as electrolyte and a solution of 0.02 M potassium ferrocyanide and 0.2 M of KCl as an electrolyte. All standard solutions were prepared by utilizing purified water.

3.2.4. Synthesis of Graphene Oxide

Graphene oxide (GO) was prepared by different modification Hummers method [32-33], by utilizing natural carbon powder as a basic material scheme 3.2. The procedure synthesis of GO is described as graphite powder (1 g) was added to 23 ml concentrated sulfuric acid (H_2SO_4) and 100 g of sodium nitrate ($NaNO_3$) into a 250 ml flask which was then kept at 5 C in ice under stirring for 30 min. Then, 3 g of ($KMnO_4$,) was added drop by drop into the solution. After heating solution from 35 to 40 °C, the solution was stirred again for 30 minutes. Then, 46 ml of distilled water was pour to the flask under steering for another 25 minutes. Eventually, 140 mL of purified water and 10 mL of 30% H_2O_2 were added.

Then centrifugation and filtration of solution (first by 5% HCl and then with water) and the resulting product were rinsed with purified water and dried at 65 °C [34].

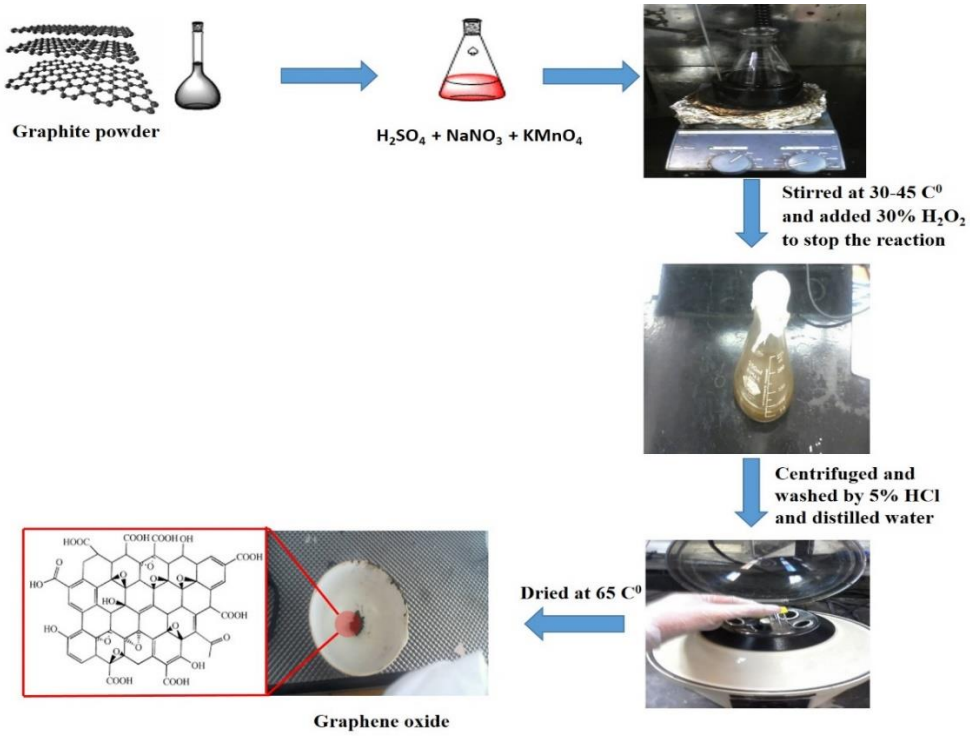

Scheme 3.2: Synthesis steps of graphene oxide by modification hummer method.

3.2.5. Preparation of Working Electrode

The carbon paste electrode (CPE) was constructed by blending 70 % of carbon powder and 30 % of low-density paraffin oil, the product paste was packed into the electrode cavity (0.1 mm diameter). The copper wire was used as an electrical contact within the past. Blending of 69 mg of graphite powder to 1mg graphene with 30 mg paraffin oil use to prepared graphene paste electrode (GCPE) as modified electrode, our preliminary results indicate that the best percentage (w/w) for mixing graphite with graphene was 65 % of graphite and 5 %of graphene with 30% (W/W) of paraffin oil. The soft paper was used to

smooth the surface of the electrode, then washed by distilled water all time of measurements.

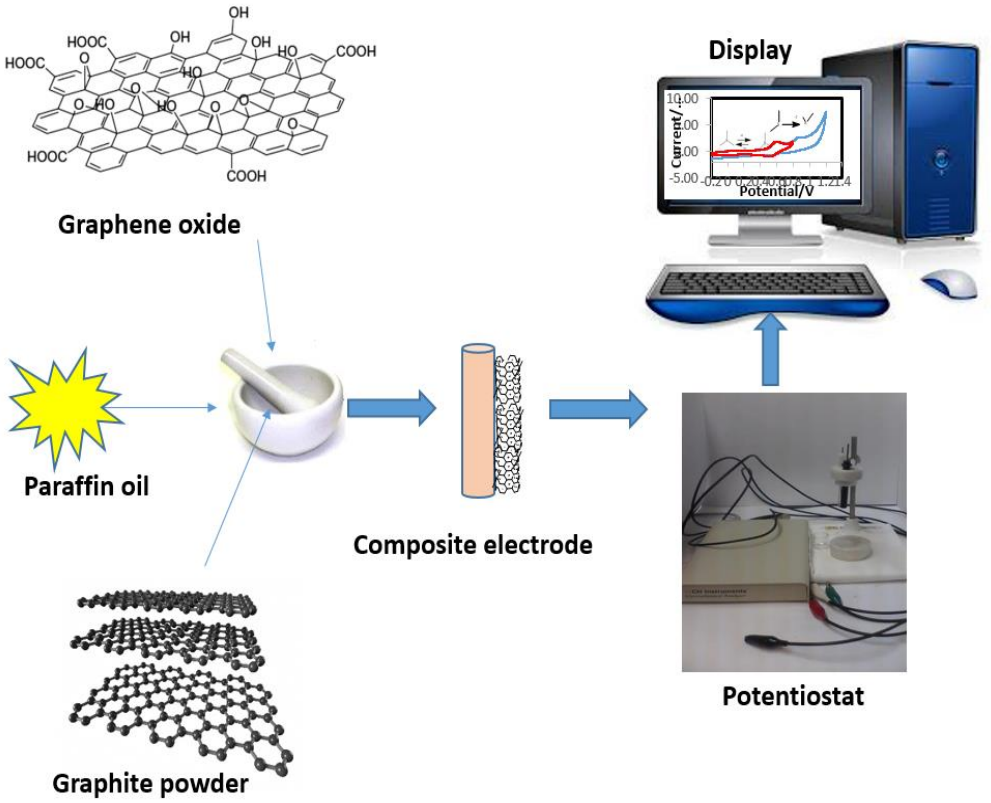

Scheme 3.3: Illustration of the preparation of the composite graphene electrode and used in the determination of promazine drug.

3.2.6. Procedure

Cyclic voltammetry (CV) measurements were obtained by treating the surface of the bare electrode and modified electrode at -0.7 V for 30 s in phosphate buffer (0.5 M, PH 4). This was followed by accumulation time at a suitable voltage for the target in the 0.5 M phosphate buffer pH 4 electrolyte. Then scanning the potential at 100 mV/s scan rate over the potential range from (-0.2 V – 1.2)V. Square wave voltammetry (SWV) measurements were achieved by pretreatment potential of the surface at -0.7 V for the 30 s, and then 60 s

of accumulation time at 0 V in 0.5 M pH 4 of phosphate buffer solution. This followed by utilizing the square wave stripping voltammetric waveform, with optimum conditions as increment 10 mV, frequency 50 Hz and amplitude 40 mV. A new composite electrode was utilized in all measurements by cut portion of paste from the hole of the working electrode, smoothed by soft paper, and washed by a small amount of deionized water.

3.3. Results and Discussions

3.3.1. Characterization of Graphene Oxide

The synthesis of graphene oxide (GO) depends on the oxidation process of graphite powder. GO is characterized by various techniques such as TEM, SEM, UV–Vis absorption, Raman spectroscopy, and FT-IR Fig. 1. TEM image (Fig.1a) shows the structure of GO with a transparent nanosheet with scale diameter 0.2 μm. SEM images show the monograph indicating few layers of GO (Fig. 1b), and (Fig. 1c). The GO chemical structure is consist of the benzene rings which contains π electrons. So, it displays UV–vis absorption peak at 230 nm, which is due to π- π^* transition of aromatic C=C bonds and the second peak was observed at 270 nm due to n- π^* transition of C=O bonds as shown in (Fig.1d). The FT-IR spectra (Fig. 2e) of the functional group of GO indicate the intense bands at 3450 and 1250 cm^{-1} which are attributed to the stretching of the O–H and band of C–O respectively. The band at 1650 cm^{-1} is associated with stretching of the C=O bond of carboxyl groups. Raman spectroscopy is important for analyzing crystalline structures of carbon materials instance GO. The characteristics of the Raman spectrum (Fig 2f) of graphene oxide observed two peaks; one that In-phase vibration (G band) of GO at 1567

nm and the disorder band (D-band) of GO at 1339nm. Isotherm shows adsorption hysteresis indicating the presence of mesopores (Fig. 1H). The nitrogen adsorption and desorption measurements were performed at 77 K. The Brunauer-Emmett-Teller (BET) surface area, pore volume and pore size of GO, were 805.8022 m^2/g, 0.985760 cm^3/g, and 48.9331 Å respectively.

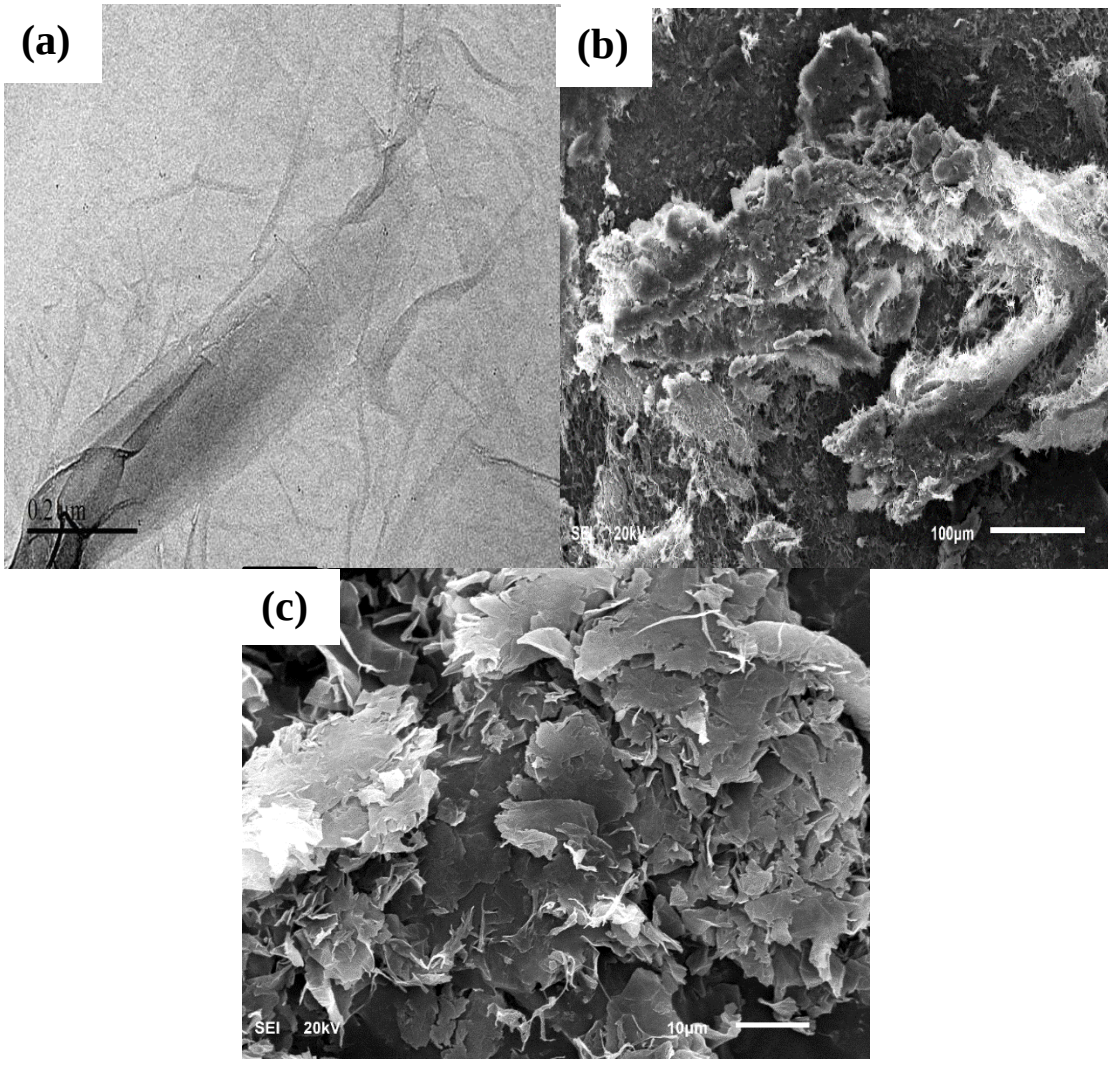

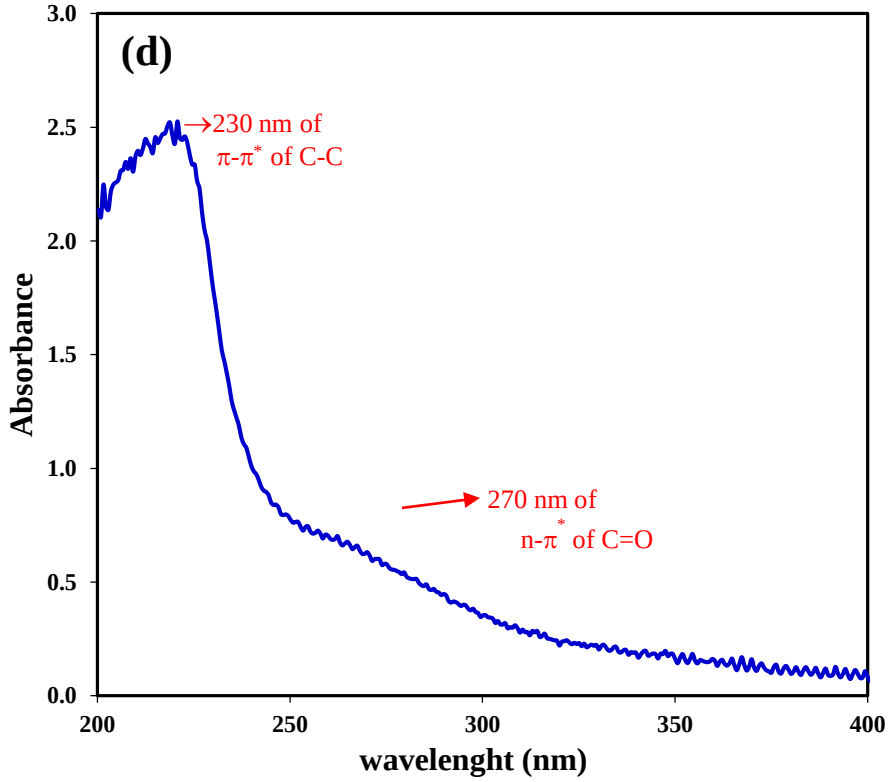
(d)
→230 nm of
π-π* of C-C
270 nm of
n-π* of C=O
Absorbance
wavelenght (nm)
3.0
2.5
2.0
1.5
1.0
0.5
0.0
200
250
300
350
400

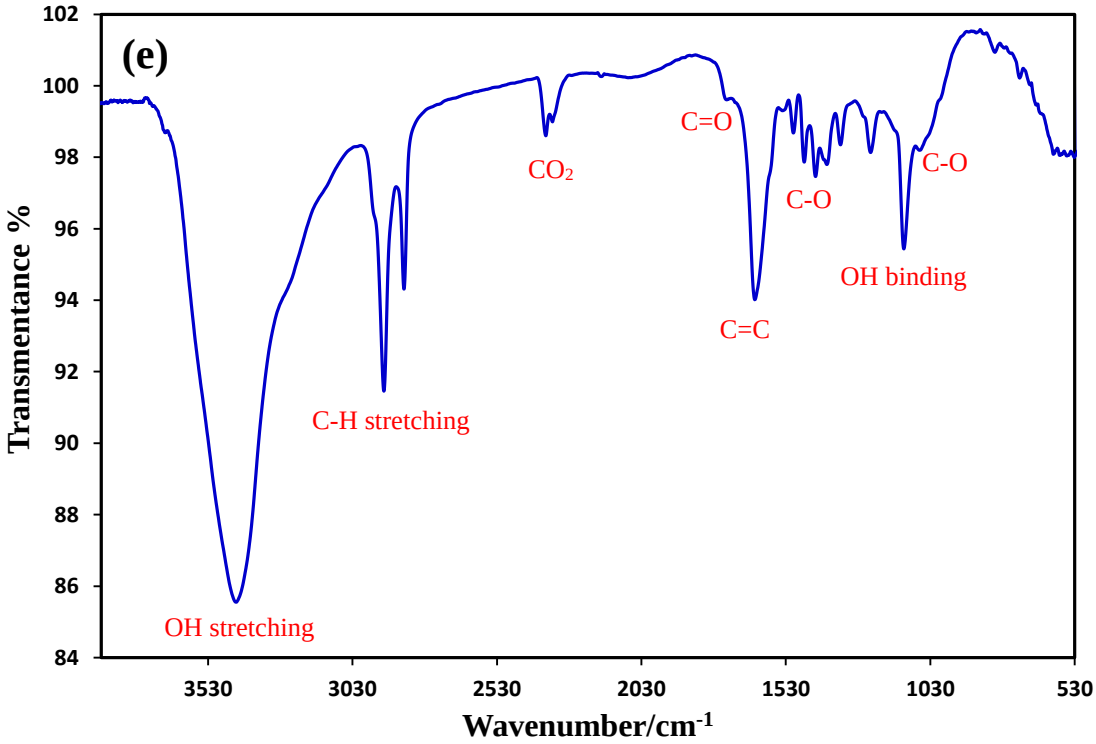
(e)
OH stretching
C-H stretching
CO2
C=O
C=C
C-O
C-O
OH binding
Transmentance %
Wavenumber/cm-1
102
100
98
96
94
92
90
88
86
84
3530
3030
2530
2030
1530
1030
530

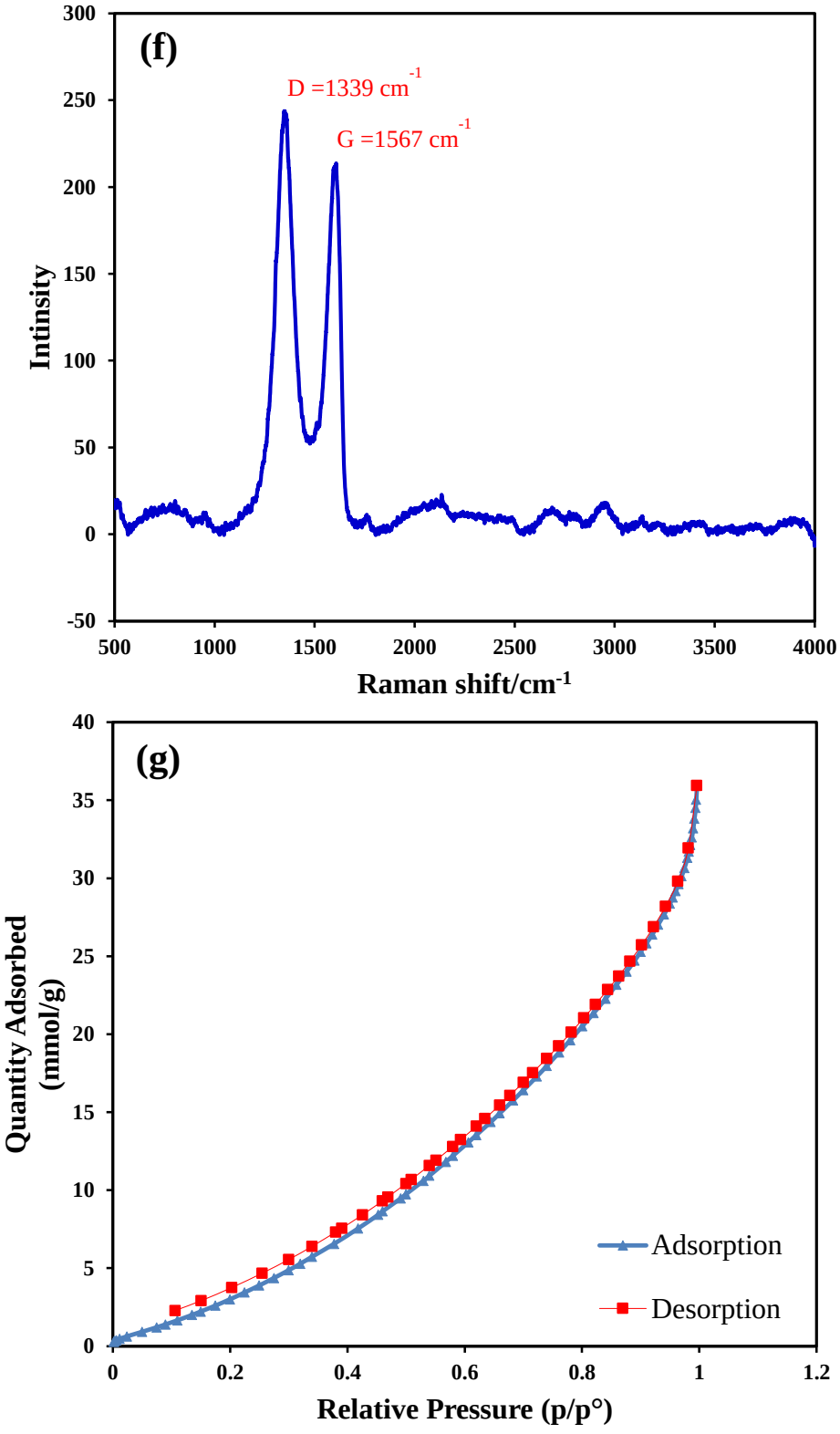

Figure 3.1: (a) TEM image (b) SEM image of GO at low magnification at 100 µM (c) SEM image of GO at high magnification at 10 µM (d) UV-Visible spectrum, (e) FT-IR spectrum, (f) Raman spectrum of GO, and (g) Typical N adsorption- desorption isotherm of GO.

3.3.2. Characterization of GCPE and CPE

The SEM images for the CPE electrode showed microstructures grain with a crystal structure EDX analysis illustrates the composition elements of CPE. Data analysis show that CPE is mainly composed of carbon was shown in Fig. 3.2 (a, b). The structure of the CPE electrode showed the graphite particles are covered with a small amount of paraffin oil. To investigate the morphology of the surface of modified electrode made of this mixture, the SEM image is depicted in Fig. 3.2(a, b) which indicate homogeneous surface.

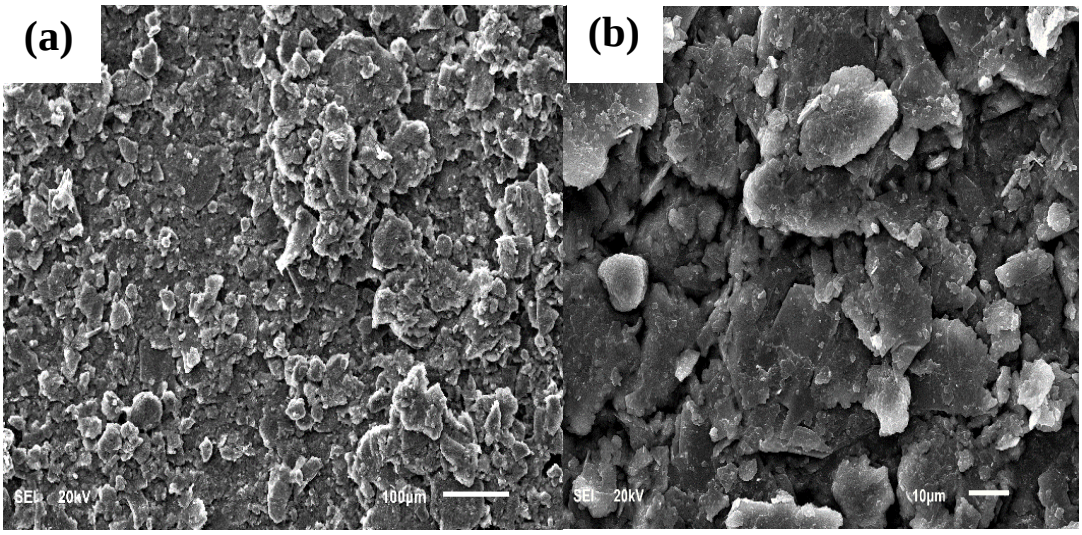

Figure 3.2: SEM images of carbon paste electrode, (a) low magnification at 100 µm and (b) high magnification at 10 µm.

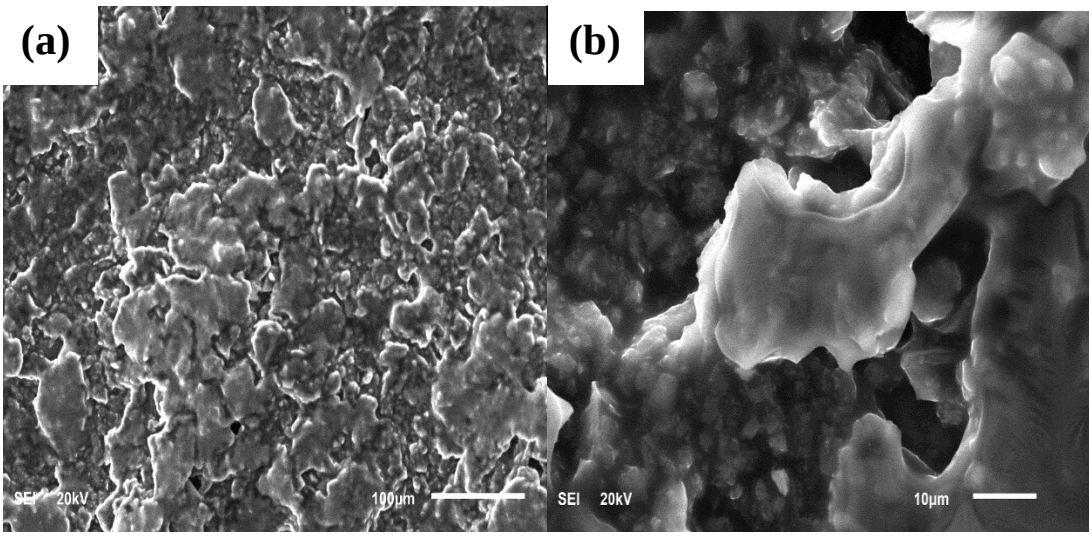

Figure 3.3: SEM images of GCPE, (a) low magnification at 100 µm and (b) high magnification at 10 µm.

3.3.3. Comparison of Different Percentage (w/w) of GCPE Electrodes

CV technique was utilized to perform the influence of graphene amount in the mixture. As shown in Fig. 3, the best amount of graphene was 5% with (w/w) 65% graphite and 30% paraffin oil. This mixture showed the best enhancement of signals compared to another percent. It also showed very good background shown in orange line (c) compared to other. To obtain the surface morphology of electrode, the SEM image is depicted in Fig. 3.4 which indicate homogeneous surface.

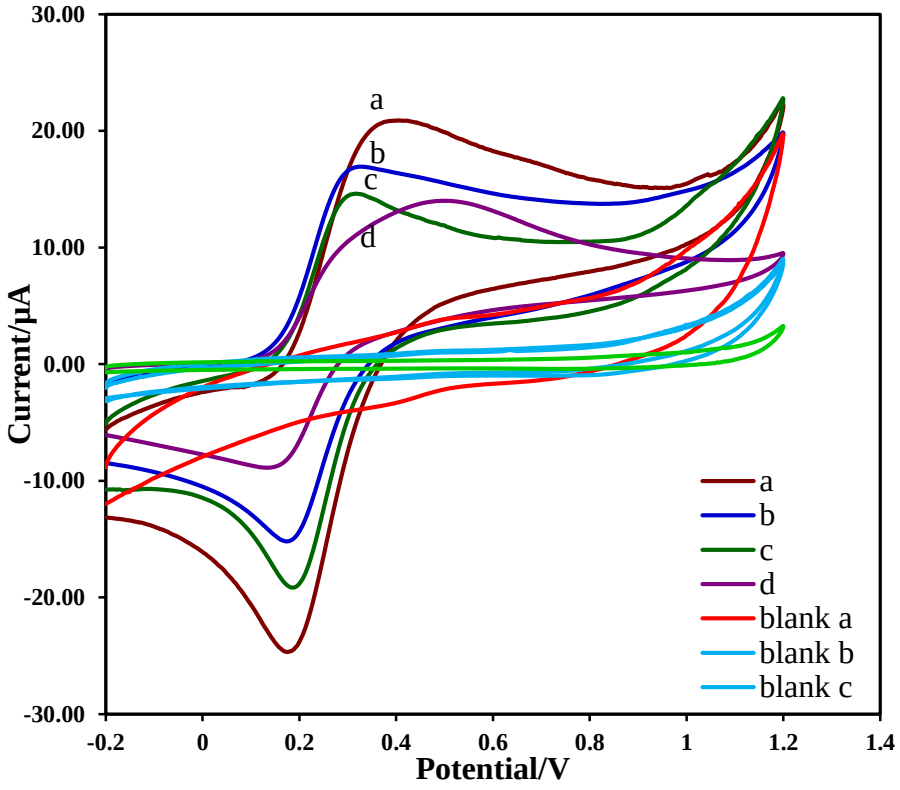

Figure 3.4: CVs for 0.02 M $K_4Fe(CN)_6$ of different percentages (w/w) of mixing graphite: graphene. Phosphate buffer of pH 4 as electrolyte solution, Scan rate100 mV/s (a) 60%graphite with 10% graphene and its blank a, (b) 50% graphite with 20% graphene and its blank b, (c) 65% graphite with 5% graphene and its blank c, and (d) 69% graphite with 1% graphene and its blank d.

3.3.4. Comparison of GCPE and CPE

Cyclic voltammetry is a good technique used for comparison between the two different kinds of electrodes, GCPE, and CPE. Fig. 5 shows the CVs for 0.02 M $[Fe_4(CN)_6]^{3-/4-}$ record at the GCPE and CPE. The two redox peaks were appeared at CPE due to the less conductivity of carbon in CPE compares with GCPE which contained a graphene of high conductivity. The signal is enhanced for anodic and cathodic reactions because of the in electrons transfer. The background of GCPE is narrower than the background of CPE. It is clear that there is a good enhancement of redox peak potentials observed in 0.2 V and 0.4

V on GCPE electrode. By studying the electrochemical behavior of $K_4Fe(CN)_6$ with 0.5 ml of 0.2 M KCl at scan rate 100 mV/s the intensity of the signal at GCPE is more enhancement than the signal at CPE electrode as shown in Fig. 3.5. The results show the current intensity derived from the cyclic voltammograms at the surface of the two various electrodes with a scan rate of 100 mV/s... The presence of graphene causes the good conductivity results of the electrode. The graphene-modified electrode exhibited an important oxidation peak with the intensity peak current of around 17 µA. As a result, low redox intensity peak was appeared at bare CPE electrode under conditions. This indicated that the presence of the graphene nanosheet promoted charge transfer reactions, the good enchantment of conductive properties.

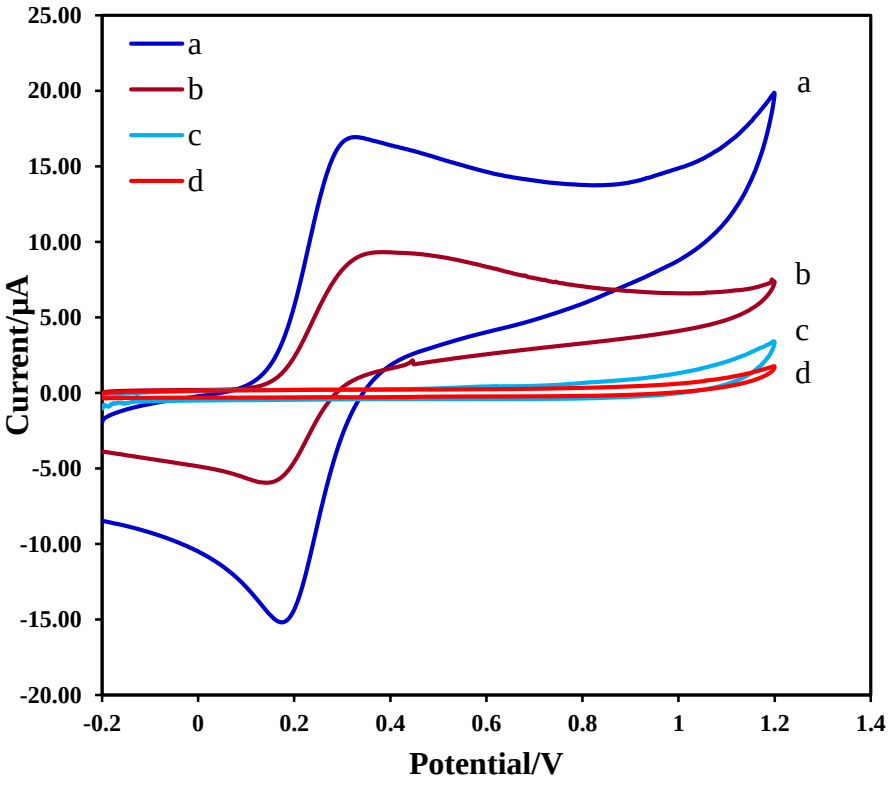

Figure 3.5: CVs for 0.02 M $[Fe_4(CN)_6]^{3-/4-}$ using (a) GCPE, (b) CPE, (c) blank of GCPE, and (d) blank of CPE A phosphate buffer of pH 4.0 as an electrolyte solution, Scan rate 100 mV/s.

3.3.5. Pretreatment Potential at GCPE

The modified graphene with carbon paste electrode (GCPE) was investigated through studying the electrochemical behavior of $[Fe(CN)_6]^{-4,-3}$ oxidation and reduction couple. A potential pretreatment has effected on the peak separation as. The electrochemical intensity of $[Fe(CN)_6]^{-4,-3}$ at the +1.3 V pretreated (GCPEs). It was found the longer pretreatment time, the larger the response of 0.02 M $K_4Fe(CN)_6$ in 0.5 ml of 0.2 M KCl solution. Fig.3.6 shows the pretreatment potential at1 min at different potentials from range (-0.7– 1.3) V at $K_4Fe(CN)_6$ and observed the potential -0.7 V is a good optimum pretreatment potential to select due to the higher oxidation signal peak and narrow background.

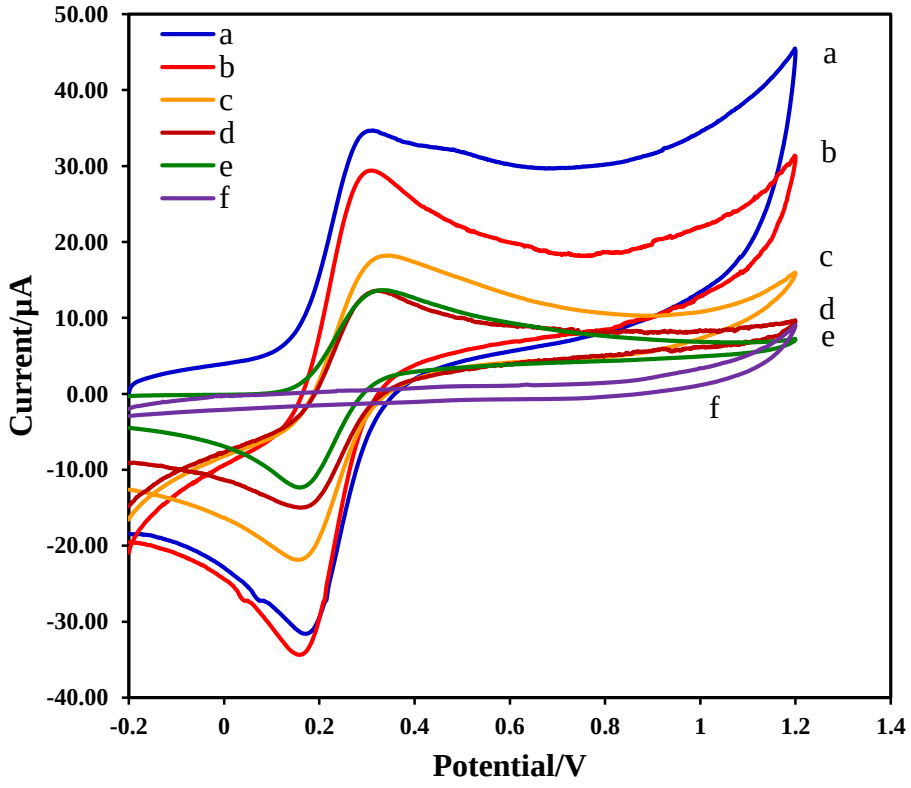

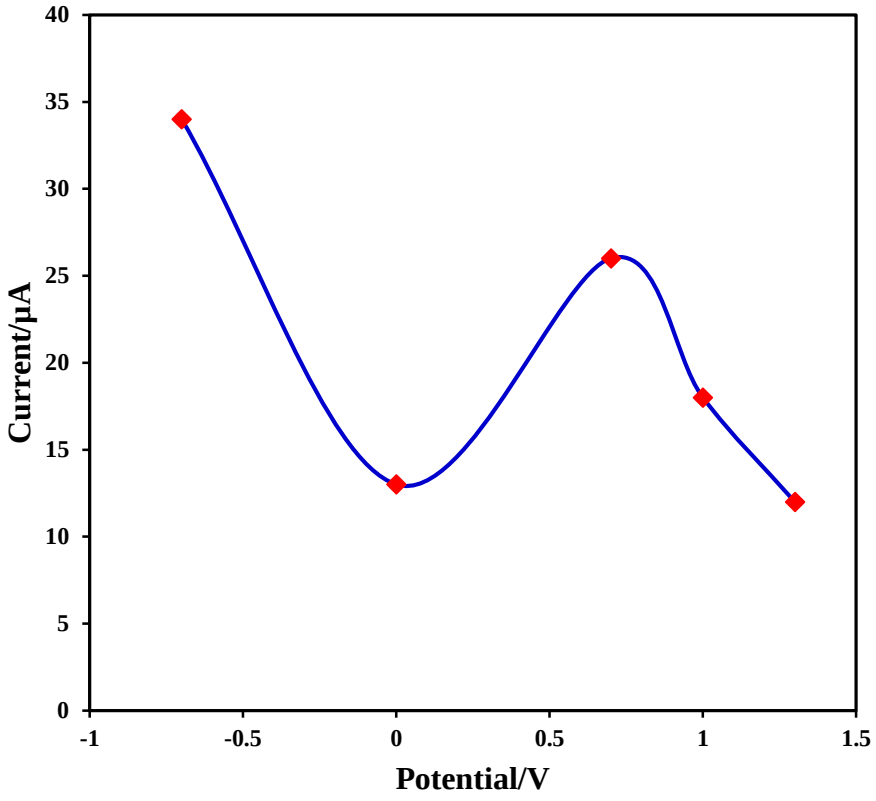

Figure 3.6: Cyclic voltammetry of 0.02 M $K_4Fe(CN)_6$ using GCPE at pretreatment potential at 1 min and different potentials : (a) -0.7 V , (b) +0.7 V , (c) +1 V , (d) +1.3 V , (e) 0 V, and (f) blank of buffer . Phosphate buffer of pH 4 as electrolyte solution, scan rate 100 mV/s.

3.3.6. Pretreatment Time at GCPE

The best optimum of pretreatment time at potential -0.7 V and the different time from range (0 – 30) s. A solution of $K_4Fe(CN)$ was used as an electrolyte and investigate better time at 30 sec. this value of Pretreatment time was selected due to the higher oxidation signal peak and narrow background as shown in Fig. 3.7.

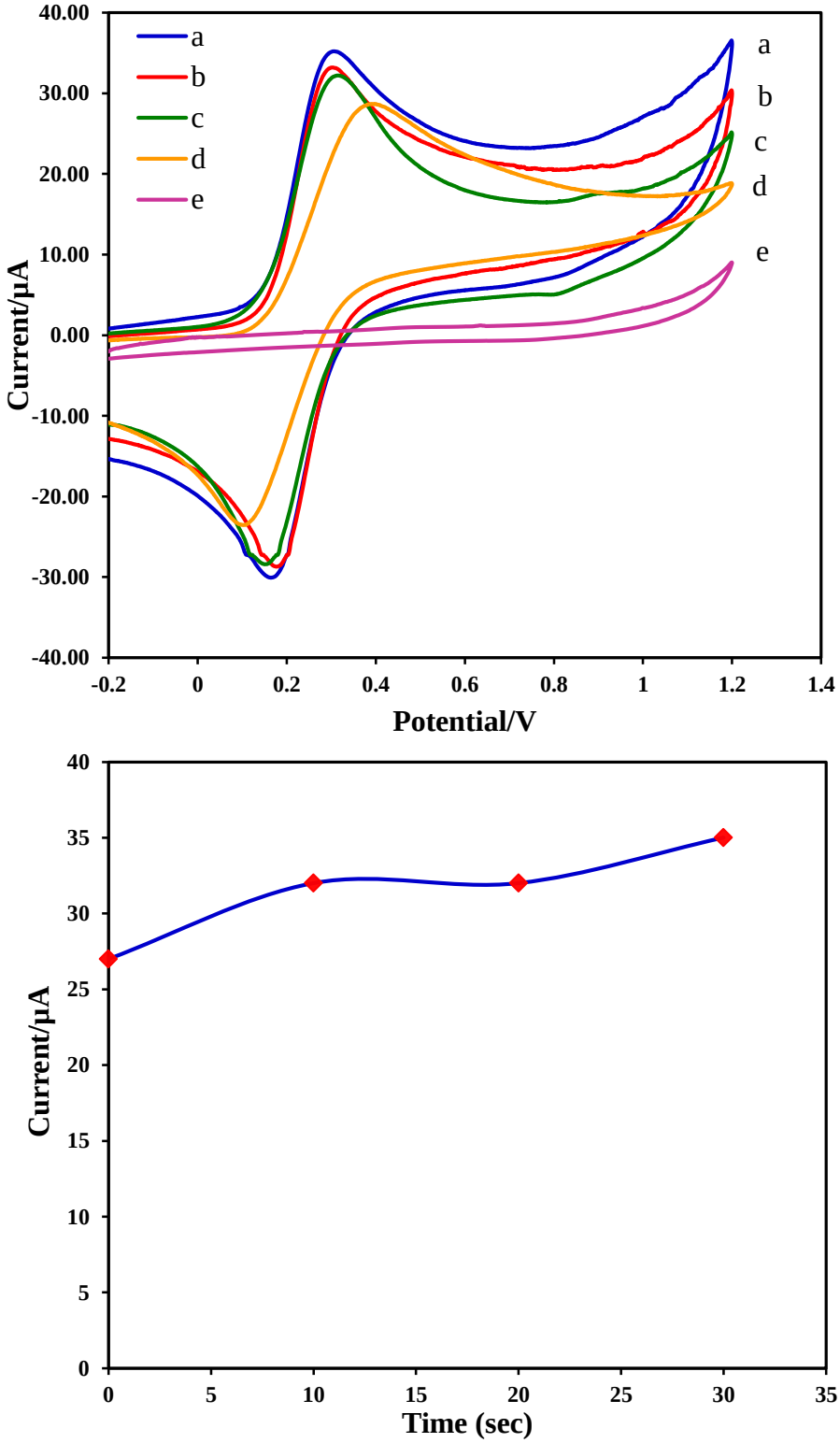

Figure 3.7: Cyclic voltammetry of 0.02 M $K_4Fe(CN)_6$ used graphene carbon paste electrode (GCPE) at pretreatment time at potential -0.7 V and different time :(a) 30 s , (b) 20 s , (c) 10 s , (d) 0 s, and (f) blank . A phosphate buffer of pH 4 as an electrolyte solution, and 100 mV/s of scan rate.

3.3.7. Electrochemical Behavior of Promazine

In Fig. 3.8. Shows the CVs of 0.1 mM promazine at GCPE and CPE electrodes. At GCPE shows, a voltammogram of promazine with two electrochemical oxidation peaks and a high signal of reduction peak compare to CPE electrode due to the high electronegativity and high surface area of graphene. For the CPE, the two redox peaks were observed; the reduction observed at 0.57V and oxidation potential peaks observed at 0.6 V and 0.9 V. The difference in potential of promazine drug ΔE_{PZ} was 30 mV and the peak current ratio (Ip_C/Ip_A) was recorded 0.5, which perhaps attributed to less conductivity and less surface area of the bare CPE. While the difference potential (ΔE) of promazine on GCPE was recorded 60 mV, and peak current intensity ratio (Ipc/ Ipa) nearly unity (Fig. 3.8a). The presence of graphene was achieved a high electrocatalytic activity of GCPE and improved the electroconductivity, surface area of the electrode, and transfer rate of the electron.

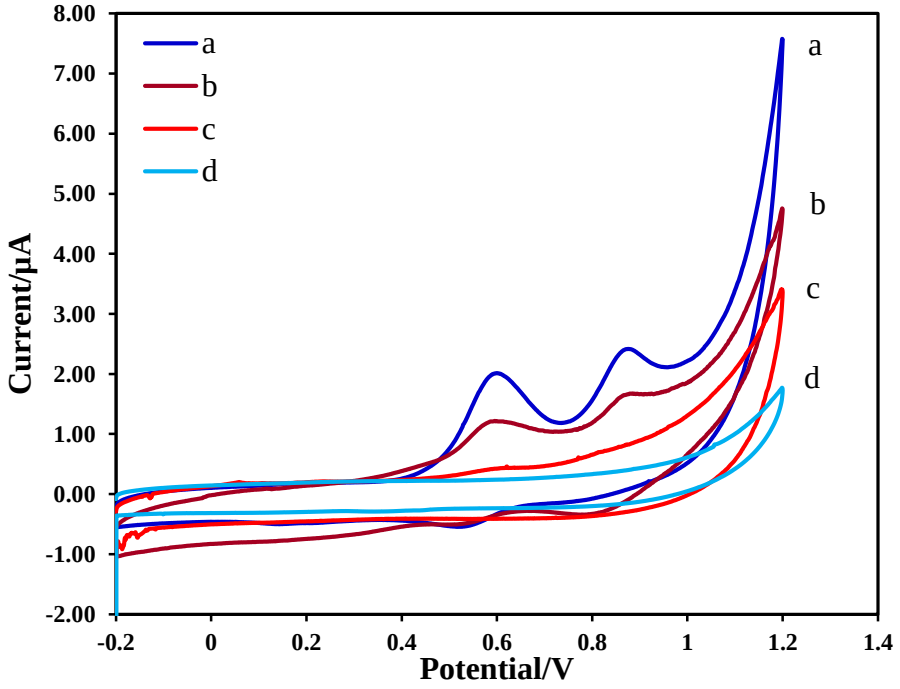

Figure 3.8: CVs for 0.1 mM promazine using (a) GCPE electrode, (b) CPE electrode, (c) blank of GCPE, and (d) blank of CPE. A phosphate buffer of pH 4.0 as electrolyte solution and scan rate 100 mV/s.

The cyclic voltammograms (CVs) of 1.0 mM promazine at GCPE were shown in Fig. 3.9. A promazine voltammogram curve is a wide range of potential with two various anodic current peaks shows in Fig. 3.9a. In the first oxidation, the anodic current peak occurred duo to the oxidation of nitrogen atom and was recorded at 0.63 V, which is reversible as a short range in Fig.3.9b. The second oxidation anodic peak occurs at the sulfur atom was observed at 0.91 V, which is irreversible (Scheme 3.4.) [27].

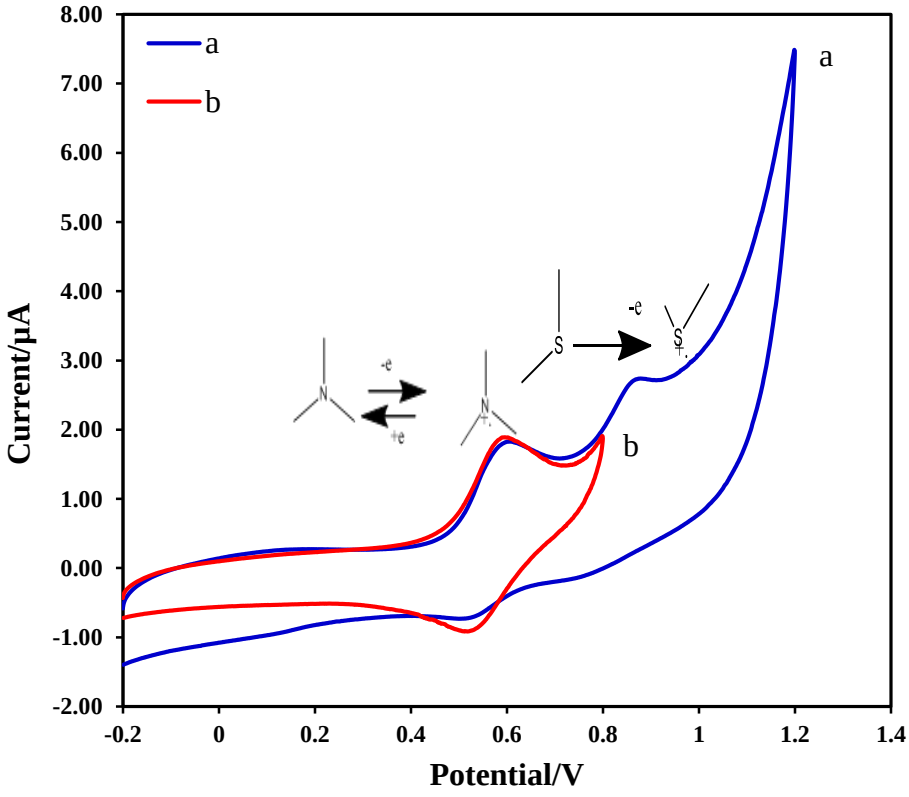

Figure 3.9: CVs of 0.1 mM promazine at the GCPE, (a) wide range, and (b) short-range Scan rate 100 mV/s and phosphate buffer of pH 4.0 as an electrolyte solution.

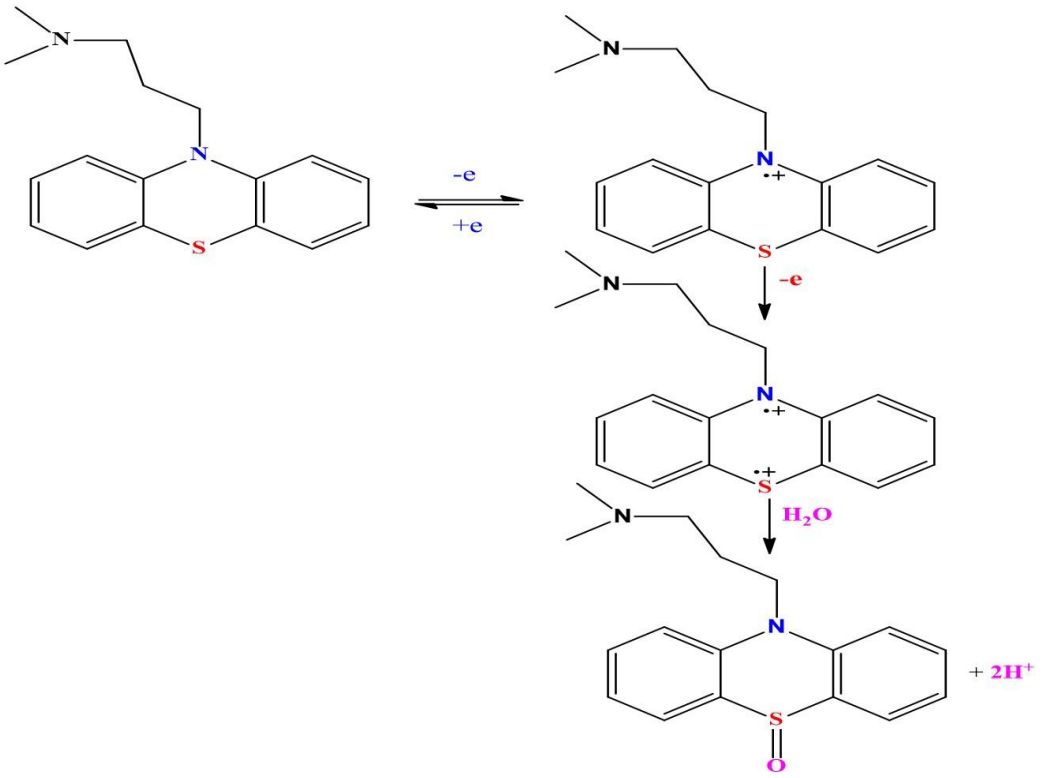

Scheme 3.4: Mechanism of redox behavior of promazine

3.3.8. Optimum Parameter of SWV at GCPE

To get more insights into the electroanalytical performance of the GCPE for promazine detection, square wave voltammetry technique was used. Fig. 3.10., shows the optimization of relevant technique parameters. The potential increment (A) was varied from 1,2,4,6,10 and 20 mV, the pulse amplitude (B) was varied from 0.025, 0.015, 0.01 and 0.04 V , and the frequency (C) was varied from, 25, 20, 15,10 and 5 Hz. From the corresponding plots shown in Fig. 3.10., potential increments of 4 mV, frequency of 15 Hz and amplitude of 25 mV were chosen as optimum parameters.

The corresponding curve of the SWV response of 0.1 mM promazine on GCPE. After accumulation times: 0 s, 30 s, 60 s, 90 s, and 120 s. The promazine signal increased up 60 sec and 60 sec used as optimum accumulation time is shown in Fig. 3.11.

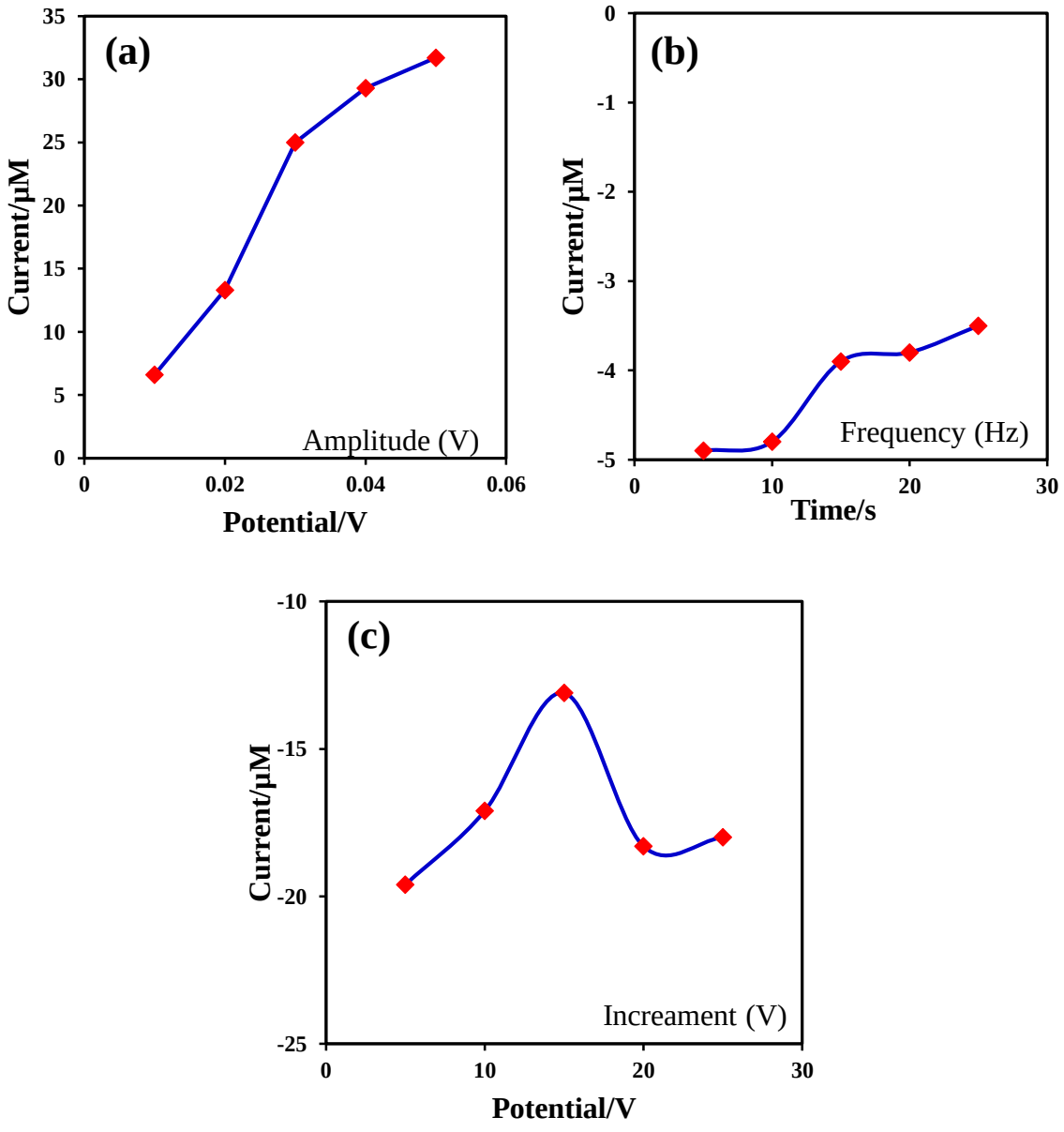

Figure 3.10: Plots corresponding to square wave voltammetric measurements of 0.1 mM promazine at GCPE (a) Pulse amplitude (b) Frequency and (c) Potential increment.

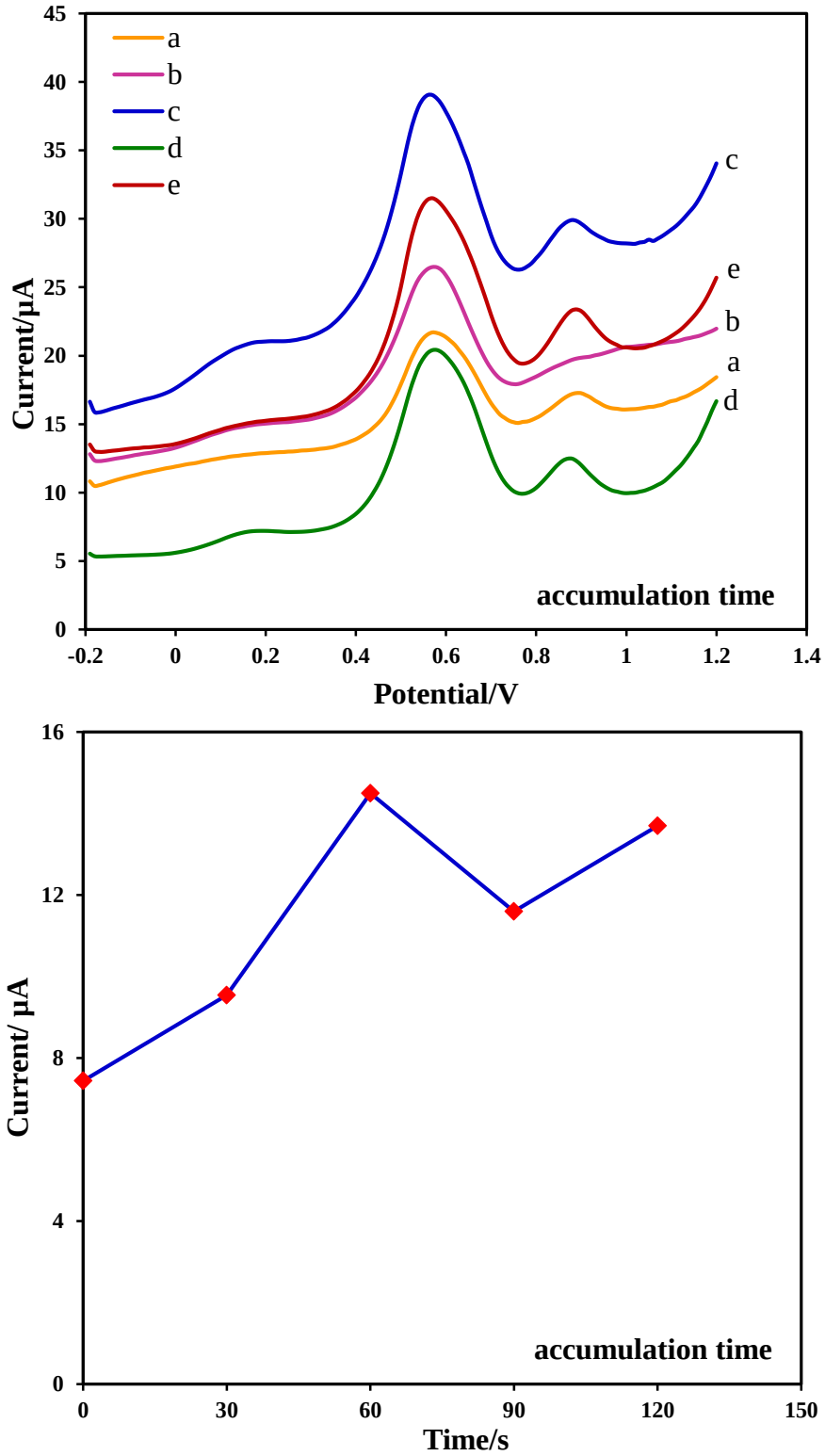

Figure 3.11: A Plot corresponding to accumulation time of 0.1 mM promazine at graphene carbon paste electrode (GCPE).(a) 0 s, (b) 30 s, (c) 60 s , (d) 90 s , and (e) 120 s.

3.3.9. Analytical Determination of Promazine

The effect of optimization parameters on the square wave stripping voltammograms, such as amplitude, increment potential, accumulation time, and frequency was studied by invariable design. The better sensitivity and better voltammograms wave with narrow peak width were investigated under optimization parameters of 15 mV increment, 4 mV amplitude, 15 Hz frequency and 60 s accumulation time were chosen. The intensity of SWV voltammogram of promazine at GCPE is more enhanced than that of promazine at the CPE electrode, as illustrated in Fig. 3.12. In addition, the intensity of square wave voltammetry of promazine at GCPE electrode is more enhanced than the CV voltammogram of promazine at the CPE as shown in Fig. 3.13. The SWV signals obtained by measuring various concentrations of PZ and the calibration curve is illustrated in Fig. 3.14. It is worth mentioning that the current intensity values, utilized for the calibration curve, are actually the absolute values of the oxidative peak current observed the different concentration of promazine solutions. The better linearity relationship is investigated over promazine concentration in the range of (0.1 – 8.0) μM. The linear equation was calibrated as Ip (μA) = 0.4602 + 0.0299C_{CPZ} (μM) with the correlation coefficient of 0.9979. The ksm^{-1} relation was used to calculate the limits of detection (LOD). In this relation k = 3 for LOD, (S) represents the standard deviation of the current peaks of the y-intercepts and blank (n = 6) and m represent the slope of the calibration curve and the mean of blank and the standard deviation of the blank were used to calculate the LOD for promazine. The value LOD was 8 nM.

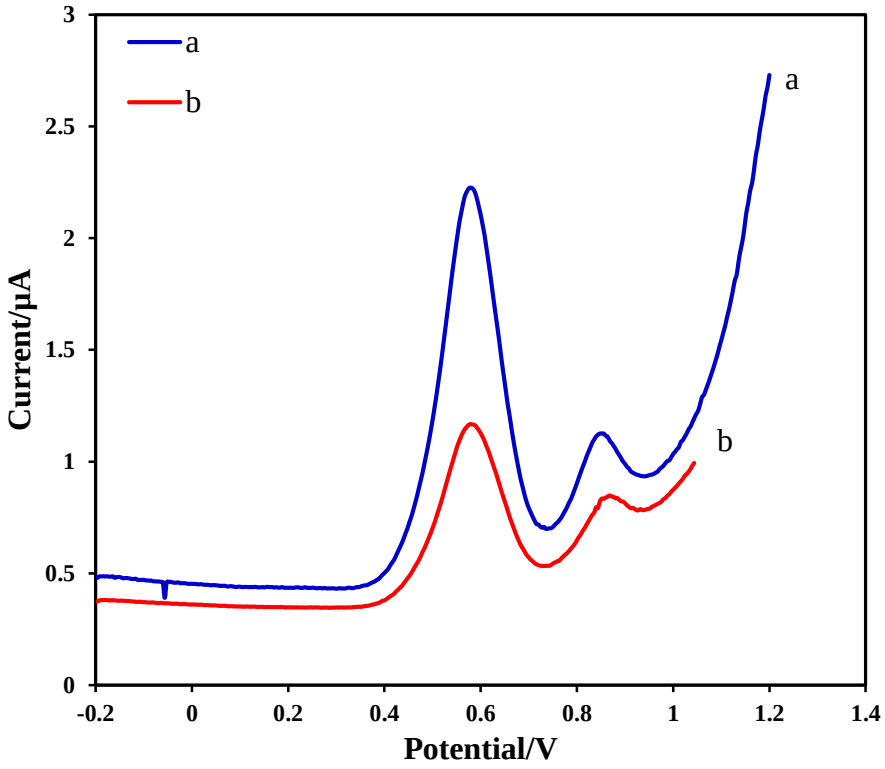

Figure 3.12: SWV of 0.1 mM promazine at GCPE (a) and SWV of 0.1 mM promazine at CPE (b).

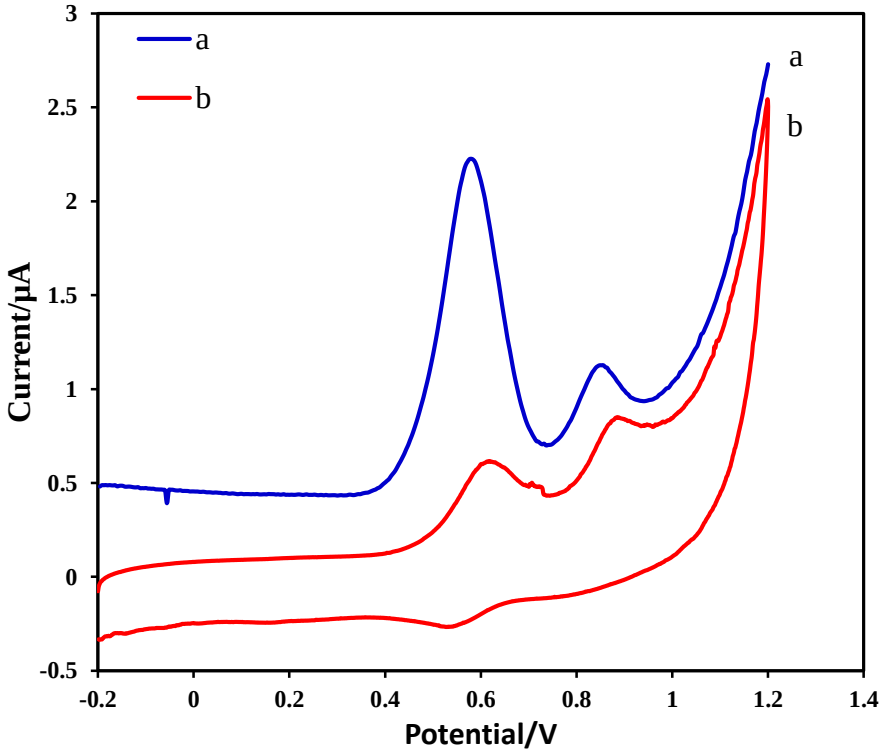

Figure 3.13: SWV of 0.1 mM promazine at GCPE (a), and CV of 0.1 mM promazine at CPE (b).

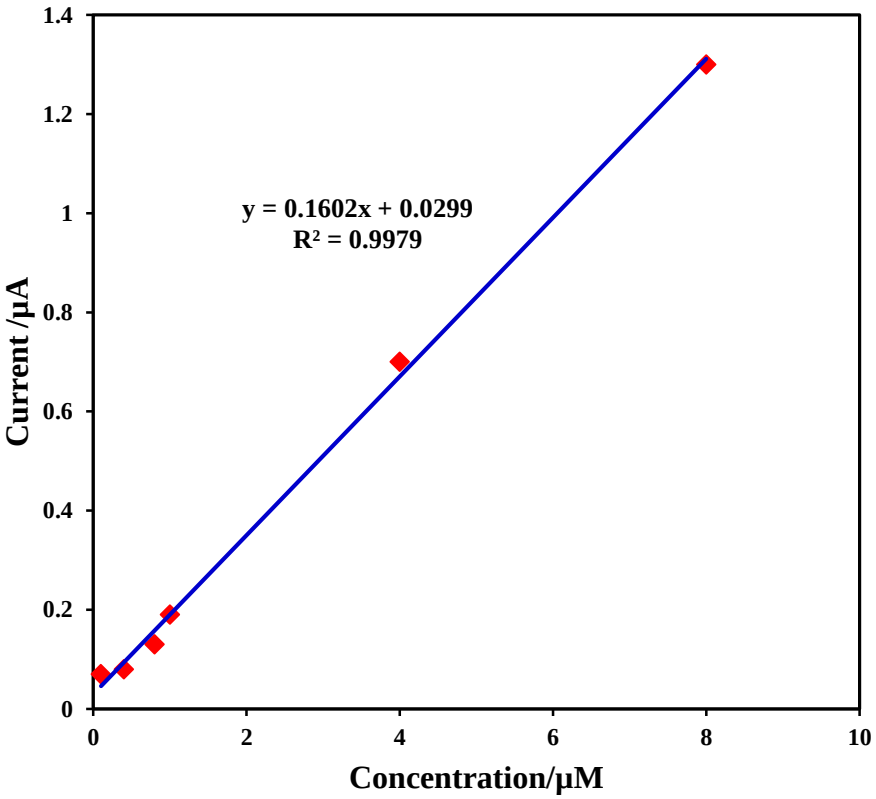

Figure 3.14: The plots of the Square wave voltammetric response (peak current) as a function of promazine concentration (from bottom 0.1, 0.4, 0.8, 1, 4, 8 µM) measurements. A phosphate buffer of pH 4 as an electrolyte solution, and other parameter condition: Accumulation time 60 sec, potential pretreatment -0.7 V, pretreatment time 30 sec and scan rate 100 mV/s.

3.4. REFERENCES

[1] A.K. Geim, Science, 324, 2009, 1530.

[2] A.K. Geim, K.S. Novoselov, Nat. Mater., 6, 2007, 183.

[3] A.L.Higginbotham,D.V.Kosynkin,A. Sinitskii, ACS Nano, 4, 4, 2010, 2059-2069.

[4] J.L. Xia, F. Chen, J.H. Li, N. Tao, J. Nat. Nanotechnol., 4, 2009, 505.

[5] Jacobs, C.B.; Peairs, M.J.; Venton, B., J. Anal. Chim. Acta, 662, 2010, 105-127.

[6] K. Zhou, Y. Zhu, X. Yang, J. Luo, C. Li, Electrochim. Acta., 55, 2010, 3055.

[7] K.Kalcher, Electroanalysis, 7, 1995, 5.

[8] L.F. Dong, R.R.S. Gari, Z. Li, M.M. Craig, S.F. Hou, Carbon, 48 ,2010, 781.

[9] Apetrei C., Apetrei I.M., Villanueva S., de Saja J.A., Gutierrez-Rosales F., Rodriguez-Mendez M.L., Anal.Chim. Acta, 663, 2010, 91–97

[10] C. Apetrei, M.L., Sensors and Actuators B: Chemical, 111–112, 2005, 403-409.

[11] C. Apetrei, M.L. Rodríguez-Méndez, V. Parra, F. Gutierrez, J.A. de Saja, Sens. Actuat. B Chem., 103, 2004, 145-152.

[12] C. Liu, S. Alwarappan, Z.F. Chen, X.X. Kong, C.Z. Li, Membraneless enzymatic biofuel cells based on graphene nanosheets Biosens. Bioelectron., 25, 2010, 1829.

[13] D.A.C. Brownson, C.E. Banks, Analyst 135, 2010, 2768.

[14] D.R. Kauffman, A. Star, Electrochemistry Communications, 13, 2011, 366–369

[15] H. Wang, L.-F. Yang, Y. Yang, H.S. Casalongue, J.T. Robinson, Y. Liang, Y. Cui, H. Dai, J. Am. Chem. Soc., 132, 2010, 13978.

[16] J. J. Gooding, Electrochim. Acta, 50, 2005, 3049–3060.

[17] J.C.Ruiz-Morales,J.Canales-Vázquez, D. Marrero-López, S.N. Savvin, P. Núnez, A.J. Dos Santos-García, C.Sánchez-Bautista, Carbon, 48, 2010, 3964-3967.

[18] M. Pumera, Chem. Soc. Rev., 39, 2010, 4146.

[19] M.H., parvin. Electrochem.Commun., 13, 2011, 366-369.

[20] M.L.; Gay, M.; Apetrei, C.; De Saja,, J.A. Electrochim. Acta, 54, 2009, 7033-7041.

[21] M.S. Goh, M. Pumera, Electrochem. Commun., 12, 2010, 1375.

[22] M.S. Goh, M. Pumera, Chem. Asian J. 5, 2010, 2355.

[23] M. Liang, L. Zhi, J.A. Electrochim. Acta., 54, 2009, 7033-7041.

[24] M. Pumera, A. Ambrosi, A. Bonanni, E.L.K., Trends Anal. Chem. 29, 2010, 954.

[25] Makhotkina O., Kilmartin P.A., J. Electroanal. Chem. 633, 2009, 165-174.

[26] R.N. Adams, J Electroanal.Chem., 143, 1983, 89.

[27] Svancara I., Vytřas K., Barek J., Rev. Anal. Chem. 31, 2001, 311–345.

[28] D.C. Le, C.J. Morin, M. Beljean, A.M. Siouffia, J. Chromatogr. 1063, 2005, 235.

[29] J. Karpinska, H.P. Tarasiewicz, B. Branch, Anal. Lett. 30, 1997, 2365.

[30] B. Zeng, F. Huang, Talanta, 64, 2004, 380.

[31] T.J.R. Lambert, D.J. Castle, Schizophr. MJA, 178, 2003, S57.

[32] W.S. Hummers, R.E. Offeman, J. Am. Chem. Soc., 80, 1958, 1339.

[33] Y. Liu, D.Y.C. Zeng, Z. Miao, L. Dai, Langmuir, 26, 9, 2010, 6158.

[34] Yakovleva, K.E.; Kurzeev, S.A., Appl. Biochem. Microbiol, 43, 2007, 661-668.

[35] Francisco J. Lara, Analytica Chimica Acta, 535 , 2005, 101-108.

[36] Anatol Kojlo, Helena Puzanowska-Tarasiewicz, J. Martinez Calatayud, Journal of Pharmaceutical and Biomedical Analysis Spectrophotometric , 10, 1992, 785-788.

[37] Helena Puzanowska-Tarasiewicz, E12bieta Wotyniec, Anatol KojIo, Journal of Pharmaceutical and Biomedical Analysis, 14, 1996, 267-271.

CHAPTER 4

Voltammetric Behavior of Ketoconazole and its Determination Using Carbon Paste Electrode Modified by Gold Nanoparticles

4.1. Introduction

Ketoconazole (cis-1-acetyl-4- {4- [[2-(2, 4-dichloro-phenyl)-2-(1H-imidazol-1-ylmethyl)-1, 3-dioxolan-4-yl]-methoxy] phenyl} piperazine, KCZ), the structure of ketoconazole contains the imidazole group which is used as an anti-fungal agent. In addition, KCZ (ketoconazole) exhibits many changes in cytochrome, which is significant in biomedical compounds as detoxification in human organisms [1]. The assaying of the ketoconazole in biomedical application, pharmaceutical compounds and formulations are essential. The determination of KCZ has been carried out by high-performance chromatography (HPLC) [2-5], spectrophotometric techniques [6-8], electrophoresis technique [9]. The electrochemical techniques are commonly used nowadays to determine the pharmaceutical compounds due to that these methods are more sensitive, and requires high accuracy, precision [10]. Certain electrochemical techniques used different materials to detect the KCZ like mercury electrode [11], urine carbon paste electrode [12] and glassy carbon electrode [13]. A working electrode which detects oxidation processes usually enhanced the determination of KCZ since the electrochemical reaction take place on the surface of

the electrode, thus high sensitivity, reproducibility and accuracy are achieved [14]. The voltammetric technique has more advantages such as no the matrix effects, and the high selectivity and the sensitivity due to the dilute sample used during the detection. The development method is considered fast, simple and more accurate to be applied for the assaying of pharmaceutical and biological samples. Electroanalytical techniques are highly recommended for the analysis of organic compounds, involving drug compounds such as cephalosporin's [15-17] in dosage formulation and biological organism solutions [18-21]. The bare carbon paste electrode is commonly used in the electrochemical methods: This is due to its simple fabrication, better sensitivity, and its surface can be easily modified. Such modifications for some surface immobilization and act as a conducting material which enhances the electron transfer between the surface of gold nanoparticles and the target analyte. Many procedures have been constructed to development to construct the immunosensor by using modified carbon paste electrode with gold nanoparticles [23-29]. This improvement leads to better selectivity, sensitivity, detection limit and other properties of the graphite paste electrodes modified with AuNPs [30-35]. The process of modifying the graphite paste electrode depends on the features of the modifier, which can enhance the selectivity and the sensitivity to the target analyte [36]. Gold nanoparticles (AuNPs) have high surface areas, better biocompatibility, high electron conductivity and unique properties that initiate electro-catalysis. AuNPs have been applied in the determination of Pharmaceutical compounds [37-42]. Square wave voltammetry is considered as a fast electro-analytical method of advantages, like low detection limit, high analysis speed, and low consumption of the electro-active species [43]. The unmodified bare (CPE) and the modified (CPE) are commonly used in the assaying of Pharmaceutical

compounds, and biological materials. These electrodes have a window of wide potential range from (-1.4 to +1.3 V) based on conditions applied [44-45]. Compared to glassy carbon electrodes, the carbon paste electrode develops a current that is 10 times lower than that of glassy carbon electrode [46].

The type of the modifier has a significant influence on the selectivity of the modified electrode. For instance, imidazole group is adsorbed on the surface of AuNPs/CPE electrode [48]. Gold nanoparticles have been utilized as a better modifier substrate to carbon paste and used in the determination of ketoconazole. In this work different electroanalytical techniques such as cyclic voltammetry, square wave voltammetry, and differential pulse voltammetry were applied for the determination of KCZ. The carbon paste electrode modified with AuNPs was used as a working electrode. The structure of ketoconazole drug shown in Scheme 4.1.

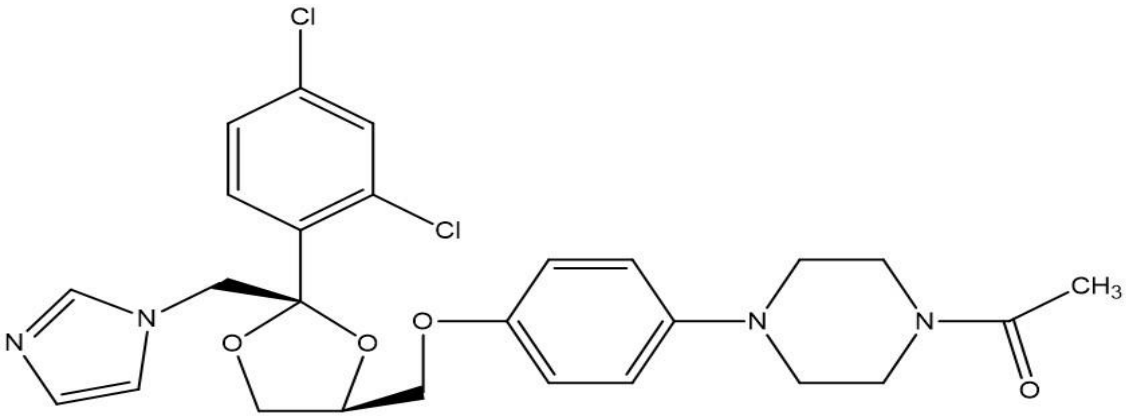

Scheme 4.1: Molecular structure of ketoconazole

4.2. Experimental

4.2.1. Chemical and Material

Ketoconazole (cis-1-Acetyl-4-(4- [(2- [2, 4-dichlorophenyl]-2-[1H-imidazol-1-ylmethyl]-1, 3-dioxolan-4-yl)-methoxy] phenyl) piperazine (analytical standard,>98% purity), the CAS number 65277, were purchased from Sigma-Aldrich. Gold (III) chloride trihydrate (HAuCl4. $3H_2O$, > 49 % Au basis), and was purchased from Sigma-Aldrich.

4.2.2. Reagents and Solutions

A solution of 1.0 mM of KCZ was prepared by dissolving a small amount of KCZ in a phosphate buffer pH 4.0 solution. A volume of five drops of nitric acid was added to the solution to dissolve KCZ. The buffer solution was prepared by dissolve 100g of phosphate buffer in a 100 ml distilled water and poured in a volumetric flask. A solution of commercial AuNPs was used.

4.2.3. Construction of the Work Electrode

Graphite nanocomposite electrode was constructed by mixing an amount of the carbon powder with a small amount of an organic liquid such as paraffin oil of a percentage (70 %, w/w) of graphite to (30%, w/w) of paraffin oil to make a paste composite. Electrical contact was made by using a copper wire that was placed into the porthole of the syringe within the paste mixture. The modified electrode (AuNPs/CPE) was constructed by blending of carbon powder (65 %, w/w) with gold nanoparticle (5%, w/w) and paraffin oil (30%, w/w). The composite mixture was packed into a plastic syringe. Modified carbon paste electrode was rinsed with deionized water before each experiment.

4.2.4. Procedure

The cyclic voltammetry carried out by treating ketoconazole on the surface of the modified electrode, where a potential voltage range of (0.4 – 1.2) V was applied. This was followed by a different scan rate for a preselected time at a suitable voltage for the KCZ in the phosphate buffer pH 4 solution. The cyclic voltammetry in potassium ferrocyanide as an electrolyte solution to show the enhancement of the signals when used the gold nanoparticles to modify the carbon paste composite by using the potassium chloride from potential (-0.4 – 0.8) V. Then scan rate of potential at 100 mV/s over the potential range. Square wave voltammetry experiments were investigated by immersing the modified electrode in KCZ solutions. This was followed by using a square wave voltammogram, with optimum conditions of increment 4mV, frequency 15 Hz and an amplitude of 25 mV.

4.3. Results and Discussions

4.3.1. Characterization of Gold Nanoparticles

SEM images have illustrated that the spherical particles of gold nanoparticles, uniform homogeneous structure and morphology. The white spots were represented the particles of gold nanoparticles with scale dynamic range of 50 μm in Fig.4.1a.

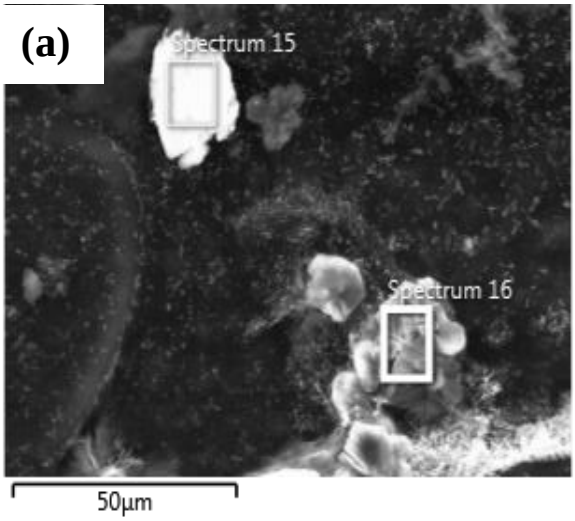

Figure 4.1: (a) SEM image of gold nanoparticles.

4.3.2. Characterization of AuNPs/CPE

SEM of composite AuNPs/CPE electrode was illustrated the grain particles of gold nanoparticles attached with graphite. The images show the morphology and homogeneous distribution of AuNPs on the CPE surface are shown in Fig. 4.2.

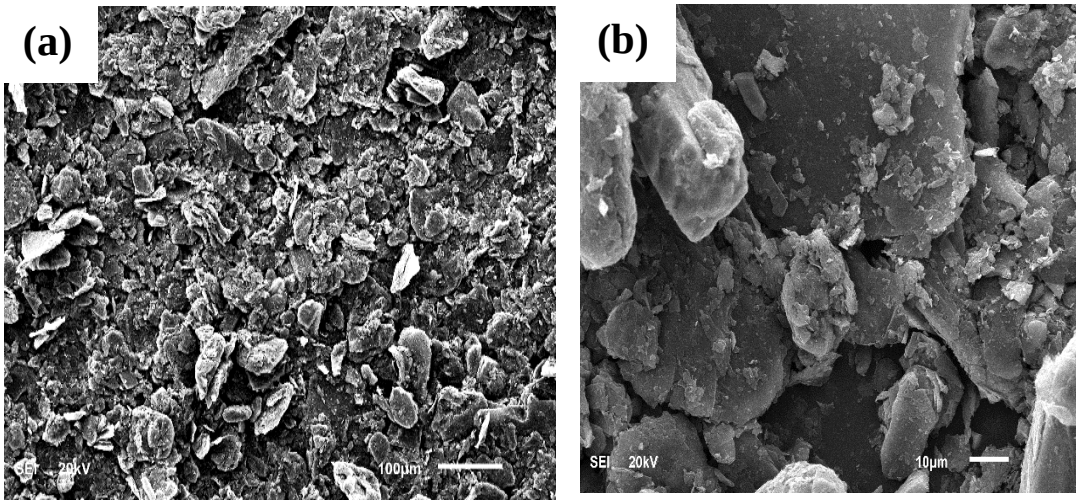

Figure 4.2: SEM images of AuNPs/CPE electrode, (a) low magnification at 100 µm, and (b) high magnification at 10 µm.

4.3.3. Optimum Percentage (W/W) of AuNPs/CPE

The accumulation the KCZ at the modified AuNPs/CPE electrode depends on the nature of its adsorption on the surface of the electrode. However, the concentration percentage of AuNPs in the composite mixture plays an important role in the voltammetric responses. Therefore, the influence of the AuNPs on the intensity of the electrode was obtained by employing CV. The peak of maximum current was investigated for 5% of AuNPs in the composite, and high amount of concentration of AuNPs (>5%) show no change in the peak oxidation of the current. This is because the surface of the modified electrode was saturated by KCZ particles. Therefore, an electrode which consists of 5% AuNPs, and 65% carbon paste was employed.

Cyclic voltammogram which is a comparison between two different types of electrodes like gold nanoparticles (AuNPs/CPE), and (CPE) electrode. Cyclic voltammetry using 0.02 M $K_4Fe(CN)_6$ record at (AuNPs/CPE) electrode and bare CPE. The modified electrode (AuNPs/CPE) have shown high conductivity due to the presence of gold nanoparticles and the signal is an enhancement for both anodic and cathodic reactions because of the high rate of electrons and the background of (AuNPs/CPE) is narrower compared to the background of CPE. Thus, enhancement of signals has resulted. By studying the electrochemical behavior of $K_4Fe(CN)_6$ with 0.5 ml of 0.2 M KCl at a scan rate 100 mV/s. as shown in Fig. 4.3.

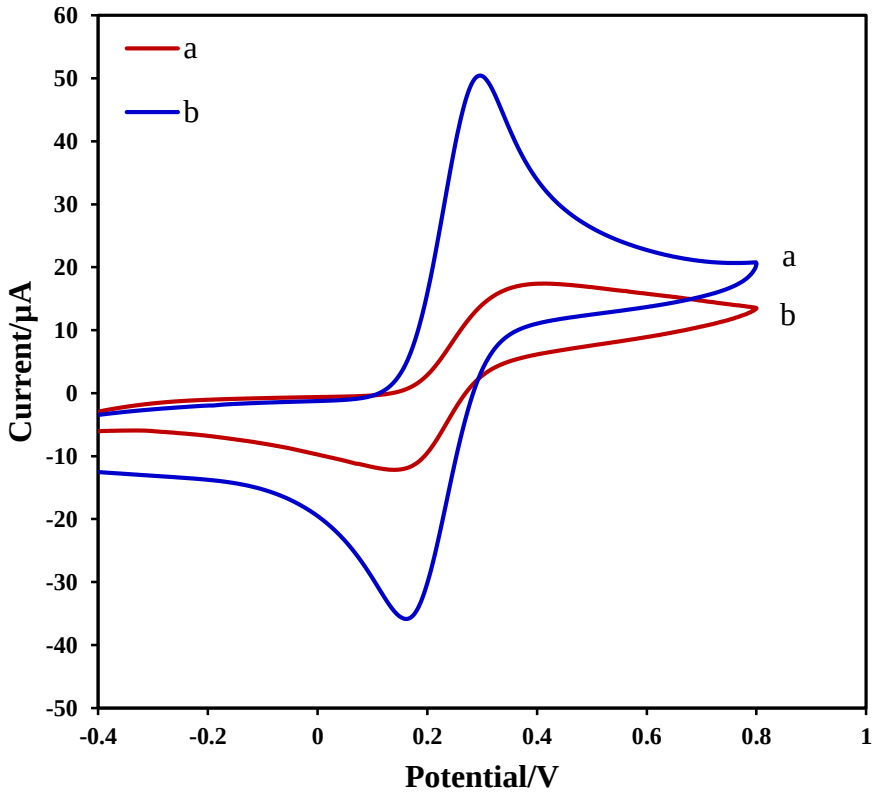

Figure 4.3: CVs of 0.02 M $[Fe(CN)_6]^{3-/4-}$ using CPE (a), and AuNPs/CPE (b). Scan rate 100 mV/s.

4.3.4. Electrochemical Enhancement of KCZ on the Surface of AuNPs/CPE

CV technique was utilized to show the redox reaction of the electrode having KCZ on its surface. The cyclic voltammetry was recorded from potential (0.4 – 1.2) V in a phosphate buffer solutions of pH 4 and a little amount of $1*10^{-3}$ M of KCZ on both electrodes, the CPE, and (AuNPs/CPE) modified electrode. The results are shown in Fig. 4.4. Good two-oxidation anodic peaks for KCZ are shown in a cyclic voltammogram curve (a). The drug (KCZ) was electro-active species at the surface of CPE in this electrolyte solution containing KCZ. The bare CPE electrode modified with metal nanoparticle (AuNPs/CPE)

produced a clear oxidation peak current of KCZ that is 4 times higher than the current that resulted at the surface of bare CPE (CV curve a). The existence of gold nanoparticle in nanocomposite increases the surface area of bare CPE and enhances the adsorption of KCZ on AuNPs/CPE electrode and also improves the sensitivity of the oxidation peak. The imidazole group of ketoconazole structure (KCZ) plays a role in the absorption of this drug at the modified electrodes (AuNPs/CPE). This has resulted in a high oxidation peak. Furthermore, the presence of nitrogen and oxygen atoms in the structure of KCZ increases its adsorption at the AuNPs/CPE electrode, as a result, the oxidation peak has improved. The scan rate of CV voltammograms was recorded at 100 mV/s, and the initial potential was 0.4 V and high potential recorded at 1.2 V.

The influence of cyclic voltammetry at different scan rates on the oxidation current peak (Ip) and the potential peak (Ep) of KCZ was studied (Fig. 4.5). A line relationship between (ip) and the scan rate (υ) over, the scan range from (10 –250) mVs^{-1} ($R^2 = 0.9885$) which illustrate the electro-oxidation current peak of KCZ adsorbed on the AuNPs/CPE were found to increase with increased scan rate. The potential was found to shift to positive values due to an irreversible oxidation process. The plot of ($Ep = 0.0305x + 1.3274$), the slope is 0.0305 shown in Fig. 4.6a. The plot of anodic current versus the root of scan rate was observed the correlation coefficient ($R^2 = 0.9898$) and this mean the two value close to each other and lead to better diffusion occurs at the modified electrode in Fig. 4.6b.

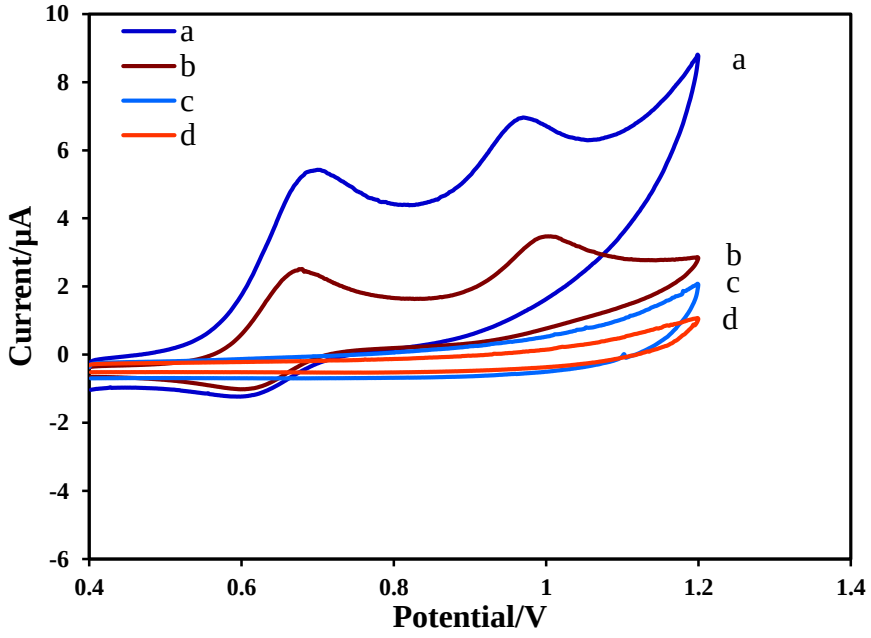

Figure 4.4: Cyclic voltammograms of KCZ (a) 1.0 mM of KCZ at AuNPs/CPE electrode (b) 1.0 mM of KCZ at CPE electrode (c) blank solution of KCZ at AuNPs/CPE, and (d) blank solution of KCZ at CPE. Experiment conditions: Phosphate buffer of pH 4.0 as electrolyte solution and 100 mV/S scan rate.

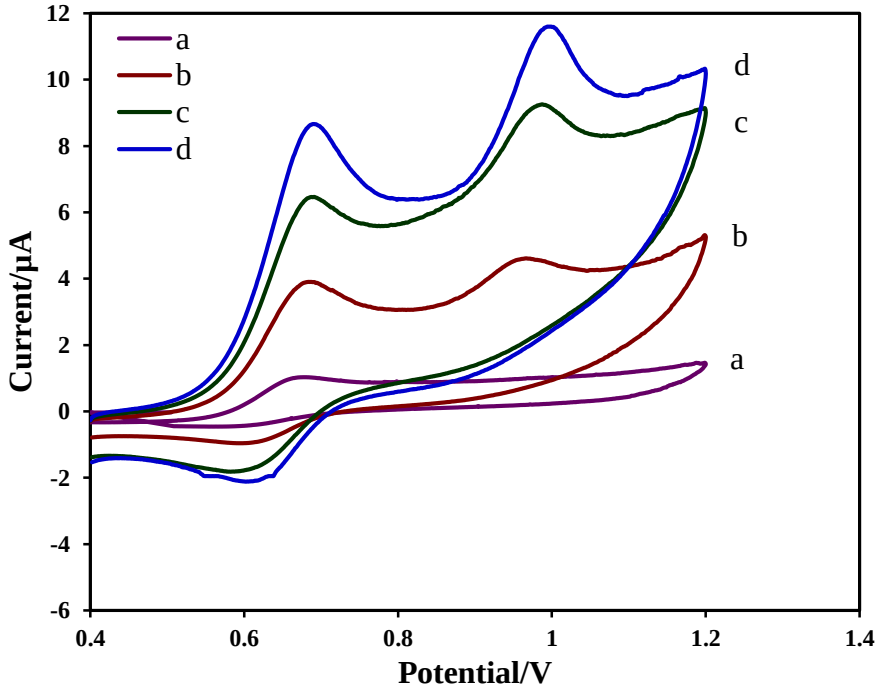

Figure 4.5: Cyclic voltammograms at different scan rates and anodic current versus scan rate of KCZ from range (a) 10, (b) 75, (c) 150, and (d) 250 mV/s at AuNPs/CPE modified electrode. 1.0 mM of KCZ in phosphate buffer of pH 4.0 solution.

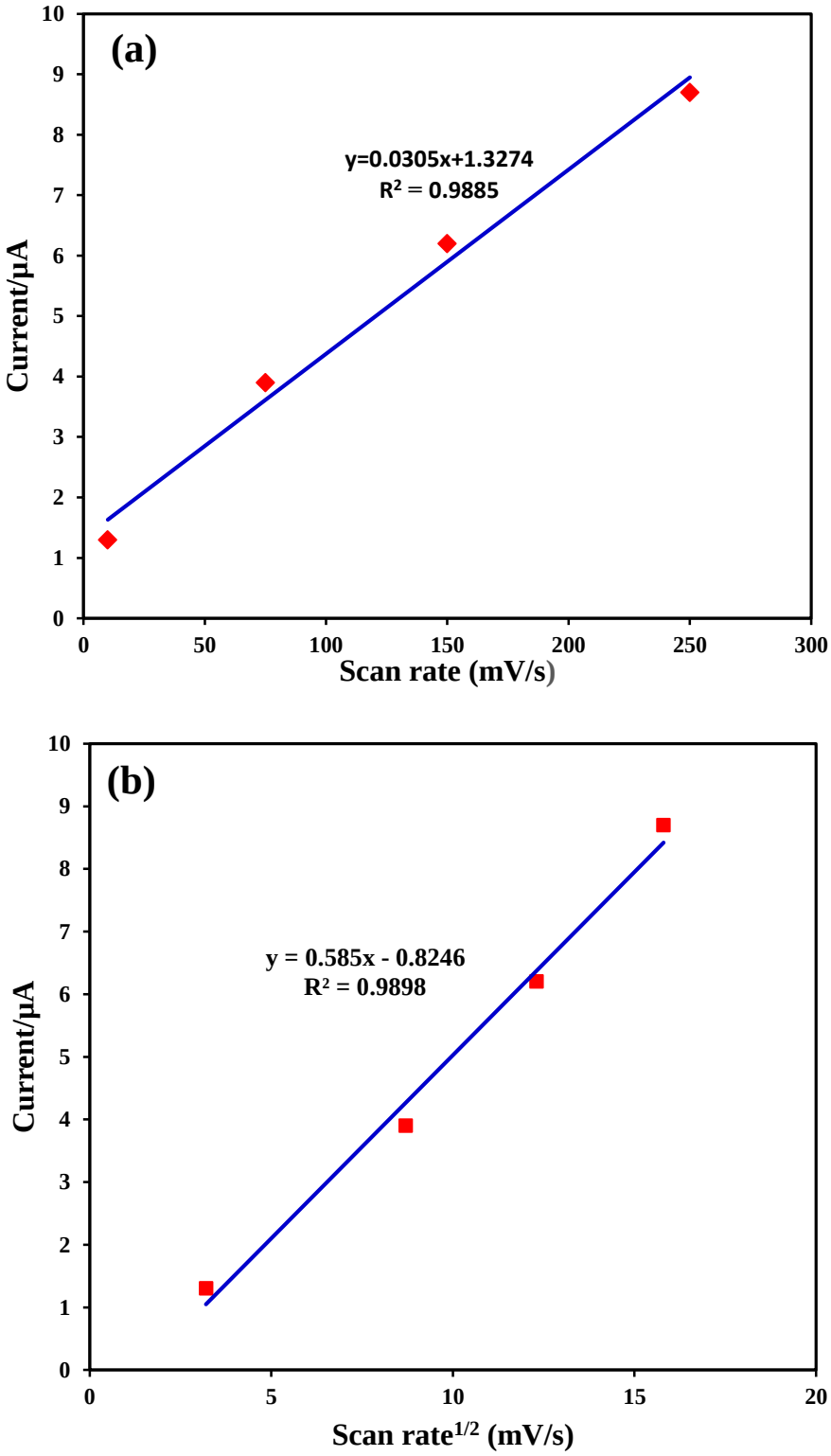

Figure 4.6: (a) the anodic current (Ip) versus scan rate (υ) of KCZ at AuNPs/CPE electrode with scan rate from range (10, 75, 100, 250) mV/s respectively, and (b) square root of scan rate. The solution contains 1.0 mM of KCZ in phosphate buffer of pH 4.0 as an electrolyte solution.

4.3.5. The pH Effect

In voltammetry, the pH of the solution affects the mechanisms of the electrochemical process. Consequently, the anodic current will be affected. Therefore, phosphate buffer of pH 2 – pH7 were used during the differential pulse voltammetry of KCZ at AuNPs/CPE electrode. The effective parameters were investigated at the ranges of (25 – 100) mV pulse amplitude, a pulse width of (30 – 200) ms pulse and a scan rate of (10 – 100) mV/s. The best signal sensitivity with a narrow peak width was achieved at the values of 50 mV pulse amplitude and 200 ms pulse width. In a buffer solution of pH 4, the current intensity was found to reach the maximum peak and then started to decrease gradually when the buffer of pH6 and pH 7 were used as can be seen from Fig. 4.7. The relation between current and pH, the relation between potential and pH were illustrated in Fig. 4.8.

On applying CV at buffer pH 3, pH 4, pH 5 and pH 6 at 0.1 mM KCZ two oxidation peaks have appeared at 0.697 V which is reversible and at 0.983 V. Furthermore, a reduction peak at 0.612 V which represents a reversible process has also appeared. In the case of pH higher than 6, this reduction peak was not observed. It is obvious from the buffers used that the electrooxidation of KCZ involves three cases were not observed and there are three cases. The first case, in which the effect of buffer solutions of pH 3 – pH 6 shows the first oxidation peak of KCZ at 0.697 V indicative of a reversible, due to the oxidation of imidazole group to form ketone structure. In addition, a reduction peak at 0.612 V due to the deprotonation of the imidazole group. The second oxidation occurs at 0.983 V which is irreversible, in the phosphate buffer solution of pH 3 – pH 6 as a result of oxidation of piperazine group at high potentials as the same process of oxidation piperazine group of trazodone [49], and doxazosin molecule [50]. Which is attributed to the loss of one electron

from the nitrogen atom of the carbonyl group [51]? The second case, at pH 2 illustrates two oxidation peaks and two reduction peaks, the first oxidation peak has shifted toward 0.761 V which is reversible due to the oxidation of imidazole group attributed the loss of two electrons from the imidazole group. The second oxidation peaks attributed to the oxidation of nitrogen atom and the peak has shifted to 1.125 V. In addition, two reduction peaks were observed. The first reduction peak at 0.451 V is attributed to the reduction of the carbonyl group in highly acidic buffer [52]. The third case, the effect of pH 7 on the KCZ molecule, shows one oxidation peak at 0.697 V, and there is no reduction peak which shows that the electrochemical reaction of KCZ at AuNPs/CPE electrode is irreversible. For an irreversible process, the number of electrons transferred (n) could be obtained from Eq. (1) [53].

$\Delta Epa = Epa - Epa/2 = (47.7/\alpha n)$ mV (at 298 K) (1)

Where Epa/2 is the half peak potential, α represents the electron transfer coefficient ($0.3 < \alpha < 0.7$), α is assumed to be 0.5 for an irreversible process. In this paper, a value of 47 mV for |Epa-Epa/2| was obtained from equation 1 and the value of n is ≈ 2 is yielded referring to Eq. (1) [54]. Therefore, the electrochemical oxidation of KTZ undergoes 2 e^- transfer process. The buffer pH 4 was chosen for the assaying of KCZ, and the results were investigated and the mechanism was proposed for the redox reactions of KCZ (Scheme 4.3).

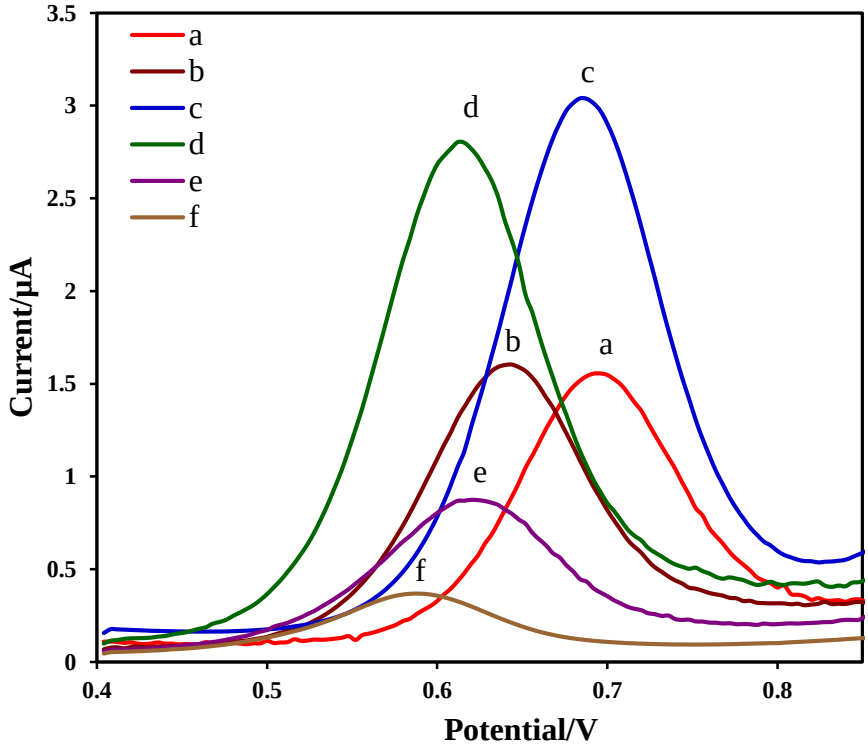

Figure 4.7: Influence of different pH buffer of 1.0 mM KCZ solutions from range (a) pH 2, (b) pH 3, (c) pH 4, (d) pH 5, (e) pH 6, and (f) pH 7 on the differential pulse voltammetry (DPV) oxidation peak current. Optimum conditions are the values of 50 mV pulse amplitude, 200 ms pulse width, and 100 mV/S scan rate.

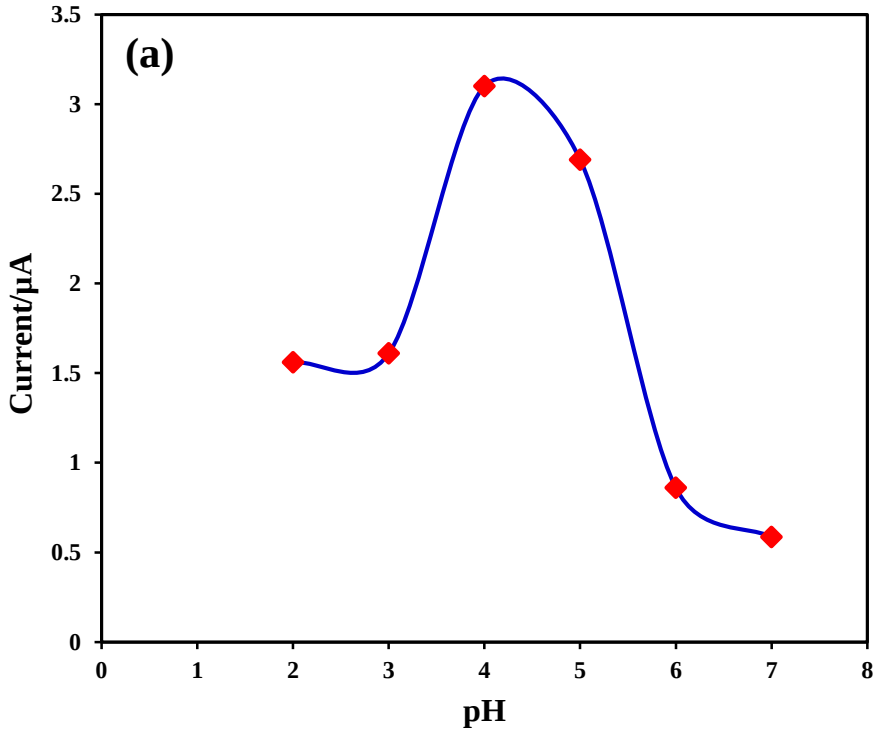

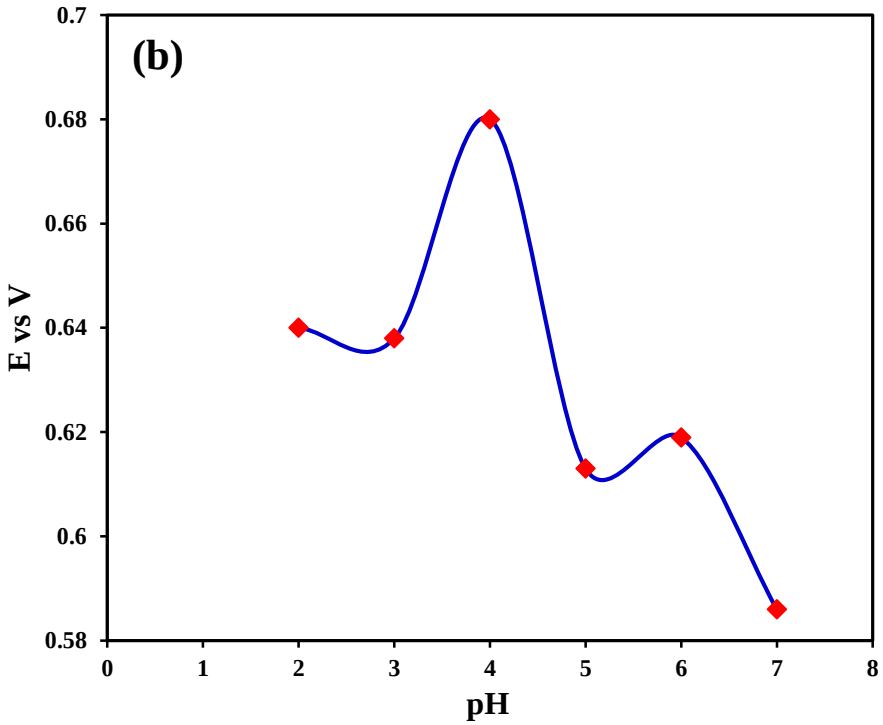

Figure 4.8: (a) The relation between anodic current versus values of pH and (b) the relation between anodic potential versus pH.

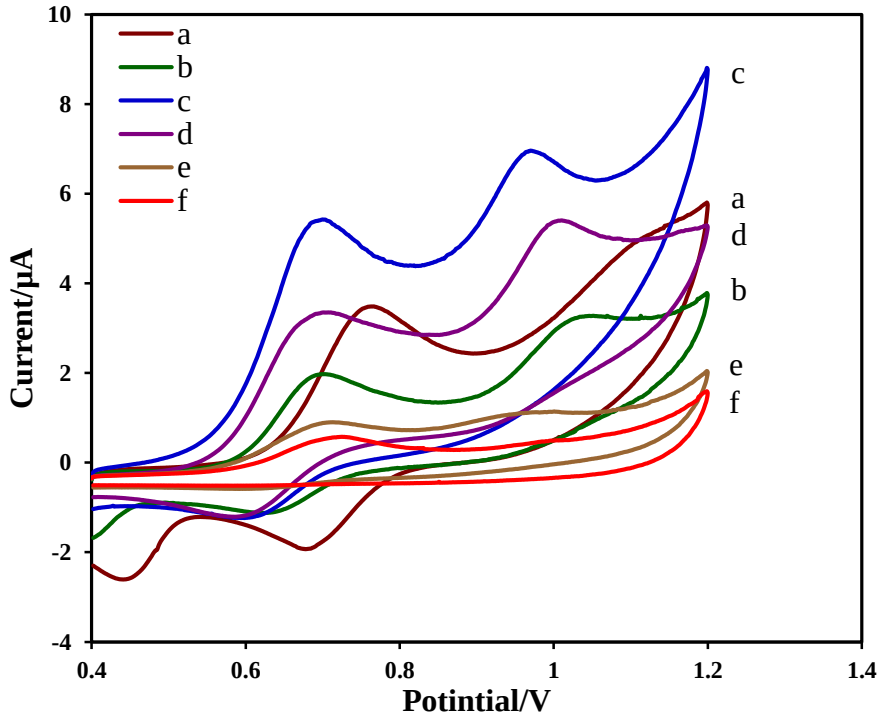

Figure 4.9: Effect of the different pH buffer of 1.0 mM KCZ solutions from range (a) pH 2, (b) pH 3, (c) pH 4, (d) pH 5, (e) pH 6, and (f) pH 7 on cyclic voltammetry (CV) oxidation peak current. Optimum condition is the value of 100 mV/S scan rate.

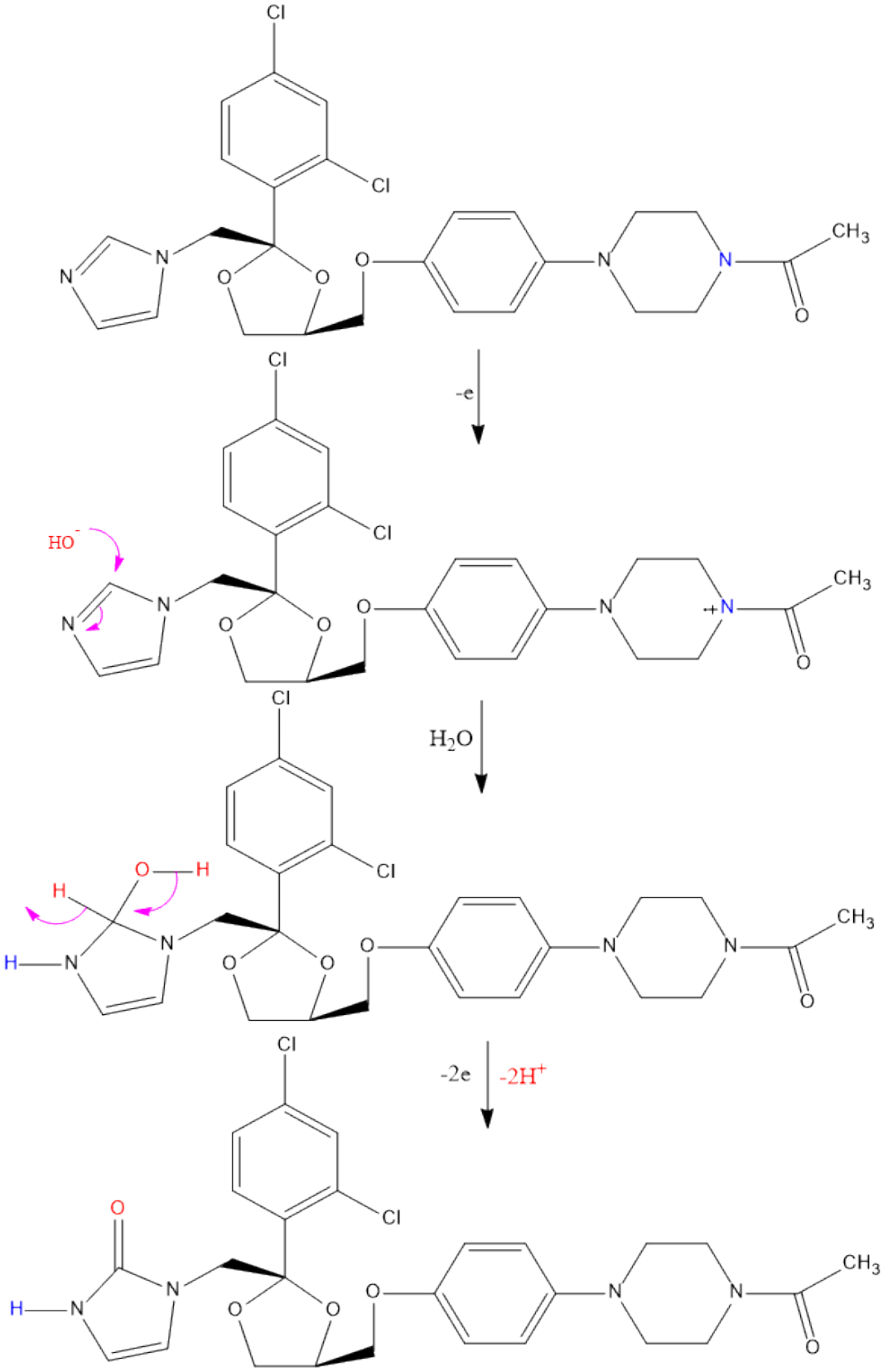
Cl
Cl
N
N
O
O
O
N
N
CH3
O
-e
HO-
H2O
H
O
H
H
N
-2e
-2H+

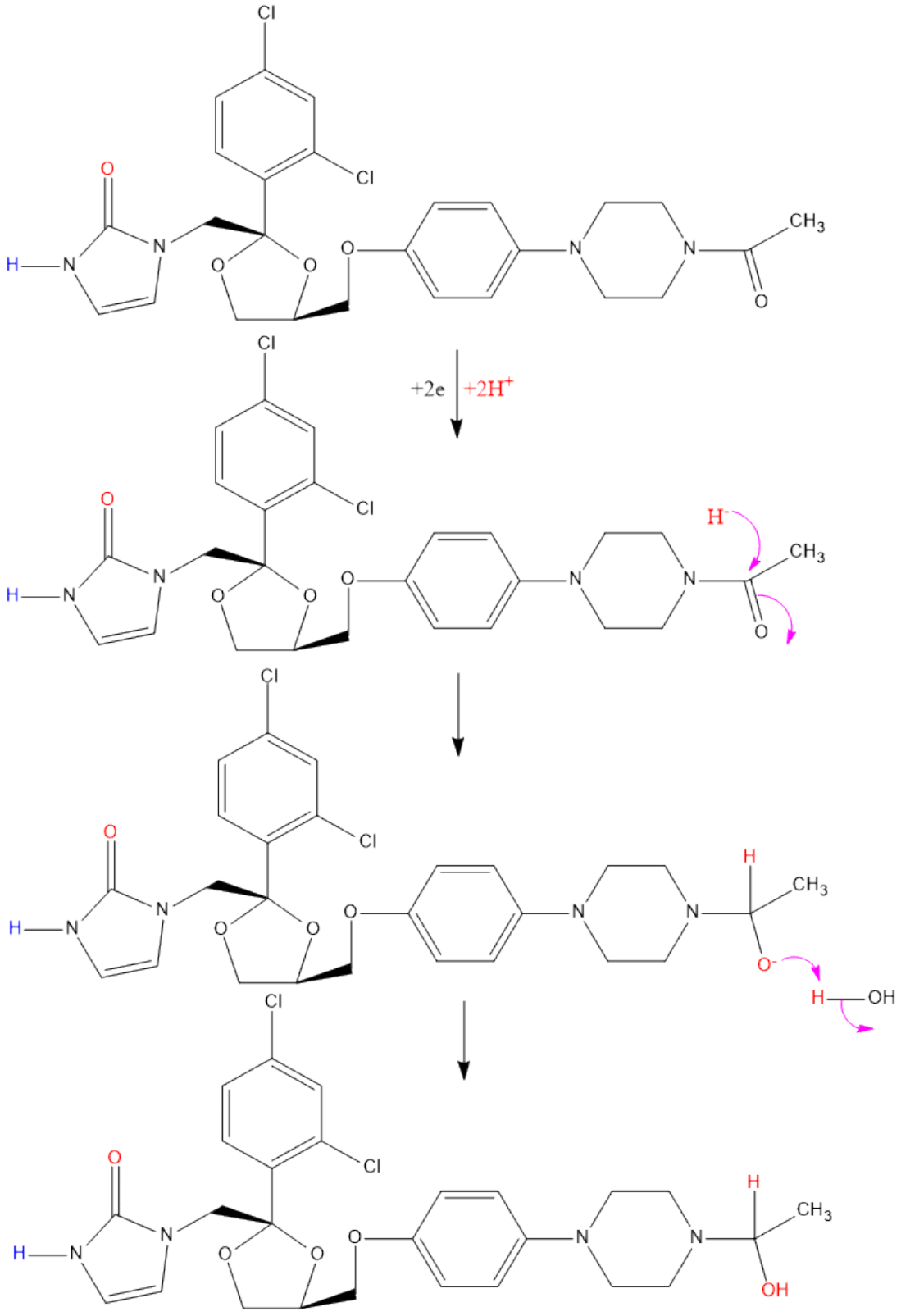

Scheme 4.2: Mechanism reduction of ketoconazole.

4.3.6. Electrochemical Determination of Ketoconazole

The voltammetric parameters that affect the square wave voltammetry (SWV) technique in the determination of KCZ was investigated. These parameters included the amplitude, the increment, and the frequency. The optimum parameters were found to be: An amplitude of 25 mV, a potential increment of 4mV and a frequency of 15 Hz. Fig.4.10. Shows the SWV voltammogram curves of various concentrations of KCZ at AuNPs/CPE using the optimum parameters. The better linearity relationship between the intensity of the current and the concentration of KCZ in the range of (1.0 – 80.0) µM was observed. The linear equation is $I_a = 0.0252C_{(KCZ)} + 0.6339$, correlation coefficient of ($R^2 = 0.998$), where I_a is the current anodic peak in µA and C is the concentration of KCZ in µM. The relation ks/m was used to calculate the limits of detection (LOD), where k = 3 for LOD (S) representing the standard deviation of the intensity currents of the blank (n = 6) and the slope of the calibration curve of KCZ was 0.0252. The LOD was calculated from the relation of the standard deviations of the blank and the mean of the blank. The LOD value was found to be 0.59 µM in the analysis of KCZ.

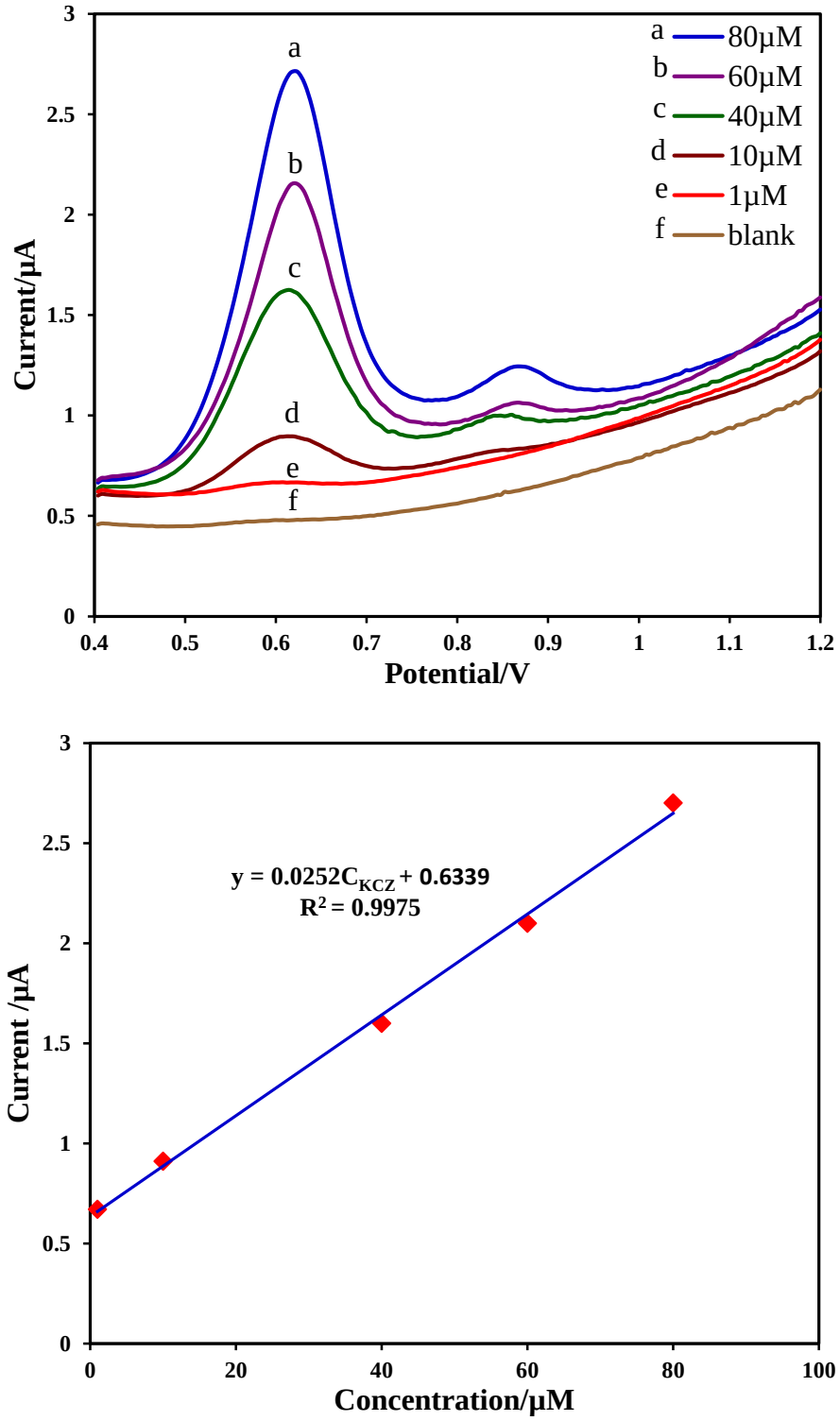

Figure 4.10: Square wave voltammograms of different concentrations of KCZ (from bottom to top: 1.0, 10.0, 40.0, 60.0, 80.0 µM) and a calibration curve of oxidation peak current against the concentration of KCZ at AuNPs/CPE. The electrolyte of pH 4.0 phosphate buffer solution with and 25 mV amplitude, 4 mV potential increment, and 15Hz frequency.

4.4. REFERENCES

[1] W. Martindale, in: J.E.F. Reynolds (Ed.), Martindale: The Extra Pharmacopeia, the Pharmaceutical Press, London, 1989.

[2] Gordien JB, Pigneux A, Vigouroux S, Tabrizi R, Accoceberry I, Bernadou JM, Rouault A, Saux MC, Breilh, JPharm. Biomed. Anal., 50, 2009, 932-938.

[3] Y.V. Heyden, A. Nguyen, M. Nguyet, M.R. Detaevernier, D.L. Massart, J. Plaizier-Vercammen, J. Chromatogr., 958, 2002, 191.

[4] A. Nguyen, M. Nguyet, A.M. Van Nederkassel, L. Tallieu, S. Kuttatharmmakul, E. Hund, Y. Hu, J. Smeyers-Verbeke, Anal. Chim. Acta, 516, 2004, 87.

[5] A. Nguyen, M. Nguyet, L. Tallieu, J. Pharm. Biomed. Anal., 32, 2003, 1.

[6] P.Y. Khashaba, S.R. El-Shabouri, J. Pharm. Biomed. Anal., 22, 2000, 363.

[7] M. Pandeeswaran, K.P. Elango, Spectrochim, Acta Part A, 72, 2009, 789.

[8] M. Pandeeswaran, K.P. Elango, Spectrochim, Acta Part A, 69, 2008, 1082.

[9] A. Arranz, C. Echevarria, J.M. Moreda, J. Chromatogr A, 871, 2000, 399.

[10] T. Peng, Q. Cheng, C.F. Yang, J Anal Chem, 370, 2001, 1082

[11] P. Arranz, A. Arranz, J.M. Moreda, J. Pharm. Biomed. Anal., 33, 2003, 589.

[12] M. Shamsipur, K. Farhadi, Analyst, 125, 2000, 1639.

[13] M.A. El Ries, M.F. Abdel Ghany, L.A. Hussin, Elsevier, 51, 2013, 49–55.

[14] F.W.P. Ribeiro, A.S. Cardoso, R.R. Portela, J.E.S. Lima, S.A.S. Machado, P. de Lima- Neto, D. De Souza, A.N. Correia, Electroanalysis 18, 2008, 2031.

[15] S.A. Ozkan, B. Uslu, P. Zuman, Analytica Chimica Acta, 457, 2002, 265.

[16] A.H. Al-Ghamdi, M.A. Al-Shadokhy, A.A. Al-Warthan, Journal of Pharmaceutical and Biomedical Analysis, 35, 2004, 1001.

[17] P. Zuman, V. Kapetanovic, M. Aleksic, Analytical Letters, 33, 2000, 2821.

[18] B. Uslu, S.A. Ozkan, Electrochimica Acta 49, 2004, 4321.

[19] S.A. Ozkan, B. Uslu, H.Y. Aboul-Enein, Talanta, 61, 2003, 147.

[20] B. Uslu, S.A. Ozkan, Analytica Chimica Acta, 462, 2002, 49.

[21] M.M. Ghoneim, W. Baumann, E. Hammam, A. Tawfik, Talanta, 64, 2004, 857.

[22] C.F. Ding, M.L. Zhang, F. Zhao, Analytical Biochemistry, 378, 2008, 32.

[23] H.X. Ju, S. Liu, B. Ge, F. Lisdat, F.W. Scheller, Electroanalysis, 14, 2002, 141.

[24] M.B. Gonzlez-Garca…etal, Biosensors and Bioelectronics, 15, 2000, 315.

[25] M.L. Mena, P. Ynez-Sedeno, Analytical Biochemistry, 336, 2005, 20.

[26] J. Manso, L. Agü, P. Yjnez-Sedeno, Analytical Letters, 37, 2004, 887.

[27] L. Agüe, J. Manso, P. Yjnez-Sedeno, Sensors and Actuators B, 113, 2006, 272.

[28] L. Agüe, J. Manso, P. Yjnez-Sedeno, J.M. Pingarron, Talanta, 64, 2004, 1041.

[29] L. Agüe, C. Pena-Farfal, P. Yjnez-Sedeno, J.M. Pingarron, Talanta, 74, 2007, 412.

[30] A. Afkhami, H. Ghaedi, Multiwalled, Anal. Methods, 4, 2012, 1415.

[31] A. Afkhami, T. Madrakian, H. Ghaedi, Electrochimica Acta 66, 2012, 255.

[32] A. Afkhami, H. Bagheri, H. Khoshsafar, M. Saber-Tehrani, M. Tabatabaee, A. Shirzadmehr, Analytica Chimica Acta, 746, 2012, 98.

[33] A. Afkhami, T. Madrakian, S.J. Sabounchei, M. Rezaei, S. Samiee, M. Pourshahbaz, Sensors and Actuators B, 161, 2012, 542.

[34] A. Afkhami, T. Madrakian, Sensors and Actuators B, 174, 2012, 237.

[35] A. Afkhami, T. Madrakian, A. Shirzadmehr, H. Bagheri, Ionics, 2012, 881

[36] A. Afkhami, H. Ghaedi, T. Madrakian, Biosensors and Bioelectronics, 44, 2013, 34

[37] W. Huang, W. Qian, P. Jain, M. El-Sayed, Nano Letters, 7, 2007, 3227

[38] O.P. Khatri, K. Murase, H. Sugimura, Langmuir, 24, 2008, 3787.

[39] L. Guczi, G. Peto, A. Beck, K. Frey, O. Geszti, G. Molnar, C. Daroczi, Journal of the American Chemical Society, 125, 2003, 4332.

[40] N.F. Atta, A. Galal, F.M. Abu-Attia, J. Electrochemical Society, 157, 2010, 116.

[41] Z.F. Chen, Y. Zu, Langmuir, 23, 2007, 11387.

[42] H. Qiu, G. Zhou, G. Ji, Y. Zhang, Colloids and Surfaces B, 69, 2009, 105.

[43] P.T. Kissinger, W.R. Heinemann (Eds.), Laboratory Techniques in Electroanalytical Chemistry, second ed., Marcel Dekker, New York, 1996.

[44] M.H. Mashhadizadeh, A. Mostafavi, Actuator B, 113, 2006, 930.

[45] M.H. Parvin, Electrochem. Commun., 13, 2011, 366.

[46] K. Kalcher, J.M. Kauffmann, J. Wang, Electroanalysis, 7, 1995, 5.

[47] N.A. Ulakhovich, E.P. Medyantseva, G.K. Budnikov, Kazan' State University. Translated from Zhurnal Analiticheskoi Kimii, 48, 1993, 682.

[48] S.I. Stoeva, J.S. Lee, C.S. Thaxton, Angew. Chem. Int. Ed., 45, 2006, 3303.

[49] J.-M. Kauffmann, J.-C. Vire, G.J. Patriarche, L.J. Nunez-Vergara J.A. Squella, Electrochim. Acta, 32, 1987, 1159.

[50] A. Arranz, S. Fernandez de Betono, J.M. Moreda, Analyst, 122, 1997, 849.

[51] Mojtaba Shamsipur and Khalil Farhadi, Electroanalysis, 12, 2000.

[52] H. Knoth, T. Petry, P. Gärtner, pharmzine, 67, 2012.

[53] Bard AJ, Faulkner LR., Electrochemical methods: fundamentals and applications. New York 2nd ed, 1980, Wiley**.**

[54] Stela P, Florina P, Alexandru R, Biris, Stefania A, Valentin C, Gabriela B, Enkeleda D, Alexandru S Biris. J Phys Chem C, 115:23, 2011, 387–23394.

CHAPTER 5

DETERMINATION OF METHIMAZOLE BY MODIFIED CARBON PASTE ELECTRODE WITH DECORATED SILVER NANOPARTICLES WITH GRAPHENE

5.1. Introduction

Methimazole (MMZ, 2-mercapto-1-methylimidazole), is a thioureylene kind of drugs used as an antithyroid drug. Its oxidation mechanism of action of the oxidized of iodine in tyrosyl radicals of the thyroglobulin molecule to form monoiodothyronine (IT) and diiodothyronine (IIT). As results, the drug is used as a substrate for the enzyme [1-4].

The pharmaceutical development depends on the drug analysis which is tested during various phases. For example, formulation of the drug, measuring its stability, pharmacological testing, pharma-toxicology and the experimental quality control. Experiments in drug analysis such as, bioavailability, monitoring therapeutic drugs, and pharmacokinetic require reliable and validated analytical techniques. So drug analysis is important in hospitals in order to can be measure drugs in formulations, biofluids and supporting clinical test [5]. MMZ has been determined by different techniques in pharmaceutical fields. For instance, UV–Vis technique coupled with performance liquid chromatography (HPLC) has been used as a detection system consisting of iodine/azide column [6-9]. Iodine/azide as a detection system has been developed for the determination

of MMZ in tablets [10-11]. Also, MMZ has been determined by amperometric technique at the surface of a modified electrode such as Nafion/indium hexacyanoferrate [12]. Furthermore, chemiluminescent Spectrophotometric techniques have been reported [13-17]. However, some techniques have several disadvantages such as complexity, time consuming, effect of interferences, and the high cost. Certain techniques have many advantages such as the electrochemical techniques that proved to be simple technique, and less interference effect [18-24]. A review of the pharmaceutical analysis using electrochemical techniques has been recently reported. In square wave voltammetry (SWV) a large waveform amplitude is employed and an excellent sensitivity with a great speed are achieved. The scan rate of square wave voltammetry can reach 500 V/s. Furthermore, the sensitive square wave voltammetry is higher than differential pulse voltammetry, due to both the forward current and the reverse current. [25].

In the present work, the electro-oxidation of MMZ at modified Ag/GO/CPE electrodes was studied. Hydration and self-association effect on the reaction mechanism of proton transfer in methimazole (3-methyl-1H-imidazole-2(3H)-thione) and1H-imidazole-2(3H)-thione (scheme 5.1) was surveyed. This tautomeric mechanism could be responsible for its pharmacological activity [26-29].

In this work, an electrochemical sensor of CPE modified with silver nanoparticles and decorated with graphene oxide (AgNPs/GO) was used in the voltammetric analysis of methimazole is reported. From the point of view of analytical optimization and the oxidation mechanism of MMZ, the Ag/GO/CPE electrode is favorable because, among other reasons, is cheap and easy to fabricate. The modified electrode, when used in the assaying of MMZ, shows better sensitivity.

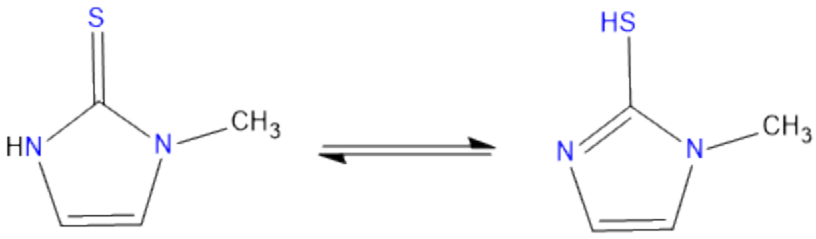

Scheme 5.1: Tautomeric structures of methimazole.

5.2. Experimental

5.2.1. Chemical and Material

Methimazole (1-Methyl-2-imidazolthiol) (≥ 99% purity) with the CAS number 60560 and was purchased from Sigma-Aldrich. Silver nitrate (AgNO3, 99.8%), a material with number 30087, was purchased from BDH-Chemicals Ltd Poole England. Carbon nanotube prepared in a chemistry lab. Potassium bromide (KBr 99%) was purchased from Sigma-Aldrich Company.

5.2.2. Synthesis of Silver Nanoparticle

Colloidal Ag/NPs were prepared by using a solution of 50 ml of aqueous 0.0010 M $AgNO_3$ as a precursor of the Ag nanoparticles. A solution of 150 ml of aqueous 0.0020 M $NaBH_4$ was prepared and used as a stabilizer. In addition, a reducing agent (always the $NaBH_4$ solution was prepared), by dissolving an amount of 11.34 mg of NaBH4 in distilled water. The Sodium borohydride was placed on ice for 20 min. to cool, then the $AgNO_3$ solution was added to $NaBH_4$ solution at a rate of 1 drop/sec with continuous stirring when the silver nitrate is added, the color of the mixture was turned to dark yellow; this color indicates the formation of the nanoparticles [45]. The solvent and the resulting side

products were removed by centrifuging the solution, then sonicated to disperse the particles in the deionized water. The method of synthesis is shown in scheme 5.2.

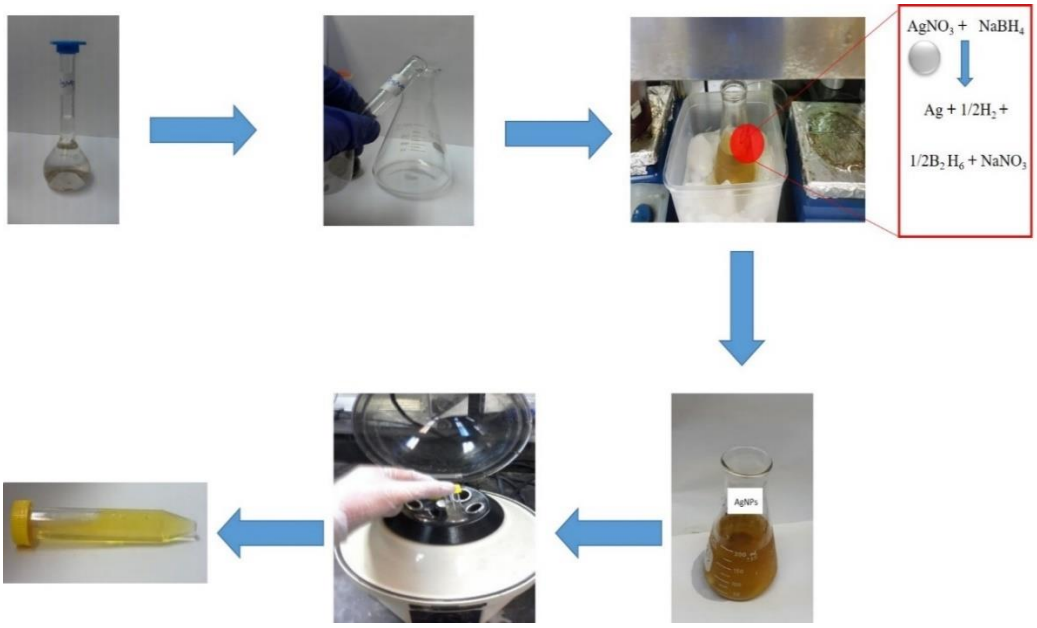

Scheme 5.2: Synthesis steps of silver nanoparticles.

5.2.3. Synthesis of Silver Nanoparticle Decorated Functionalized MWCNTs

The decoration of AgNPs on the OH- or -COOH of functionalized MWCNTs was conducted. Silver nanoparticles were prepared by a volume of 50 ml 0.2M silver nitrate was added to 25 mg of functionalized MWCNTs which was dissolved in 25 ml ethanol, then sonicated and stirred for 60 min of 60 C°. The reduction process to the Ag° NPs was undertaken by the addition of 50 ml of 0.2m $NaBH_4$. The resulting products of AgNPs/MWCNTs nanocomposites were collected by centrifugation and purified by washing with deionized water and dried under vacuum at a temp. of 120 C° for 2. The Synthesis procedure is illustrated in Scheme 5.3.

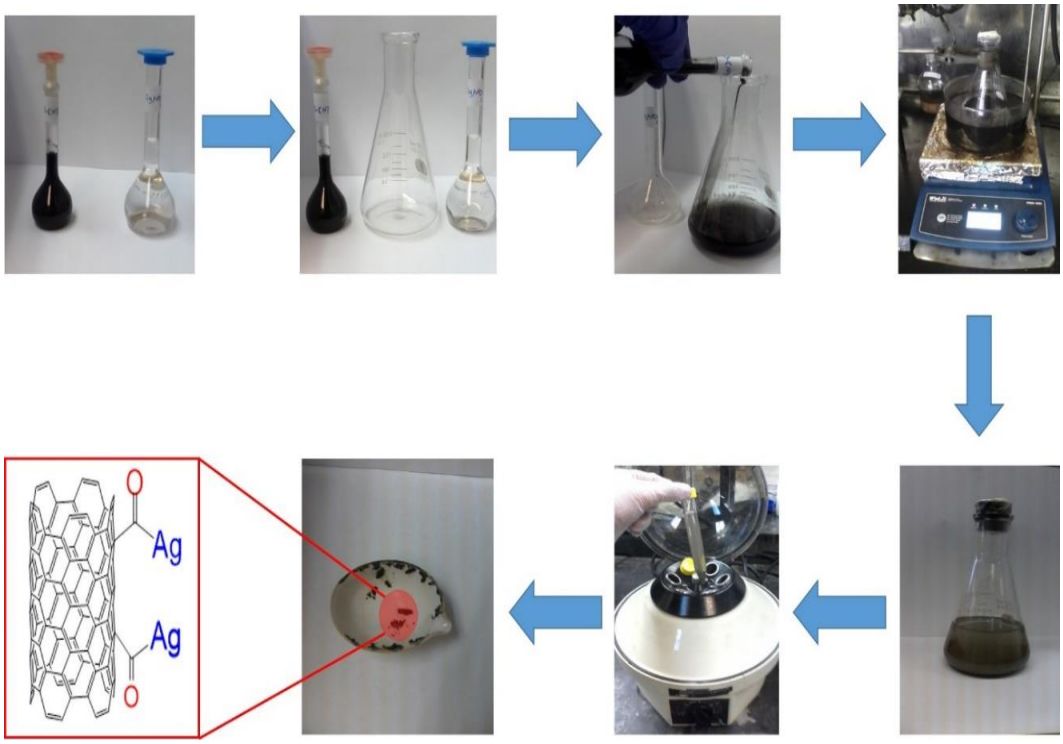

Scheme 5.3: Synthesis steps of Ag/CNT.

5.2.4. Synthesis of Silver Nanoparticle Decorated Graphene Oxide

The decoration of AgNPs on the OH^- or COOH functionalized graphene oxide was conducted. A volume of 20 ml of 0.2 M silver nitrate was added to 2mg of graphene oxide which was dissolved in 20 ml ethanol under sonication. The resulting solution was stirred for 24 hr. The reduction process to Ag° NPs was carried out by the addition of 20ml of 0.2 M $NaBH_4$ as a reducing agent and complete stirred for 12 hr. The AgNPs were decorated on surfaces of functionalized GO. The decorated solution of AgNPs/GO was heated for 1 hr. The resulting nanocomposite of AgNPs/GO was collected by centrifugation and purified by washing with deionized water and dried under vacuum at 120 C° for 2 h. Steps of preparation are shown in Scheme 5.4.

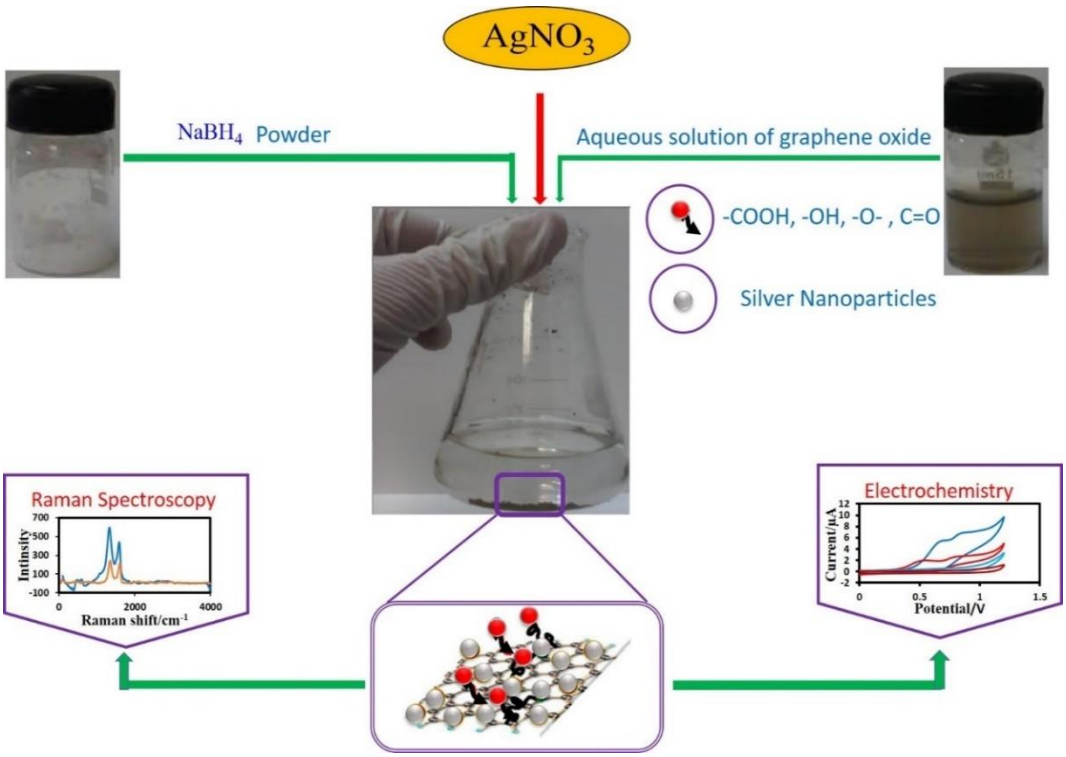

Scheme 5.4: Preparation steps of silver nanoparticles decorated graphene oxide.

5.2.5. Construction of the Modified Electrodes

The modified carbon paste electrodes (AgNPs/CPE), (AgNPs/CNT/CPE), and (AgNPs/GO/CPE) were prepared by mixing (65 %, w/w) graphite powder with (5 %, w/w) Ag nanoparticle, (5 %, w/w) AgNPs/MWCNT, and (5 %, w/w) AgNPs/GO respectively and paraffin oil (30%, w/w). Each of these mixture was placed into a plastic taps, then a copper wire was inserted.

5.3. Results and Discussions

5.3.1. Characterization of Silver NanoParticles

TEM image shows that the synthesized AgNPs are spherical particles with a diameter of 10 ± 2 nm was shown in Fig. 5.1a. SEM image shows the morphology and spherical

particles size of silver was illustrated in Fig. 5.1b. In addition, UV-Vis illustrate the absorbance peak of silver nanoparticles which was observed at 410 nm was shown in Fig. 5.1c. FT-IR shows the transmittance peak of silver nanoparticles at 430.5 nm and the O-H signal was observed at 3422.9 nm, were shown in Fig. 5.1d.

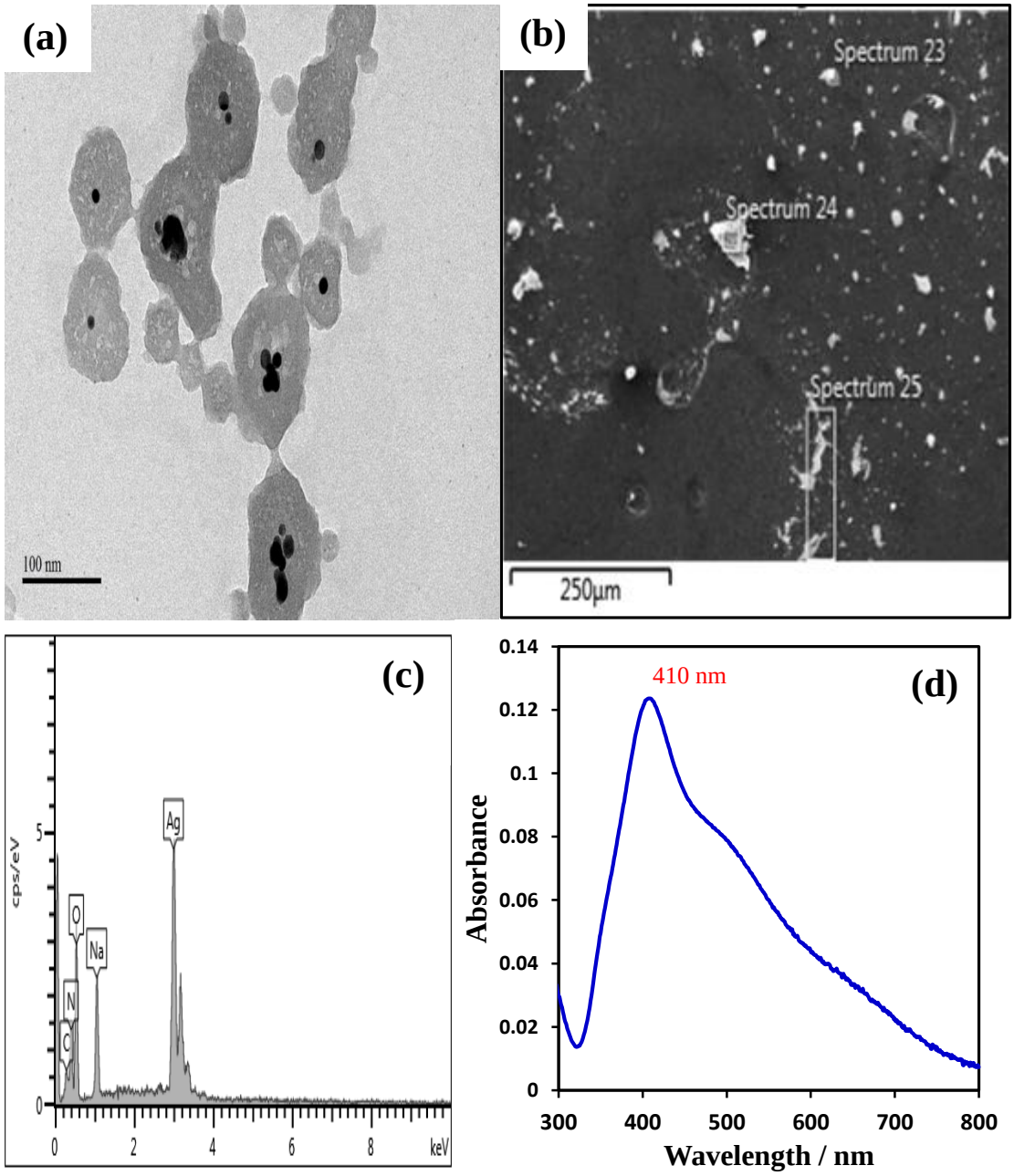

Figure 5.1: (a) TEM of AgNPs, (b) SEM of AgNPs,(c) EDX of AgNPs, and (d) UV-Vis of AgNPs.

5.3.2. Characterization of Silver NanoParticles decorated graphene Oxide

TEM image shows that the synthesized AgNPs/GO are spherical particles with a diameter of 10 ± 2 nm and scale 100 nm was shown in Fig. 5.2a. SEM image shows the morphology and homogeneous surface was illustrated in Fig. 5.2b. In addition, SEM image of liquid AgNPs/GO was showed the crystal structure of silver nanoparticles in Fig. 5.2c. EDX analysis was illustrated the chemical composition elements included in the structure of decorated silver nanoparticles with graphene in Fig. 5.2d. UV-Vis illustrate the two absorbance peak of AgNPs/GO and AgNPs were observed at 300 nm and 410 nm respectively in Fig. 5.2d. FT-IR shows the transmittance peak of different functional groups such as C=C observed at 1732 nm and O-H signal observed at 3422.9 nm for both Go and AgNPs/GO was shown in Fig. 5.3. Raman spectroscopy was illustrated the composition structure of graphene oxide and AgNPs/GO were observed two peaks; one that In-phase vibration (G band) of both GO and AgNPs/GO at 1567 nm and the disorder band (D-band) of both GO and AgNPs/GO at 1339nm. Furthermore, the ratio intensity was shower is more intensity of decorated silver nanoparticles with graphene oxide and the G band was decreased due to the fragmentation occurs as attributed the silver nanoparticles binding with the carboxyl group of GO were observed in Fig. 5.4.

XPS analysis was performed to investigate the chemical state of GO and GO-Ag nanocomposite. In Figure 5.5a, the survey spectra clearly indicate the existence of C, O in GO and C, O, Ag in GO-Ag nanocomposite. The C 1s XPS core level spectrum of GO nanosheets is displayed in Figure 5.5b. It can be deconvoluted into four components with binding energy at 284.8 eV (C=C/ C−C in aromatic ring), 286.90 eV (C−O−C), 288.4 eV (C=O), and 289.3 eV (HO−C=O). These results indicated that there are a large number of

functional groups on the surface of GO nanosheets. The C 1s and Ag 3d XPS core level spectra of GO-Ag nanocomposite are shown in Figure 5.5c, d. The C 1s core level XPS spectrum can be deconvoluted into four components with binding energies at 285.0, 287.1, 288.5, and 289.3 eV assigned to C=C, C−O, C=O, and HO−C=O, respectively (Figure5c). The intensity of the band at 287.1 eV (C−O) decreased which indicates the partial reduction of GO nanosheets to graphene nanosheets. As shown in Figure 5.5d, XPS spectra clearly show the concision of elemental Ag and the elemental status of Ag (3d). The Ag (3d) peaks are a doublet which arises from spin-orbit coupling (3d5/2 and 3d3/2). The binding energies of Ag 3d5/2 and Ag 3d3/2 peaks are 368.76 and 374.79 eV, respectively, which prove clearly that silver is present only in metallic form, indicating the formation of AgNPs on the surface of GO nanosheet.

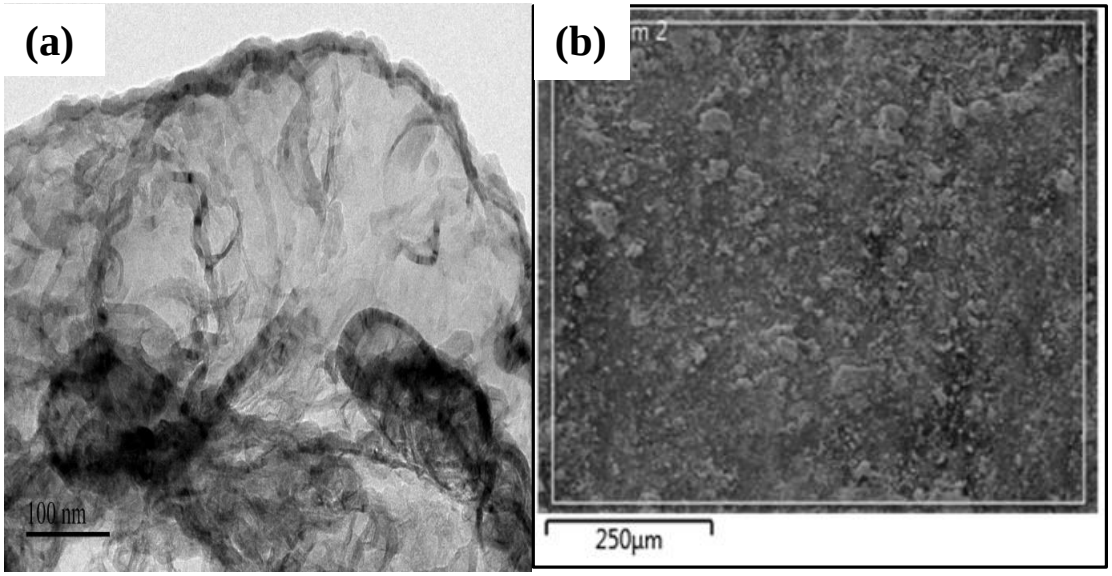

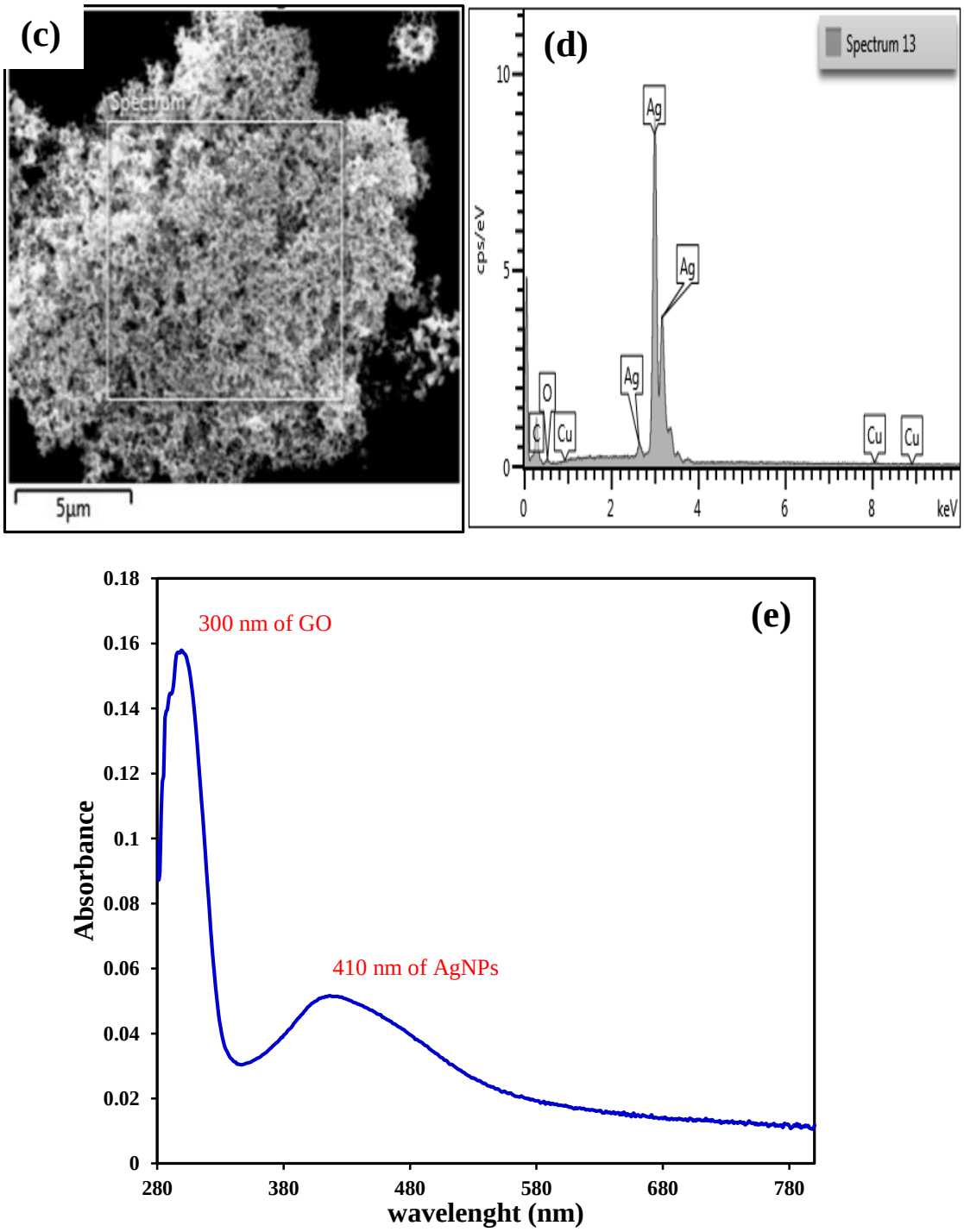

Figure 5.2: (a) TEM of AgNPs/GO (b) SEM of solid decorated AgNPs/GO (c) SEM of liquid decorated AgNPs/GO, (d) EDX of liquid AgNPs/GO, and (e) UV-Vis of AgNPs/GO.

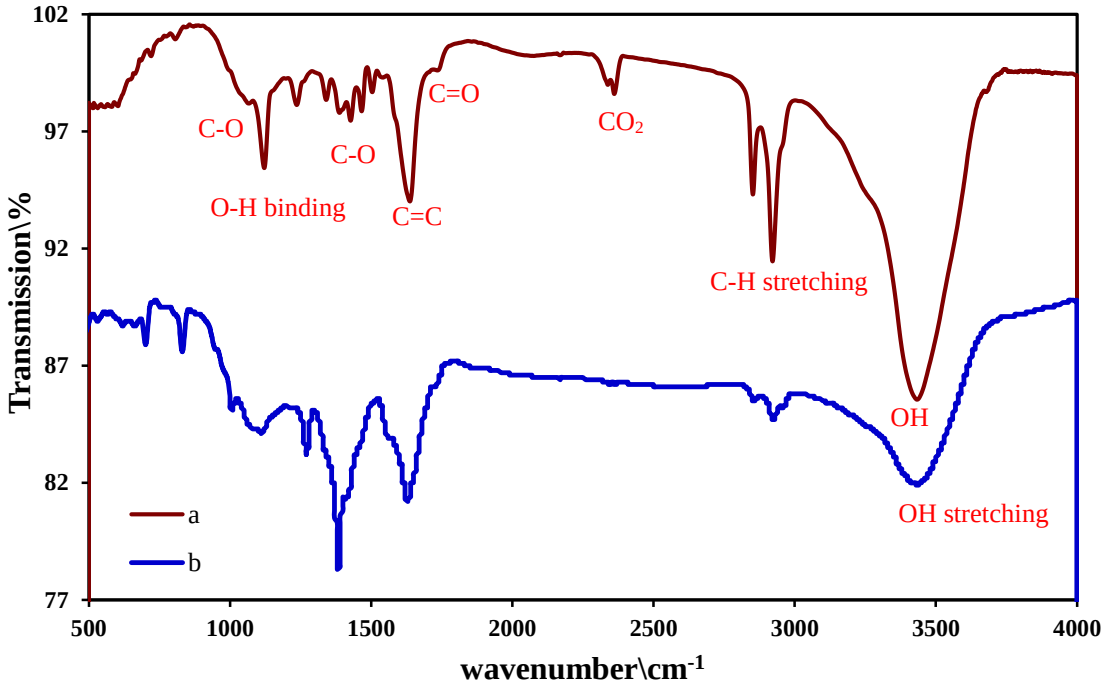

Figure 5.3: IR of (a) GO and (b) AgNPs/GO.

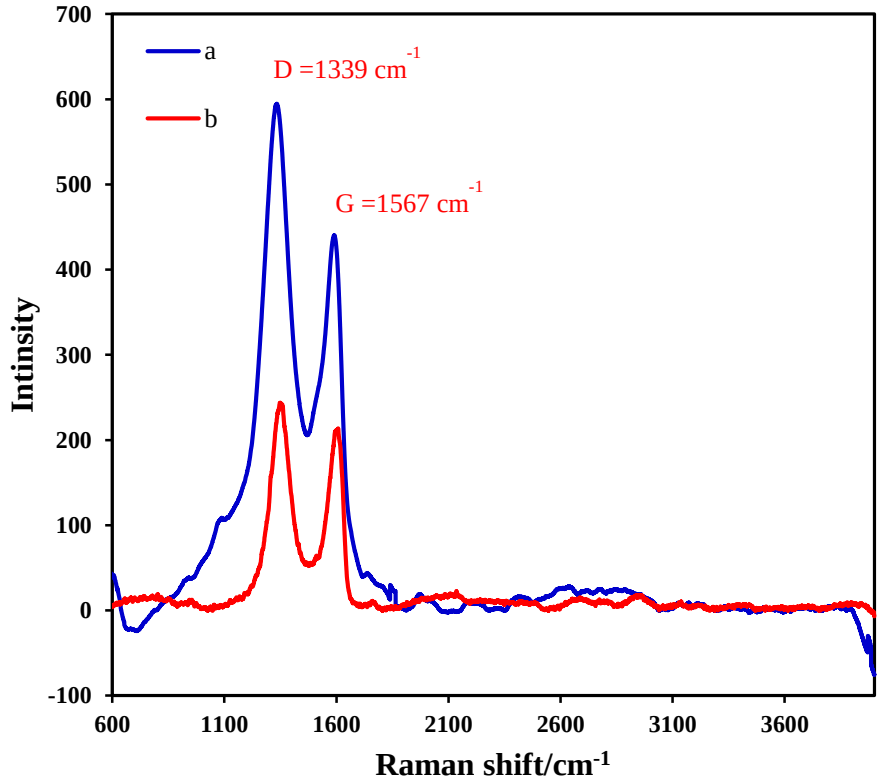

Figure 5.4: Raman of (a) AgNPs/GO and (b) GO.

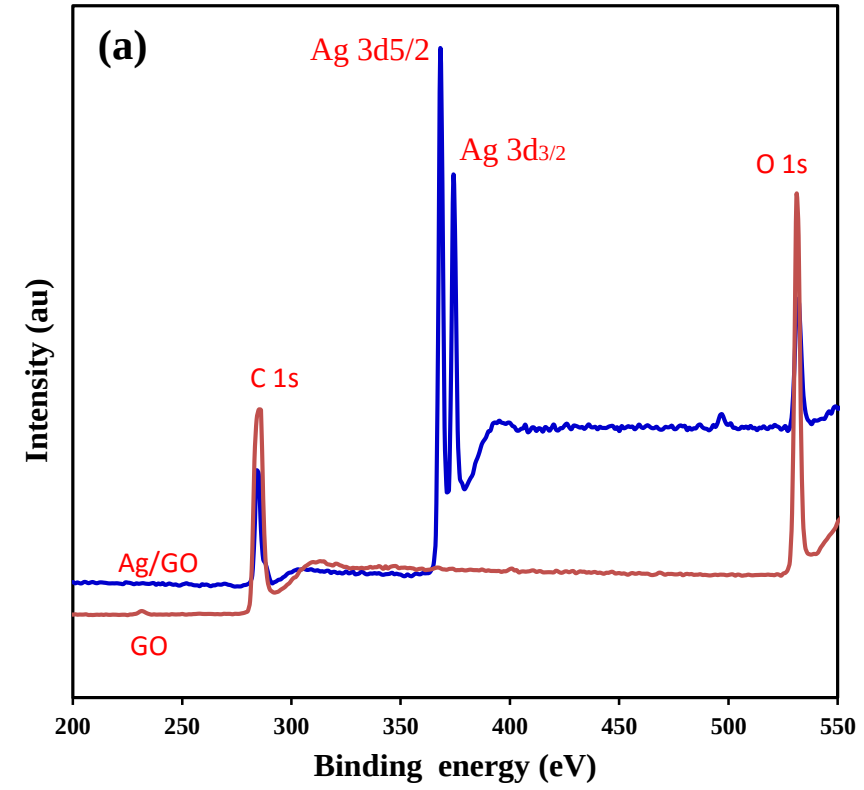
(a)
Ag 3d5/2
Ag 3d3/2
O 1s
C 1s
Ag/GO
GO
Intensity (au)
200
250
300
350
400
450
500
550
Binding energy (eV)

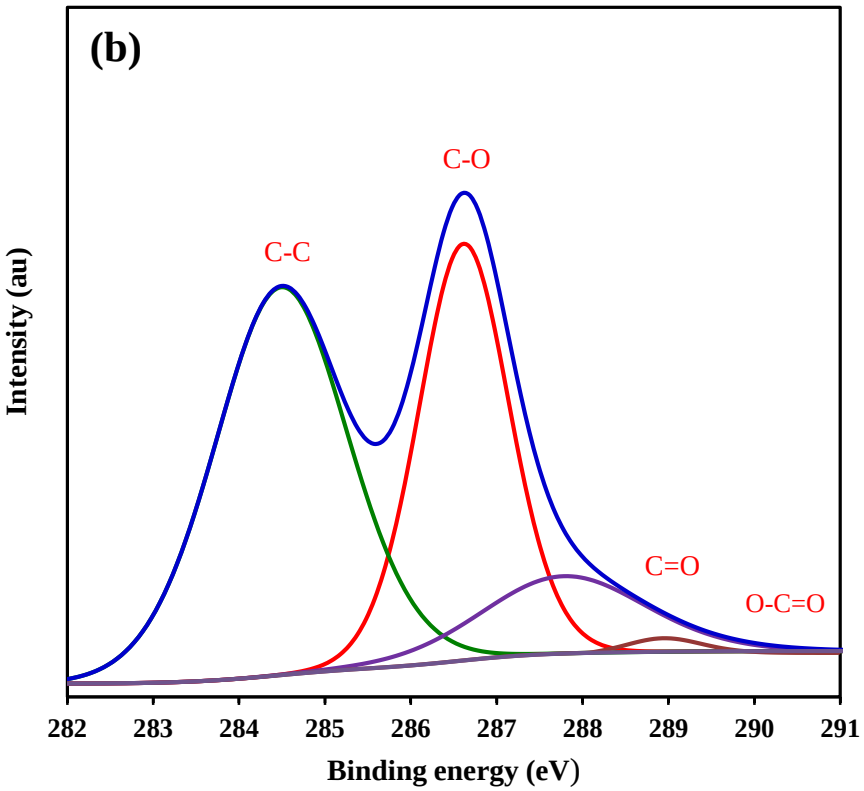
(b)
C-O
C-C
C=O
O-C=O
Intensity (au)
282
283
284
285
286
287
288
289
290
291
Binding energy (eV)

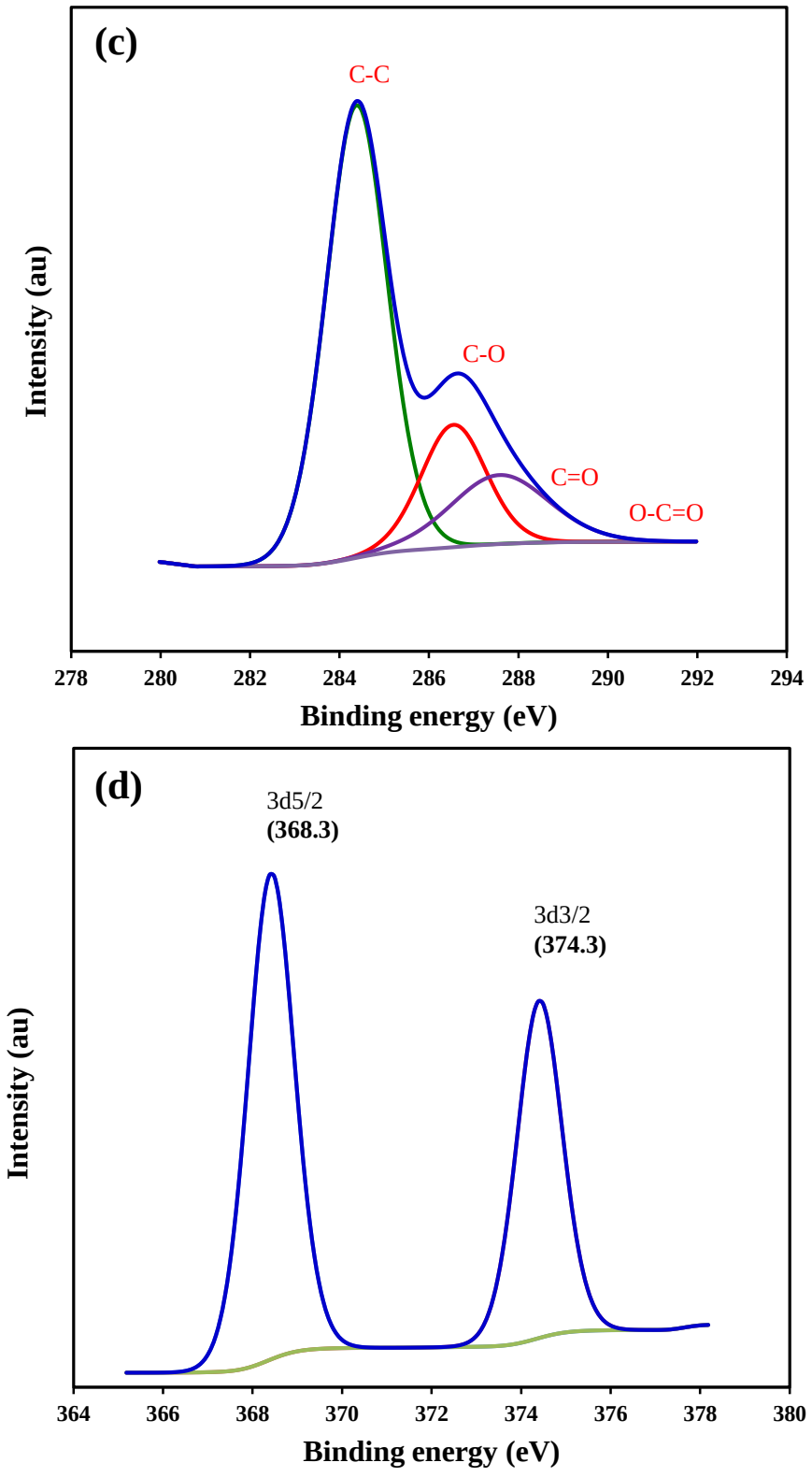

Figure 5.5: XPS survey scans of GO and AgNPs/GO (a), C 1s XPS spectra of GO nanosheets (b) and AgNPs/GO(c), and Ag 3d core level spectrum of AgNPs (d).

5.3.3. Characterization of O-CNTs and AgNPs/CNTs

SEM image shows the morphology and homogeneous surface of functionalized carbon nanotubes were shown in Fig. 5.6a. In addition, SEM image of AgNPs/CNTs was showed the crystal structure of silver nanoparticles in Fig. 5.6b. Raman spectroscopy was illustrated the composition structure of CNTs and AgNPs/CNTs were observed two peaks; one that In-phase vibration (G band) of both CNTs and AgNPs/CNTs at 1567 cm^{-1} and the disorder band (D-band) of both CNTs and AgNPs/CNTs at 1339nm. The peak at 2D was observed at 2700 cm^{-1} for both O-CNTs and AgNPs/CNTs Furthermore the ratio intensity was shower is more intensity of decorated silver nanoparticles with graphene oxide and the G band was decreased due to the fragmentation occurs as attributed the silver nanoparticles binding with the carboxyl group of CNTs were observed in Fig. 5.7.

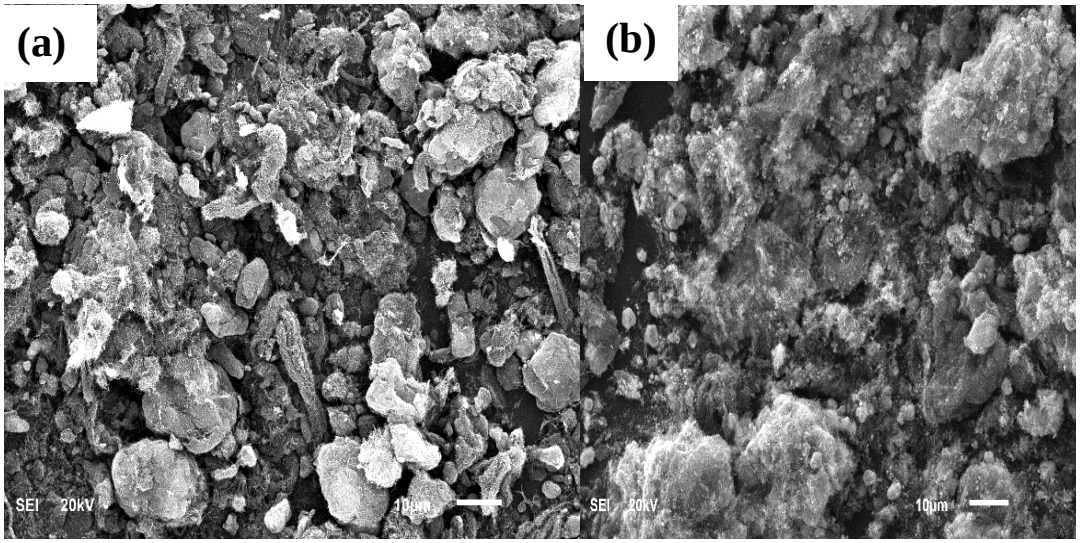

Figure 5.6: (a) SEM of O-CNT at high magnification 10 μm and (b) SEM of decorated AgNPs/CNT at high magnification 10 μm.

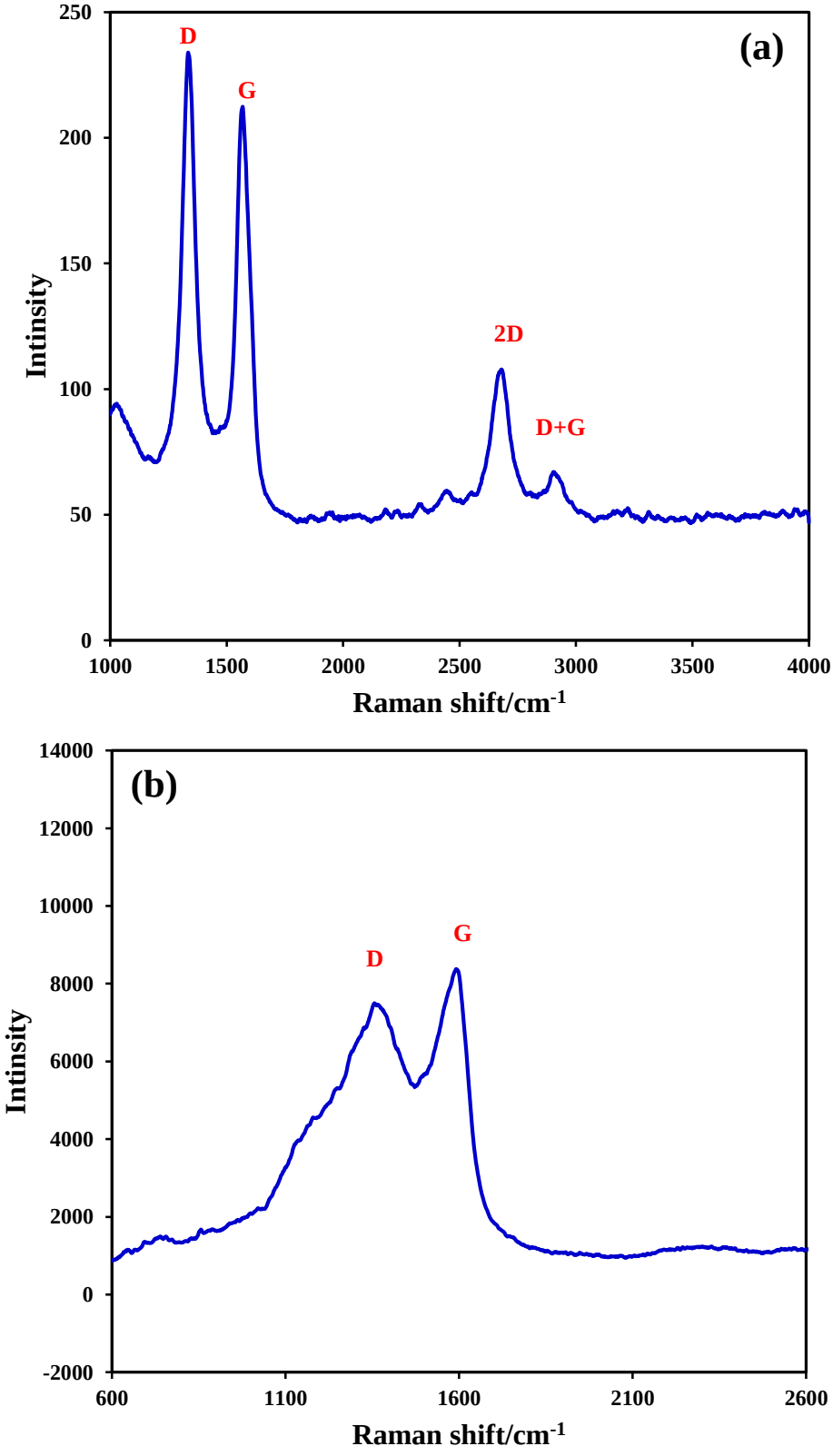

Figure 5.7: Raman of (a) MWCNT, (b) AgNPs/CNTs.

5.3.4. Characterization of Modified Carbon Paste Electrodes

The SEM images for the composite of AgNPs/CPE electrode was showed microstructures grain of silver nanoparticles and the homogeneous surface with a crystal structure was shown in Fig. 5.8a. In addition, the SEM of composite AgNPs/GO/CPE electrode illustrates the grain particles of silver nanoparticles, the morphology of homogeneous surface was shown in Fig. 5.8b. SEM of AgNPs/CNTs/CPE was shown the diameter scale of analysis 10 μM and clear to observed grains o silver nanoparticles in Fig. 5.8c

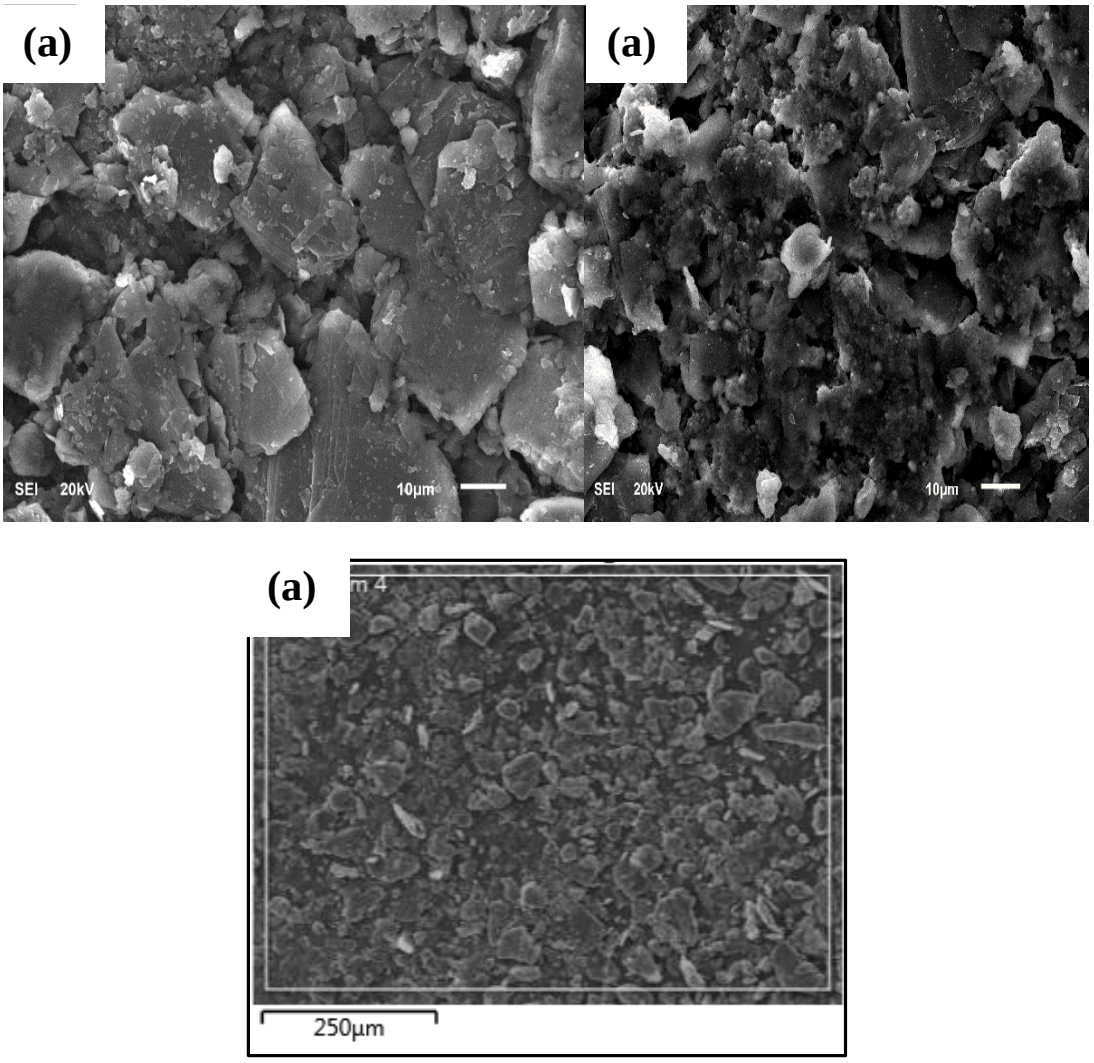

Figure 5.8: SEM images of (a) SEM images of AgNPs/CPE electrode at 10 μM, (b) SEM image of AgNPs/CNTs/CPE at 10 μM and (c) AgNPs/GO/CPE electrode at 250μm.

5.3.5. The Performance of AgNPs/GO/CPE Electrodes

The MMZ accumulation at modified AgNPs/GO/CPE electrode was depended on the nature of adsorption of MMZ on the surface of the electrode. However, the percentage composition of AgNPs/GO/CPE in the composite mixture plays a significant effect on the voltammetric responses. Therefore, the effect of the AgNPs/GO/CPE on the intensity of current was obtained by applying cyclic voltammetry. Three composite electrodes containing various amounts of AgNPs/GO/CPE (5 %, 10 %, and 20% w/w) were constructed of carbon pastes composite. The behavior of these electrodes in CV was investigated. It was found that the 5% AgNPs/GO/CPE in the composite gives a higher response. Fig. 5.9 illustrated the various percentage for the different electrode.

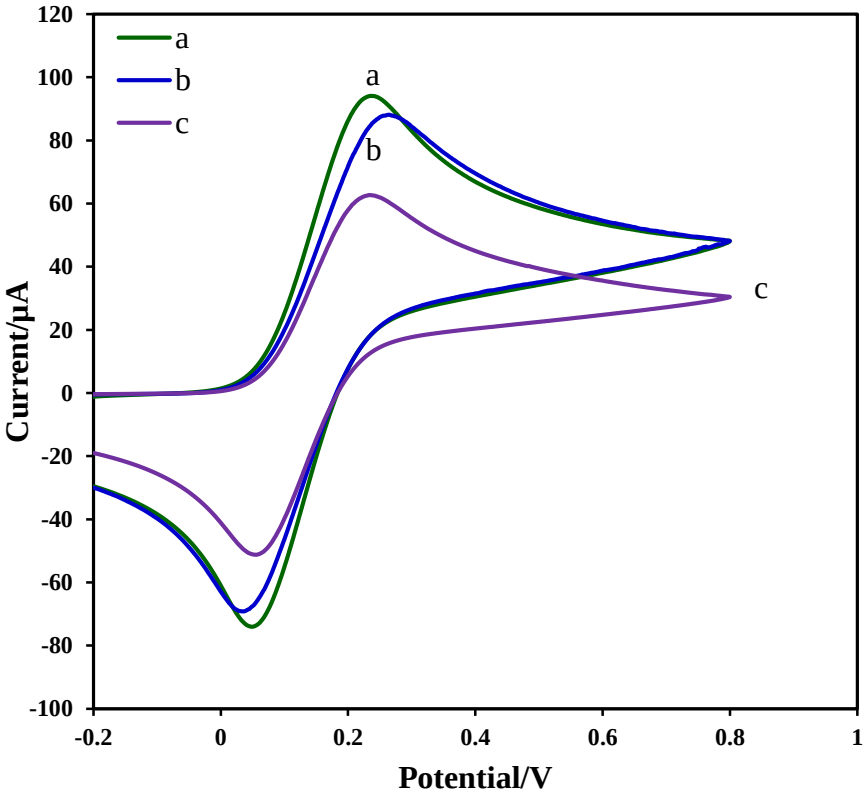

Figure 5.9: CVs of 0.02 M $[Fe(CN)_6]^{3-/4-}$ using (a), 60% graphite with 10 % AgNPs/GO 65 % graphite with 5 % AgNPs/GO (b), and 50 % graphite with 20 % AgNPs/GO (C). The percentage of oil is fixed in a, c, and d are equal 30% and experimental condition 0.5M phosphate buffer solution pH 4.0 and scan rate 100 mV/s.

5.3.6. Comparison of AgNPs/GO/CPE and CPE Electrodes

Cyclic voltammetry is sensitive and was applied to compare the response two types of electrodes. The first electrode is a bare CPE and the second is AgNPs/GO/CPE electrode in 0.02 M $K_4Fe(CN)_6$. The modified (AgNPs/GO/CPE) has shown the high current response of the signals for both anodic and cathodic reactions. This is due to the high rate of electron transfer. At a scan rate of 100 mV/s. The results are shown in Fig. 5.10 where the performance of the modified is much better than the bare electrode.

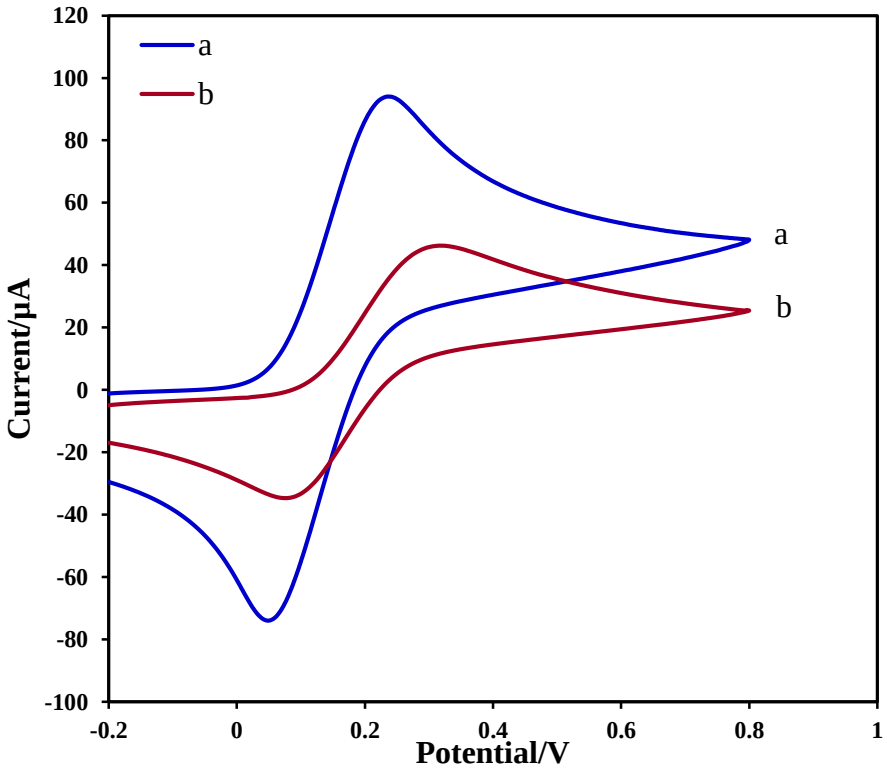

Figure 5.10: CVs of 0.1 M $[Fe(CN)_6]^{3-/4-}$ using (a) AgNPs/GO/CPE (b), and CPE, a scan rate of 100 mV/s.

5.3.7. Electrochemical Enhancement of MMZ on Different Surface of Electrodes

Cyclic voltammetric techniques were utilize to illustrate the oxidation process on the various surface of modified electrode AgNPs/GO/CPE, AgNPs/CPE, and AgNPs/CNT/CPE were applied the CV of 0.001 M of MMZ. The first electrode (AgNPs/GO/CPE) shows two oxidation peaks at 0.67 V and 0.85 V resulting from oxidation of a sulfur atom. The second electrode (AgNPs/CNT/CPE) shows one oxidation peak at 0.75 V due to the geometry of CNTs compare with graphene oxide and this lead to reduce two oxidation peaks to one oxidation peak. The third electrode (AgNPs/CPE) shows two oxidation peaks at 0.58 V and 0.85 V due to the electron transfer occurs at sulfur atom in the structure of MMZ. As are shown in Fig. 5.11.

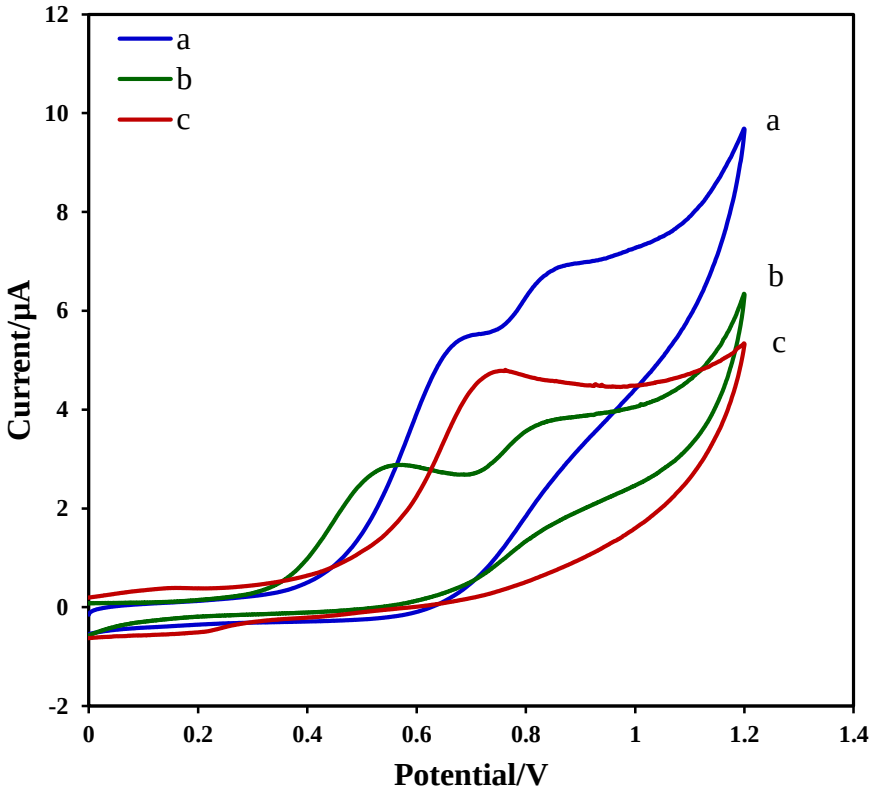

Figure 5.11: CVs of 1.0 mM MMZ at different modified electrodes, (a) AgNPs/GO/CPE, (b) AgNPs/CPE, and (d)AgNPs/MWCNT/CPE. Scan rate 100 mV/s, and pH 4.0.

5.3.8. Electrochemical Enhancement of MMZ on the Surface of AgNPs/GO/CPE

To investigate the enhancement resulting by modifying the CPE with Ag/GO and the bare CPE with its blank are shown in Fig. 5.12. Two oxidation anodic peaks of 1.0 mM MMZ are shown CV curve (a). The drug (MMZ) was electro-active species at the surface of CPE in this electrolyte solution containing 1.0 mM of MMZ. The presence of silver nanoparticle in nanocomposite increases the surface area of AgNPs/GO nanocomposite and enhanced the adsorption of MMZ on the surface of modified electrode and also improves the sensitivity of the oxidation peaks. The sulfur atom in methimazole structure (MMZ) plays a role in the adsorption of MMZ on the surface of a modified electrode (AgNPs/GO/CPE) with a scan rate 100 mV/s.

The effect of scan rates on the oxidation current peak (Ip) and the potential peak (Ep) of MMZ was investigated (Fig. 5.13). The better linearity relationship between (ip) and the scan rate (υ) over a scan range from (20 – 260) mVs^{-1} with a correlation coefficient (R^2 = 0.995). The electro-oxidation current peak of 0.001 M MMZ adsorbed on the Ag/GO/CPE electrode was found to increase the scan rate. The potential was found to shift to more positive values due to the irreversible oxidation process. The plot of (Ep = 0.0066x + 0.1195), gives a slope of 0.0066.

The plot of values of log current (Ip) versus log scan rate (ν) in a scan rate range of 20- 260 mV/s yielded a straight line with a slope of 0.7 and a colleration coefficient of 0.988. This value is close to the theoretical value of 0.5 expected for an ideal reaction condition for a diffusion-controlled electrode process. In addition, the graphs of anodic current (Ipa) versus scan rate (ν) and anodic current (Ipa) versus square root of the scan rate ($ν^{1/2}$) are shown in (Fig. 5.14) have better linearity. In the range of (20 –260) mV/s, the anodic peak

currents were proportional to the scan rate. The correlation coefficient (R^2) was found to be 0.9953 (n = 13) and 0.974 (n = 13), which indicates that the electrode reaction is of diffusion controlled.

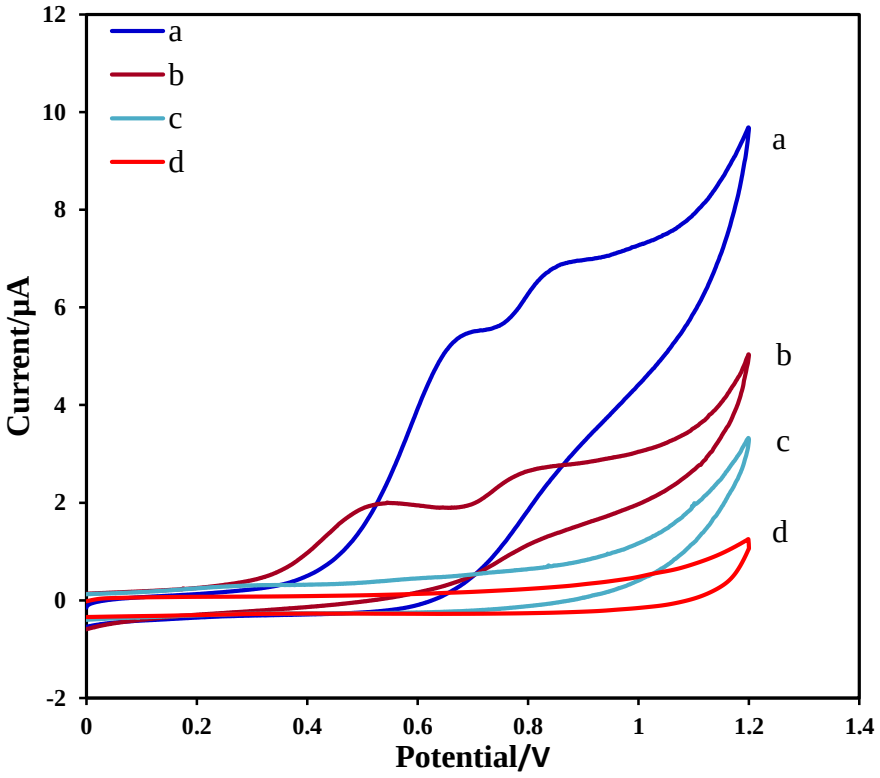

Figure 5.12: Cyclic voltammograms of 1.0 mM MMZ (a) 1.0 mM of MMZ at AgNPs/GO/CPE electrode (b) 1.0 mM of MMZ at CPE electrode (c) blank solution of MMZ at Ag/GO/CPE (d) blank solution of MMZ at CPE. Experiment conditions: 0.5 M phosphate buffer solution with pH 4.0 and scan rate was 100 mV/S.

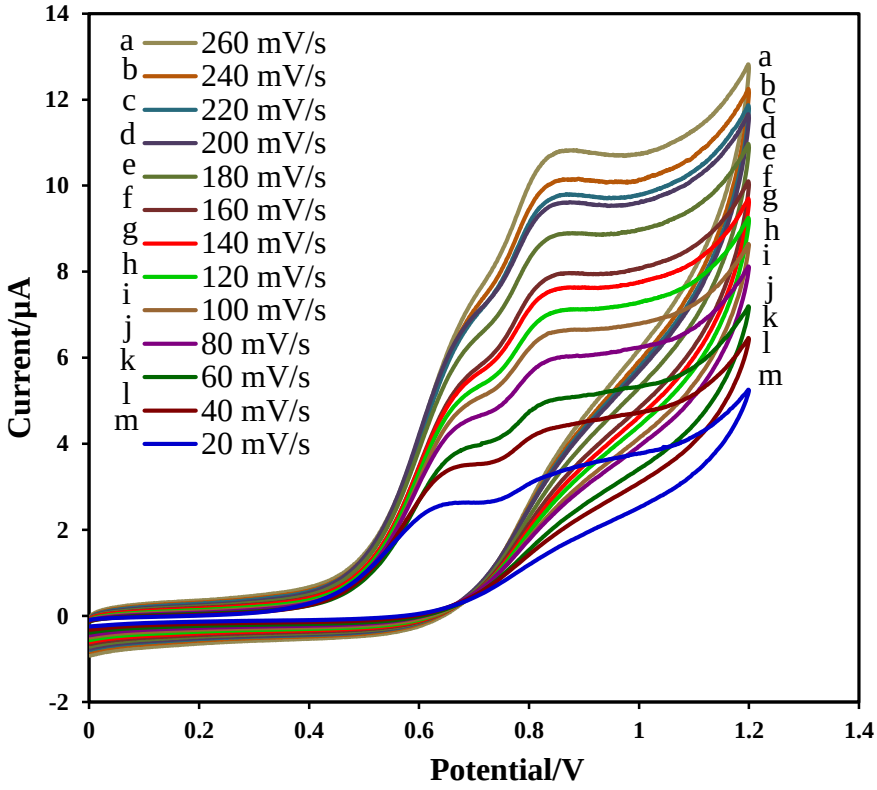

Figure 5.13: Cyclic voltammograms at different scan rates and anodic current versus scan rate of MMZ at AgNPs/GO/CPE as working electrode. The solution contains 1.0 mM of MMZ in 0.5 M phosphate buffer solution with pH 4.0.

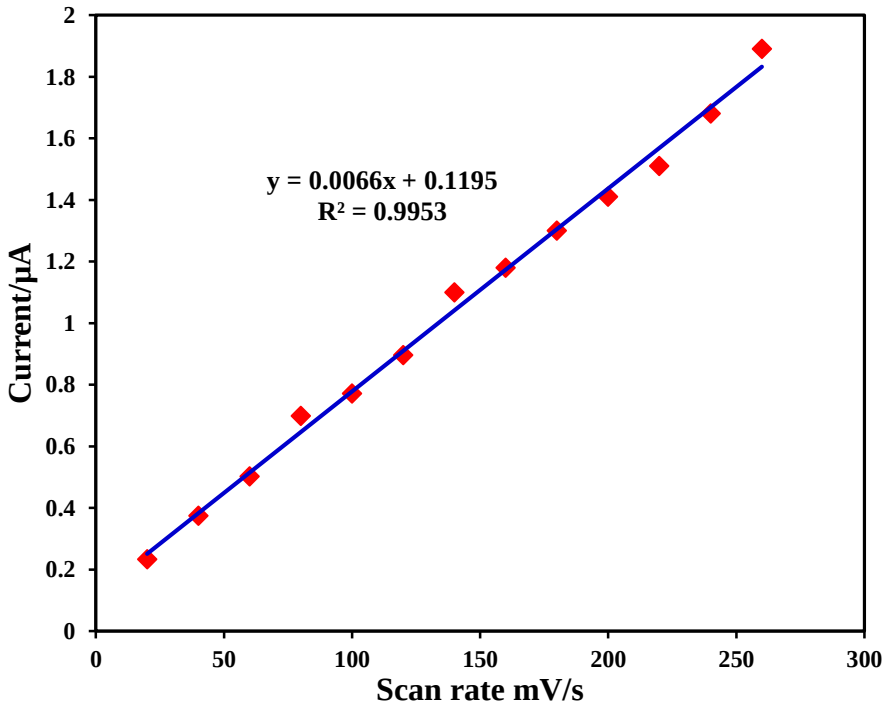

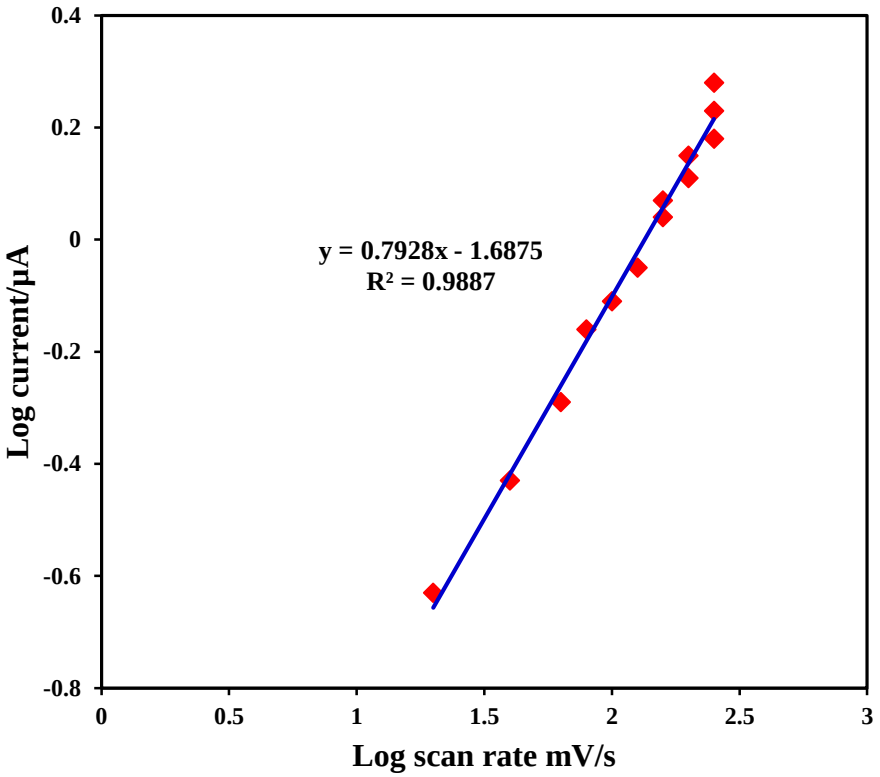

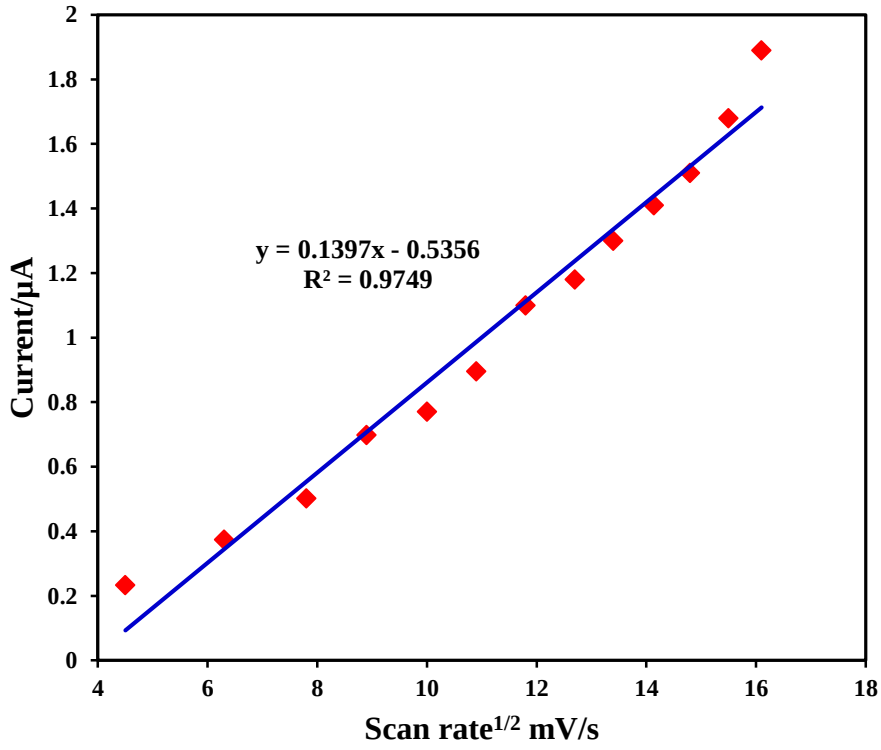

Figure 5.14: (a) The anodic current (Ip) versus scan rate (υ) of MMZ at AgNPs/GO/CPE electrode. Scan rate from (20,40,60,80,100,120,140,160,180,200,220,240,260) mV/s respectively. Solution contains 1.0 mM of MMZ in 0.5 M phosphate buffer solution with pH 4.0. (b)Plot of Ipa versus $\nu^{1/2}$ of MMZ.

5.3.9. The pH Influence

Appling cyclic voltammetry at buffers of pH 3, pH 4, pH5, pH 6, and pH 7 of 1.0 mM of MMZ at AgNPs/GO/CPE electrode. Two oxidation peaks have appeared at 0.697 V which is irreversible. Furthermore, two oxidation peaks were observed at pH 3 and pH 4 which are irreversible, while one oxidation peaks were observed at pH 5, pH 6, and pH 7 which are irreversible. The potential of the anodic peaks (Ep) of MMZ is shifted toward negative values with increasing pH above 7.0 (Fig. 5.15) by a slope of 0.05 V/pH. The linearity of the Ep/pH plot intersects at about 4 which are thought to correspond to the pKa1 value of MMZ.

The linear regression equations are Epa (V) = 0.884 - 0.05 pH for pH range of (3.0 –7.0), with the correlation coefficients 0.902. The slope of - 0.057 V/pH of 1.0 mM of MMZ oxidation indicating that the number of electrons and protons involved in the reaction mechanisms is the same and containing two electrons with two protons in the pH range of 3 to 7 were shown in Fig. 5.16. These results further indicate that proton takes part in the electrochemical reaction of MMZ. Furthermore, the electrochemical oxidation of MMZ undergoes 2 e^- transfer process. The buffer pH 4.0 was chosen for the assaying of MMZ and the results were investigated in the mechanism was proposed for electro-oxidation reactions of MMZ (Scheme 5.5).

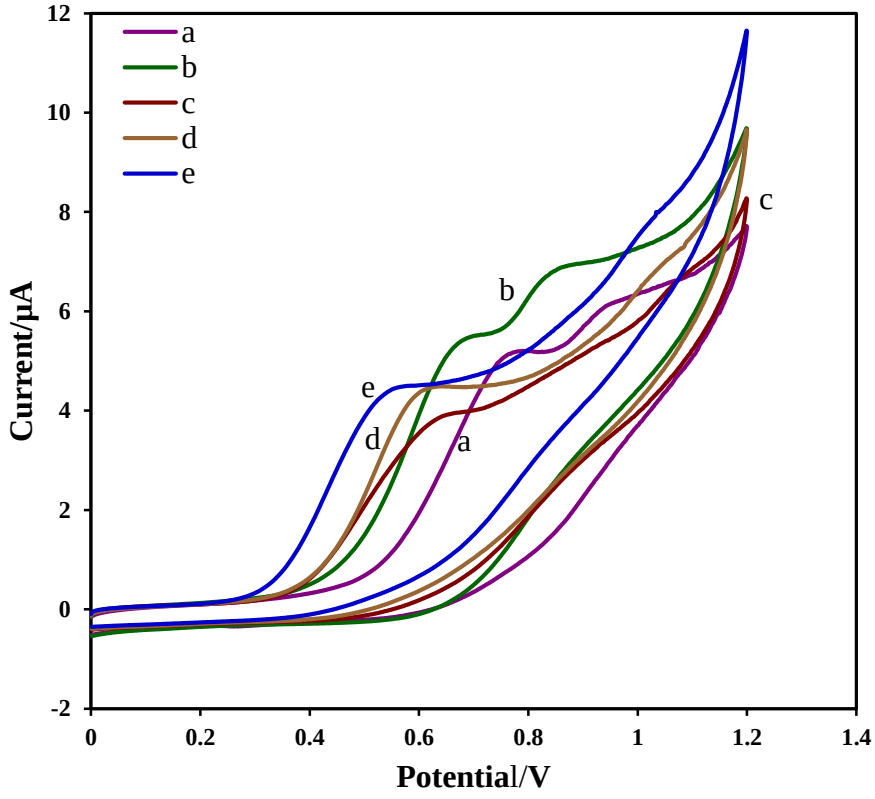

Figure 5.15: Influence of different pH buffer of 1.0 mM MMZ solutions from range (a) pH 3, (b) pH 4, (c) pH 5, (d) pH 6, and (e) pH 7, on the cyclic voltammetry oxidation peak current. Optimum conditions are 100 mV/S scan rate and pH 4.0.

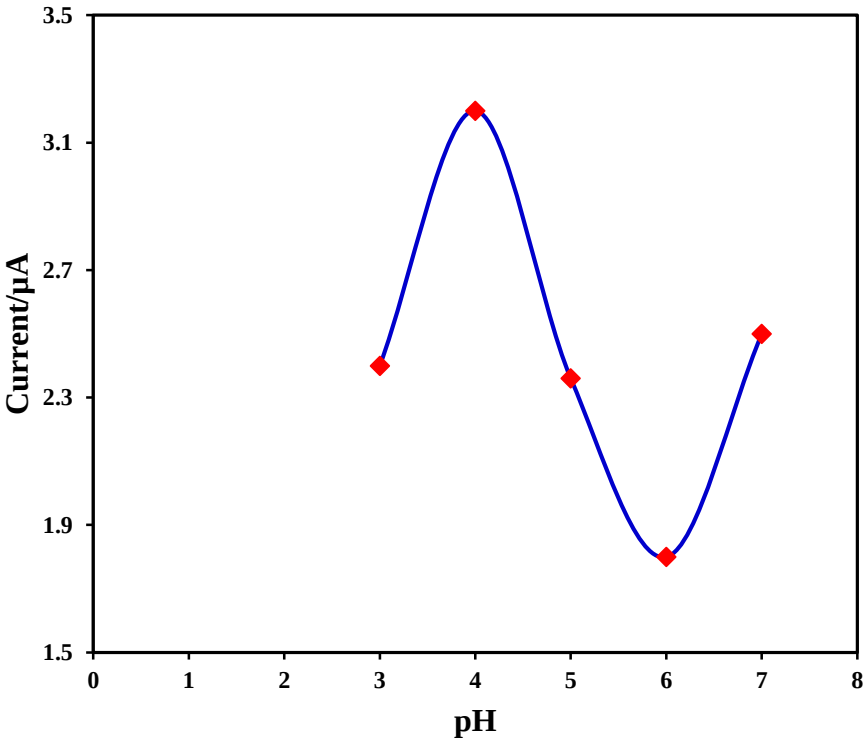

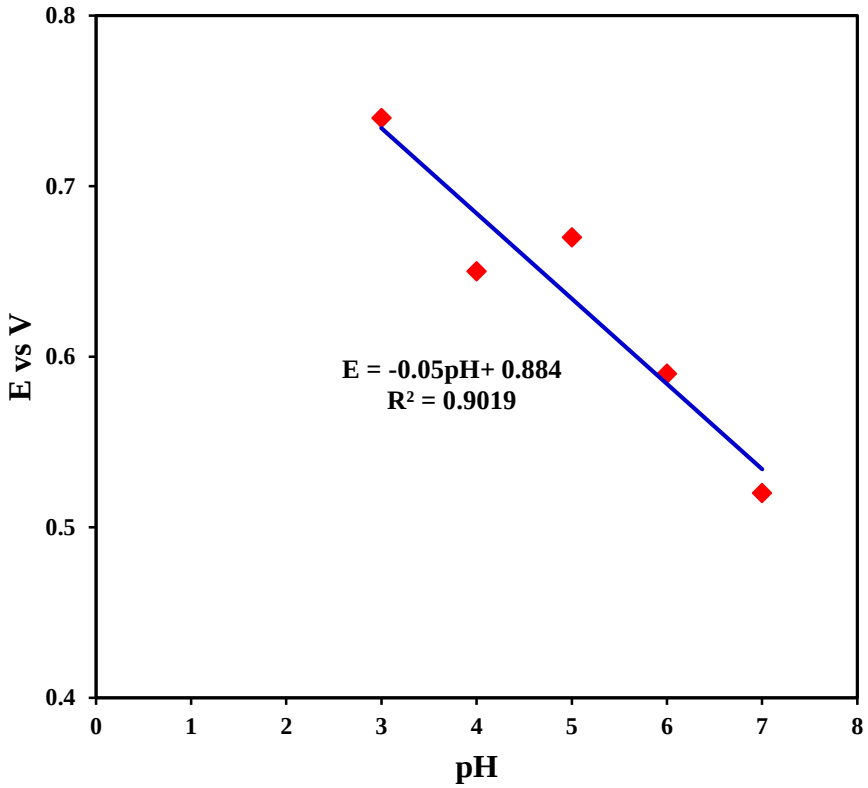

Figure 5.16: Effect of the different pH buffer of 1.0 mM MMZ solutions on cyclic voltammetry (CV) anodic oxidation peak current. Optimum condition is the values of 100 mV/S scan rate.

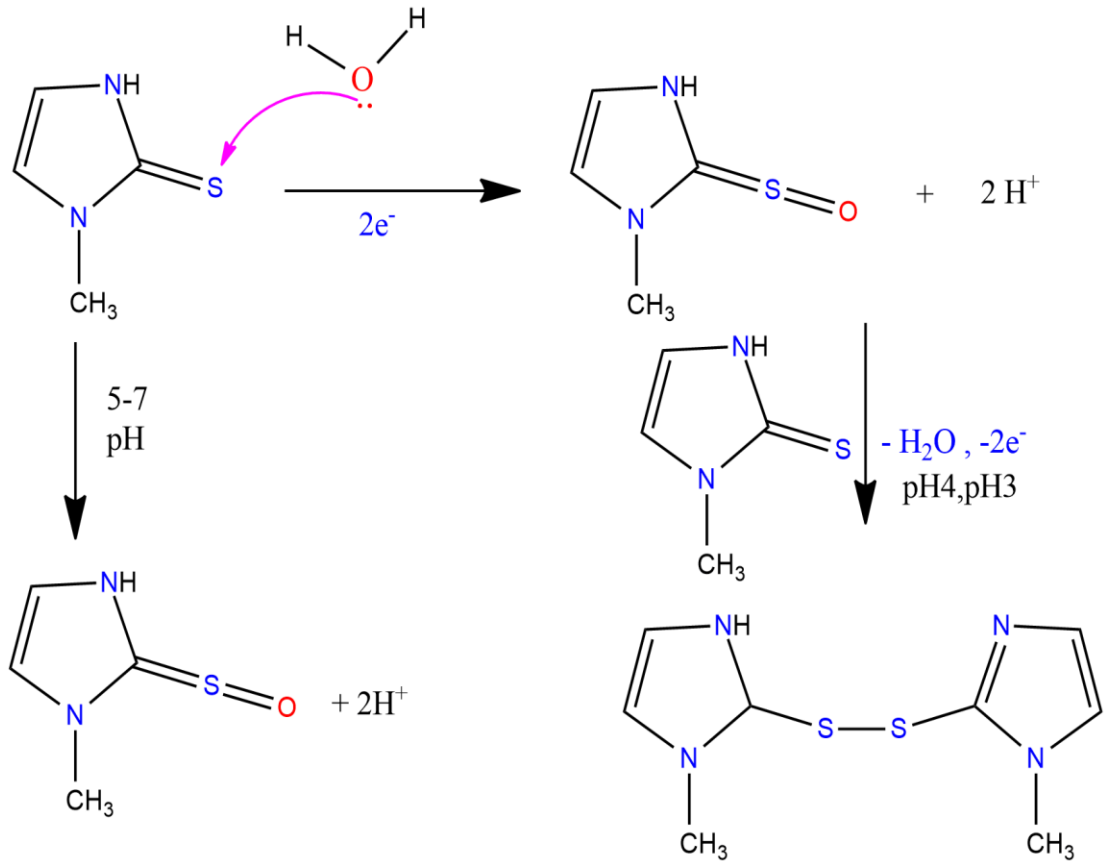

Scheme 5.5: Mechanism of electrochemical oxidation of methimazole

5.3.10. Amperometric Detection of MMZ on AgNPs/GO/CPE

Amperometry was used to calculate the diffusion coefficient of MMZ on the surface of the AgNPs/GO/CPE electrode. Fig.5.17. Illustrate the relation between the current and the time (s) and a linear relationship between the current response and concentration was obtained. The correlation coefficient of 0.9936, and a slope of 0.0114.

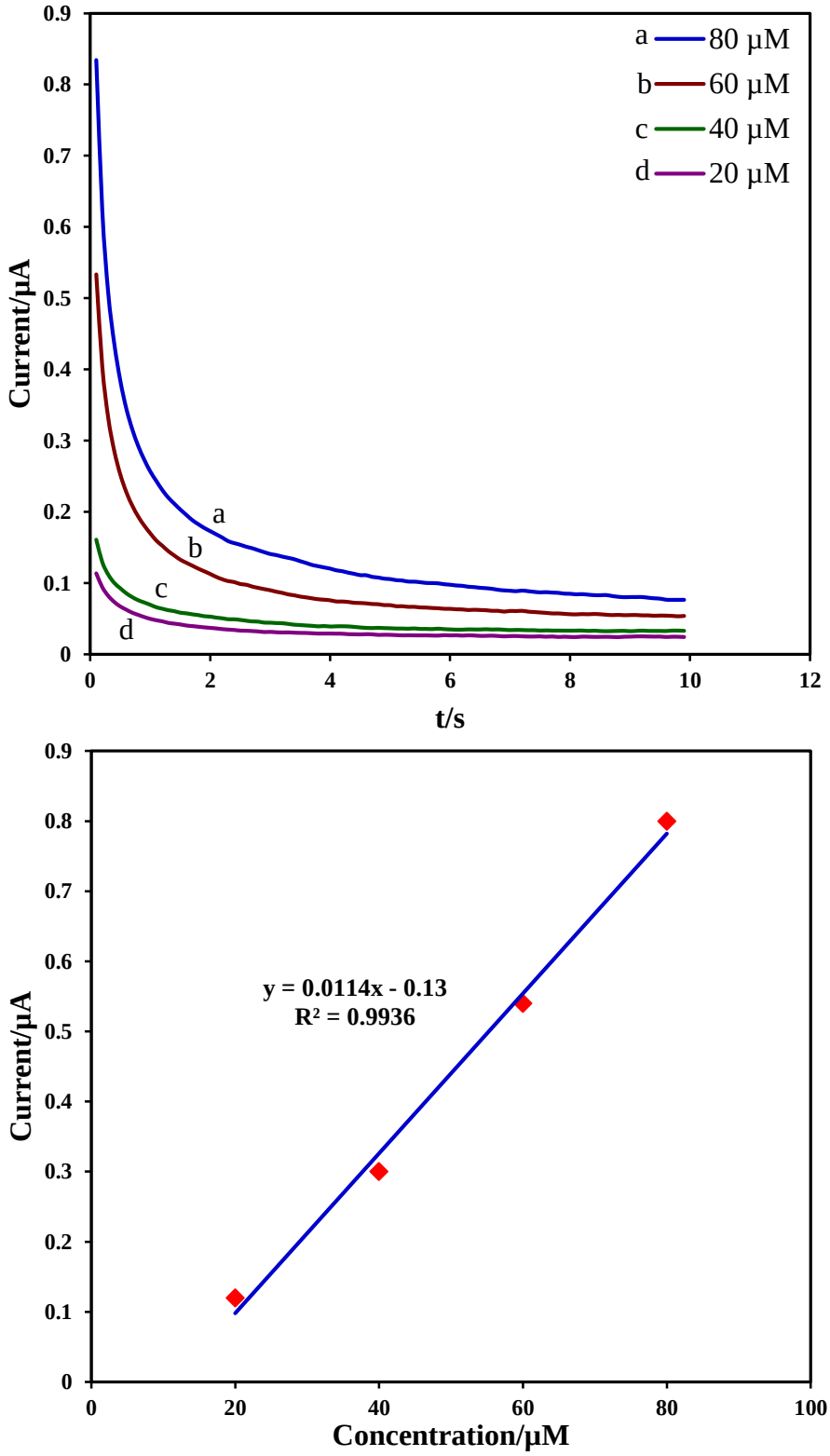

Figure 5.17: Amperometry i-t curve obtained for AgNPs/GO/CPE and concentrations of MMZ from (bottom to top 20, 40, 60 and 80 µM) MMZ in phosphate buffer pH4.0. Optimum condition of time at 10 second.

5.3.11. Square Wave Voltammetry Detection of MMZ at AgNPs/GO/CPE

The voltammetric parameters that affect the square wave voltammetry (SWV) technique in the determination of MMZ was investigated. Theses parameters included the amplitude, the increment, and the frequency. Fig. 5.18 shows SWV voltammogram of various concentrations of MMZ at AgNPs/GO/CPE using the optimum parameters. The better linearity relationship between intensity current of anodic peak and the concentration of MMZ in the range of (1 – 80) µM was observed. The linear equation is $I = 0.0826C_{(MMZ)} + 1.1444$, correlation coefficient of ($R^2 = 0.9901$), where Ia is the current of the anodic peak in µA and C is the concentration of MMZ in µM. the relation ks/m was used to calculate the limits of detection (LOD), where k = 3 for LOD and 10 for LOQ, (S) representing the standard deviation of the peak currents of the blank (n = 3) and the slope of the calibration curve of MMZ was 0.0826. The LOD was calculated from the relation of the standard deviations of the blank and the mean of the blank. The LOD value found to be 0.684 µM calculate from equation ($mean + 3SD_b$) in the analysis of MMZ.

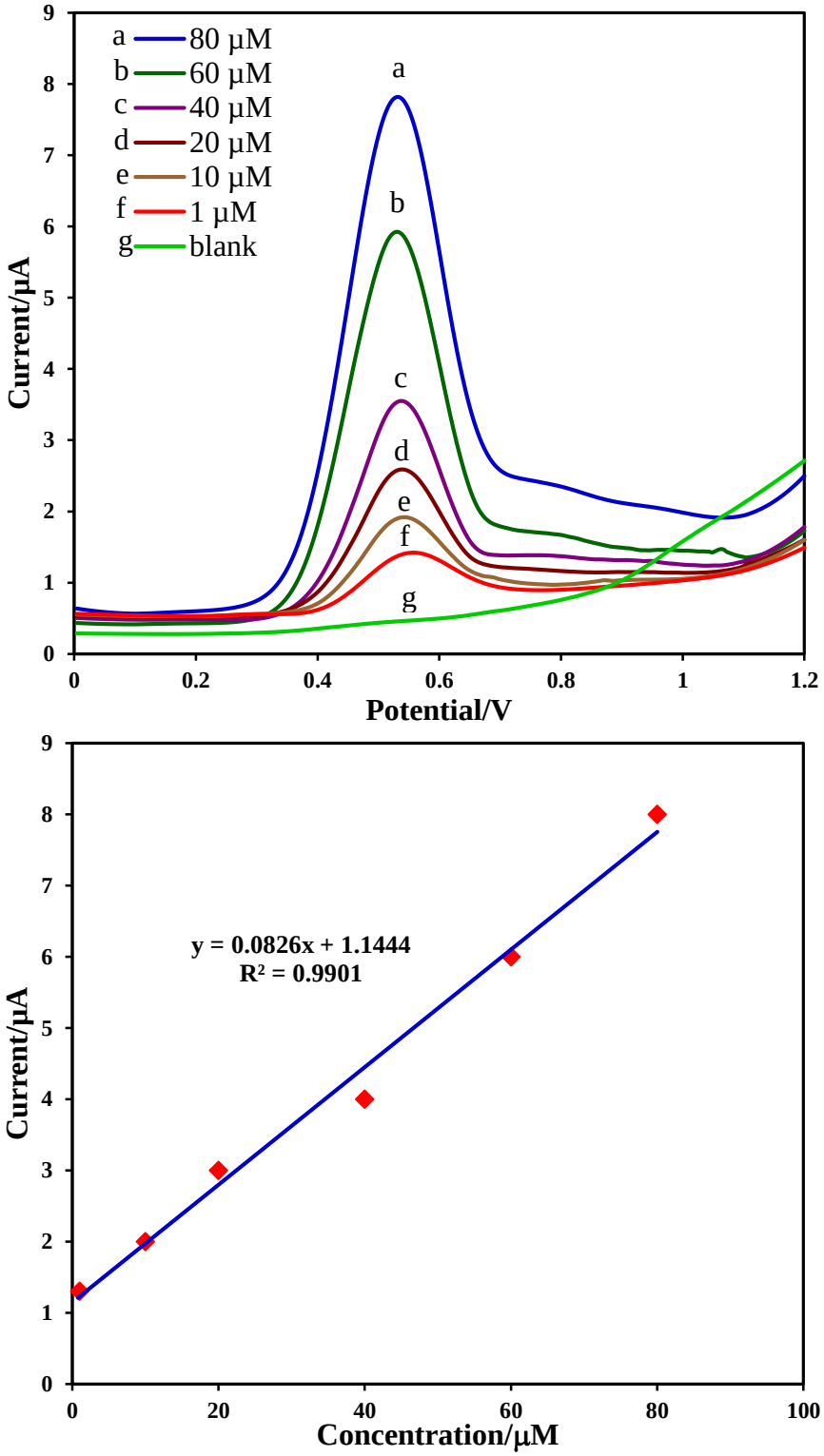

Figure 5.18: Square wave voltammograms of different concentrations of MMZ (from bottom to top: 1.0, 10.0, 40.0, 60.0, 80.0 µM) and calibration curve of oxidation peak current versus concentration of MMZ at AgNPs/GO/CPE. Supporting electrolyte in all measurements was 0.5M phosphate buffer solution with pH 4.0 and 25 mV amplitude, 4 mV potential increment, and 15Hz frequency.

5.4. REFERENCES

[1] D.S. Cooper, New England Journal of Medicine, 54, 2005, 460.

[2] E. Cano-Europa, V. Blas-Valdivia, M. Franco-Colin, C.A. Gallardo-Casas, R. Ortiz- Butron, Acta Histochemica, 113, 2011, 1.

[3] M. Kulaksizoglu, M.S. Gonen, L. Kebapcilar, F. Sahin, B. Acikgoz, T. Demir, E., Transfusion and Apheresis Science 46 (2012) 149.

[4] D.K. Papayannis, A.M. Kosmas, Journal of Molecular and Structural Theochemistry, 851, 2008, 175.

[5] N.A. El-Maali, Bioelectrochemistry, 64, 2004, 99.

[6] K. Kusmierek, G. Chwatko, R. Głowacki, J. Chromatography B, 877, 2009, 3300.

[7] M. Pan, J. Wang, G. Fang, W. Tang, J. Chromatography B, 878, 2010, 1531.

[8] L. Hollosi, A. Kettrup, K.-W. Schramm, J. Pharm. Biomedicine, 36, 2004, 921.

[9] K. Kusmierek, E. Bald, Talanta, 71, 2007, 2121.

[10] R. Zakrzewski, J. Chromatography B, 869, 2008, 67.

[11] R. Zakrzewski, J. Liquid Chromatography and Related Tech., 32, 2009, 383.

[12] S. Zhang, W.-L. Sun, W. Zhang, W.-Y. Qi, L.-T. Jin, K. Yamamoto, S. Tao, J. Jin, Analytica Chimica Acta, 386, 1999, 21.

[13] M. Skowron, W. Ciesielski, Journal of Analytical Chemistry, 66, 2011, 714.

[14] Z. Sheng, H. Han, G. Yang, Luminescence, 26, 2011, 196.

[15] L. Hua, H. Han, H. Chen, Electrochimica Acta, 54, 2009, 1389.

[16] F. Dong, K. Hu, H. Han, J. Liang, Microchimica Acta, 165, 2009, 195.

[17] A. Economou, P.D. Tzanavaras, Analytica Chimica Acta, 505, 2004, 129.

[18] M. Aslanoglu, N. Peker, J. Pharmaceutical Biomedicine, 33, 2003, 1143.

[19] W. Yazhen, Bioelectrochemistry, 81, 2011, 86.

[20] M. Pan, G. Fang, Z. Duan, L. Kong, Biosensors and Bioelectronics, 31, 2012, 11.

[21] N.A. Martinez, G.A. Messina, F.A. Bertolino, E. Salinas, J. Raba, Sensors and Actuators B: Chemical, 133, 2008, 256.

[22] J. Sun, C. Zheng, X. Xiao, L. Niu, T. You, Electroanalysis, 17, 2005, 1675.

[23] A. Wang, L. Zhang, S. Zhang, J. Pharmaceutical Biomedicine, 23, 2000, 429.

[24] S. Shahrokhian, M. Ghalkhani, Electroanalysis, 20, 2008, 1061.

[25] V.K. Gupta, R. Jain, K. Radhapyari, Analytical Biochemistry, 408, 2011, 179.

[26] N. Biswas, S. Thomas, A. Sarkar, J. Physical Chemistry C, 113, 2009, 7091.

[27] P.N. Jayaram, G. Roy, Journal of Chemical Sciences, 120, 2008, 143

[28] H. Rooh, S. Baghery, S.G. Hosseini, Chemical Society of Japan, 81, 2008, 1402.

[29] R. Zhang, Y. Wen, N. Wang, Y. Wang, Y. Wang, Z. Zhang, H. Yang, Journal of Physical Chemistry B, 114, 2010, 2450.

CONCLUSION

Different types of electrodes modified with nanomaterials were prepared. The Ag/CNTs electrodes were prepared by the CVD method and were found to have high efficiency, sensitivity, precision and stability compared with Ag/CNTs prepared by physical attachment. The former type of electrodes was applied as an indicator electrode in potentiometric titrations. For the first time, a universal indicator electrode that responds to all types of titrimetric reactions was achieved. The response of this electrode was investigated in ion combination reactions such as precipitation reactions, complexation reactions, acid-base reactions and redox reactions. Smooth potentiometric curves for all of these titrations were obtained. The nanocomposite electrodes were prepared by fabricated carbon paste with different nanomaterials such as Ag, Au, GO, Ag/GO and Ag/CNTs. The nanocomposites were characterized by various techniques like TEM, SEM, Raman, UV-Vis, FT-IR and XPS which indicate the successful preparation of nanocomposites. The GCPE electrode is noticing the graphene is ideally suitable for the applications in electrochemistry applications. The results indicated that the graphene-enhanced the sensitivity for detecting the promazine drugs by using voltammetric techniques. Square wave voltammetry (SWV) is a better technique to achieve a LOD of 8 nM and a correlation coefficient (R^2) of 0.9979. The Au/CPE electrode was applied for the determination of ketoconazole drug. This modified electrode shows a good response to the determination of KCZ where a LOD of 0.59 μM and a correction coefficient R^2 of 0.9975 were obtained.

Vitae

Name	:Khaled M. ALAqad
Nationality	:Palestinian
Date of Birth	:2/3/1987
Email	:khaqad@gmail.com
Address	:King Fahd University of Petroleum and Minerals, Dhahran
Academic Background	:Received my B.Sc. in Chemistry from Islamic University of Gaza
	Earned the MS degree in chemistry from KFUPM in May, 2016.